Universidade do Estado do Rio de Janeiro

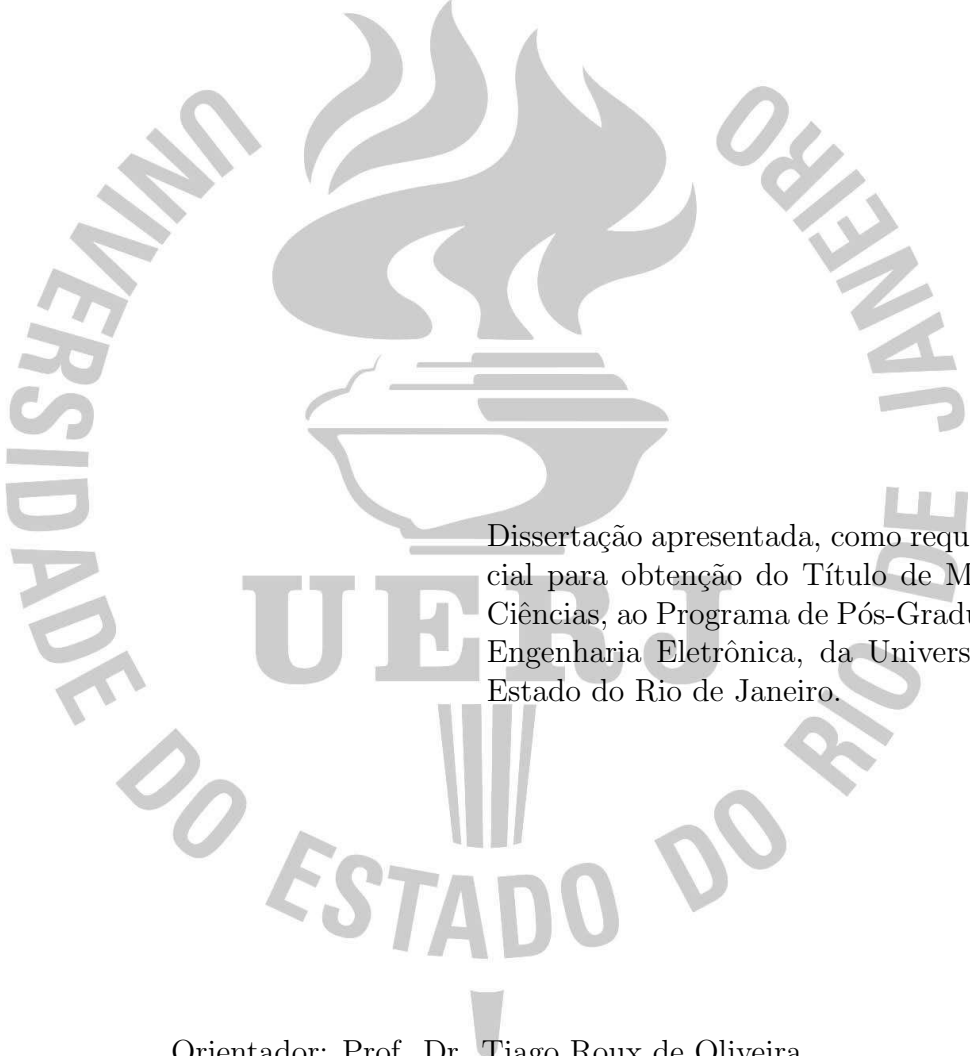Centro de Tecnologia e Ciências

Faculdade de Engenharia

Victor Hugo Pereira Rodrigues

**A Global Exact Differentiation Approach for Output-feedback
Sliding Mode and Adaptive Control**

Rio de Janeiro

2018

Victor Hugo Pereira Rodrigues

A Global Exact Differentiation Approach for Output-feedback Sliding Mode and Adaptive Control

Dissertação apresentada, como requisito parcial para obtenção do Título de Mestre em Ciências, ao Programa de Pós-Graduação em Engenharia Eletrônica, da Universidade do Estado do Rio de Janeiro.

Orientador: Prof. Dr. Tiago Roux de Oliveira

Rio de Janeiro

2018

Victor Hugo Pereira Rodrigues

A Global Exact Differentiation Approach for Output-feedback
Sliding Mode and Adaptive Control

Dissertação apresentada, como requisito parcial para obtenção do Título de Mestre em Ciências, ao Programa de Pós-Graduação em Engenharia Eletrônica, da Universidade do Estado do Rio de Janeiro. Área de concentração: Sistemas Inteligentes e Automação.

Aprovado em: 22 de Fevereiro de 2018

Banca Examinadora:

Prof. Tiago Roux de Oliveira, D.Sc. (Orientador)

Programa de Pós-Graduação em Engenharia Eletrônica - UERJ

Prof. José Paulo Vilela Soares da Cunha, D.Sc.

Programa de Pós-Graduação em Engenharia Eletrônica - UERJ

Prof. Liu Hsu, Docteur d'Etat.

Programa de Engenharia Elétrica - COPPE/UFRJ

Prof. Fernando Cesar Lizarralde, D.Sc.

Programa de Engenharia Elétrica - COPPE/UFRJ

Rio de Janeiro

2018

DEDICATÓRIA

Dedico esta dissertação a todos os meus familiares, amigas e amigos, especialmente aos meus pais, Valdevino Rodrigues da Silva Neto e Maria Aparecida Pereira Rodrigues e aos meus irmãos, Diego Pereira Rodrigues e Igor Pereira Rodrigues.

AGRADECIMENTO

"Would you tell me, please, which way I ought to go from here?

That depends a good deal on where you want to get to."

Charles Lutwidge Dodgson (Lewis Carroll)

RESUMO

RODRIGUES, Victor Hugo Pereira. *A Global Exact Differentiation Approach for Output-feedback Sliding Mode and Adaptive Control*. 172 f. Dissertação de Mestrado (Mestrado em Ciências da Engenharia Eletrônica) - Faculdade de Engenharia, Universidade do Estado do Rio de Janeiro (UERJ), Rio de Janeiro, 2018.

Nesta dissertação, um diferenciador global baseado em modos deslizantes de ordem superior (HOSM) com ganhos adaptativos é desenvolvido para resolver o problema de rastreamento usando apenas informações de entrada-saída para uma classe ampla de sistemas não-lineares com perturbações e incertezas paramétricas. O estado da planta não é medido de modo que um estimador para a norma do estado é projetado para majorar os distúrbios dependentes do estado e adaptar dinamicamente os ganhos do diferenciador proposto. Propriedades de estabilidade e o rastreamento exato e robusto podem ser obtidos quando os diferenciadores adaptativos baseados em modos deslizantes de ordem superior são utilizados na realimentação de saída. Simulações numéricas e experimentos são apresentados para diferentes controladores, tais como: controle de modo deslizante de primeira ordem, controle de modo deslizante de primeira ordem com função de monitoração, modos de deslizamento de terminal, twisting, super-twisting, super-twisting com ganhos variáveis, controle de modo deslizante quase contínuo e controle vetorial unitário. Além disso, combinamos o diferenciador global e ganhos dinâmicos com o clássico esquemas de controle adaptativo por modelo de referência (MRAC) para resolver o problema de rastreamento de trajetória via realimentação de saída para plantas lineares, incertas e de grau relativo arbitrário. Pela primeira vez, uma forma fechada é dada para controle adaptativo por modelo de referência para resolver o problema associado a plantas de grau relativo arbitrário.

Palavras-chave: Controle por Modo Deslizante. Modo Deslizante de Ordem Superior. Controle Adaptativo por Modelo de Referência. Observador da Norma. Função de Monitoração. Rastreamento Exato. Estabilidade Global e Semi-Global.

ABSTRACT

RODRIGUES, Victor Hugo Pereira. *A Global Exact Differentiation Approach for Output-feedback Sliding Mode and Adaptive Control.* 172 p. Master Thesis (Master in Science of Electronic Engineering) - Engineering Faculty, State University of Rio de Janeiro (UERJ), Rio de Janeiro, 2018.

In this thesis, a higher-order sliding mode (HOSM) based global differentiators with adaptive gains is developed to address the tracking control problem using only input-output information of a wider class of nonlinear systems with disturbances and parametric uncertainties. The state of the plant is assumed unmeasured so that a norm state estimator is designed to bound the state-dependent disturbances and dynamically adapt the gains of the proposed differentiator. Stability properties and robust exact tracking can be achieved when the proposed adaptive HOSM based differentiators for output-feedback are applied. Numerical simulations and experiments are presented for different control designs, such as: first-order sliding mode control, first-order sliding mode control with monitoring function, terminal sliding modes, twisting, super-twisting, variable gain super-twisting algorithm, nested sliding mode control, quasi-continuous HOSM finite-time controllers and unit vector control. Moreover, we combine a global differentiator based on HOSM and dynamic gains with classical model reference adaptive control (MRAC) schemes to solve the problem of trajectory tracking via output feedback for uncertain linear plants of arbitrary relative degree. For the first time a closed form is given by MRAC to solve the problem associated to plants of arbitrary relative degree.

Keywords: Sliding Mode Control. Higher Order Sliding Mode. Model Reference Adaptive Control. Norm Observer. Monitoring Function. Exact Tracking. Global and Semi-Global Stability.

LIST OF FIGURES

LIST OF TABLES

LIST OF ACRONYMS

FOAF	First Order Approximation Filter
FOSMC	First-Order Sliding Mode Control
HFG	High-Frequency Gain
HGO	High-Gain Observer
HOSM	Higher-Order Sliding Mode
I/O	Input-Output
ISS	Input-to-State Stability
MIMO	Multiple-Input Multiple-Output
MRAC	Model Reference Adaptive Control
SISO	Single-Input Single-Output
SMC	Sliding Mode Control
SOSM	Second-Order Sliding Mode
SPR	Strictly Positive Real
STA	Super-Twisting Algorithm
TA	Twisting Algorithm
UUB	Uniformly Ultimate Boundedness
UVC	Unit Vector Control
VGSTA	Variable Gain Super-Twisting Algorithm

SUMMARY

INTRODUCTION

Robust exact tracking control for uncertain systems is a longstanding problem. The most common way to solve this problem is using sliding mode control (SMC) [1–7]. In some papers ensuring finite-time exact tracking, it is supposed that the matched uncertainties are bounded [2,3] or they can be bounded by unknown constant bounds [4,5]. The presence of unmatched perturbations and uncertainties can also be found in [8]. On the other hand, the SMC design requires the knowledge of the system state vector or its estimate by using observers or differentiators.

The use of output-feedback SMC for exact tracking of disturbed systems with arbitrary relative degree is thus a challenging problem in this context [6]. This scenario is even more problematic when global stability properties are also pursued.

In [9,10], high-gain observers (HGOs) were used to generate the sliding variable and obtain output-feedback controllers. The result obtained in [9] is global but, nevertheless, only linear systems and matched disturbances were considered. In [2,3,11,12], higher-order sliding mode (HOSM) differentiators have been employed for exact state estimation and control. Such HOSM differentiators use constant [2,3] or time-varying gains [11–13]. As a result for any Lipschitz signal, exact derivative of arbitrary order is obtained by HOSM differentiators. In [11] the authors present conditions for the existence of time-varying gains which preserve the HOSM differentiation and accuracy of signals with unbounded higher derivatives. Hybrid estimation schemes combining lead filters (or HGOs) and HOSM differentiators can also be found in the literature [14].

The main problems with HGOs and the current versions of HOSM differentiators are:

- HGO based output-feedback control [9,10] achieves global or semi-global stability only with residual errors;

- HOSM differentiators with constant gains [2,3] cannot guarantee global stability;

- The time-varying gains in [11,12] can decrease when used in closed-loop since the variable bound depends on the state vector (which is not available in output-feedback scenarios), whereas in [13] they must be made strictly increasing to work over unbounded operation regions;

- The hybrid switching scheme in [14] applies two estimators (lead filter plus HOSM differentiators) running in parallel, which is not necessary to obtain global stability.

Finally, the works [2,14] considered only uniformly bounded matched disturbances. As mentioned before, the authors of [4,5] (see also references therein) envisaged approaches to circumvent exogenous disturbances with unknown constant bounds in the context of adaptive SMC. However, the price to be paid against the overestimation for the controller gain is the loss of the sliding motion thus, residual errors are implied.

In the Chapter 1 , we introduce a global exact differentiator with dynamic gains and then apply it to the global exact tracking problem via output-feedback. The main contributions are the following:

- We propose a new output-feedback strategy for disturbance domination and for differentiator gains adaptation based on state-norm observers [15]. Such state-norm observers are derived from the input-output filters commonly used in adaptive control [16];

- The proposed gains of the global differentiator are decreasing together with the system states and, consequently, the precision of the tracking is growing, while preserving in theory the globality and the sliding mode occurrence. In practice, if the gains decrease, the sensitivity of the overall closed-loop system is reduced [11];

For the first time, a HOSM based global exact differentiator is developed, guaranteeing global exponential stability when used in closed-loop control. The construction of a global upper bound for the derivative of the system states using only input-output information is derived to compute the dynamic gains of the proposed differentiator. Matched disturbances which can grow linearly with the unmeasured state and unmatched time-varying disturbances neglected before in [4, 5, 14] are now coped with.

In general, a sliding variable of *relative degree one* with respect to the control signal must be chosen for the sliding surface design in first-order sliding mode controllers. Higher-Order Sliding Mode (HOSM) algorithms rise to remove this condition and allows for an arbitrary relative degree between the sliding variable and the control signal [6]. One of the main uses of HOSM is the robust and finite-time differentiators [17] commonly applied to compute exactly the sliding variable or its higher time-derivatives.

Real-time differentiation is a classical problem in the field of control and estimation, with different applications such as output feedback and observer design [17–22]. The main obstacle for the real-time differentiator implementation is the trade-off between accuracy and robustness with respect to noise or discretization [23]. In particular, when used for control feedback, such observers/differentiators demand high gains to accommodate the plant uncertainties as well as to increase the domain of attraction, which in turns increase the sensitivity of the closed-loop system to real world imperfections as noise, unmodeled dynamics, discretization and switching delays [10]. This problem is even more challenging when the higher time-derivatives related to the gains necessary to design the differentiators are unknown or unmeasured and some kind of adaptation must be invoked [24, 25].

In this context, we can find HOSM differentiators using fixed [2, 3, 26] or time-varying gains [13, 27]. The advantages of applying variable gains is the possibility of guaranteeing global/semi-global stability results rather than local stability only, and obtaining adaptive gains that may decrease together with the system states. Note that even if semi-global results could be obtained with arbitrarily large constant gains to encompass large initial conditions for the closed-loop signals, the price to be paid there is the unnecessarily large value kept fixed when the (error) states have already ultimately converged to the origin. In practice, if the gains decrease, the sensitivity of the overall closed-loop system is reduced while the precision of the tracking is growing [11, 23]. In addition, the time-varying gains in [11, 13, 27] would not decrease when used in closed-loop feedback for global stability purposes since the variable bound depends on the state variables (which are not available in an output-feedback scenario), otherwise it must be made strictly increasing to work over unbounded operation regions leading again to overestimation of the gains.

In Chapter 2, we introduce a HOSM exact differentiator with adaptive gains applying it to the exact tracking problem via output feedback. We consider uncertain plants with time-varying disturbances of unknown bounds and nonlinear terms with a linear (unknown) growth condition with respect to the state variables. Based on the conditions for the existence of variable gains presented in [11, 28], we propose a new output-feedback strategy for disturbance domination and for differentiator gains adaptation using switching monitoring functions [29]. Hybrid state-norm observers are also employed in the sense of [30] in order to norm bound the unmeasured state preserving the HOSM diffe-

rentiation and accuracy of signals with unbounded higher derivatives, while guaranteeing global stability properties. The general methodology can be used to obtain a quite general family of output-feedback sliding mode controllers, which is illustrated in our simulation examples for the first order SMC case. An application example concerning the suppression of wing rock oscillations of *Slender Delta Wings* for high angles of attack of the aircraft is also presented to evaluate the proposed adaptive output-feedback control strategy.

The rejection of uncertainties and disturbances in nonlinear systems is a long lasting problem for which Sliding Mode Control (SMC) has shown to be a very efficient solution [1, 31–33]. However, the so called "chattering phenomenon" represents the main disadvantage of such control strategy. While in some applications a discontinuous control signal can be implemented (e.g., in electric drives and converters in power electronics), there are several control applications (e.g., some electromechanical systems and valves in hydraulic actuators to name a few) which simply does not match with the "chattering scenario" of non ideal first-order sliding mode control (FOSMC).

Controller designs using second-order sliding-mode (SOSM) concept [21, 23, 34–38] has been proposed for chattering elimination and attenuation. These SOSM algorithms can ensure finite-time convergence to zero of the sliding variable and its first derivative. It can be found plenty of applications using SOSM based algorithms reported recently, for instance: real-time differentiation [11, 13, 27], estimation of gasoline-engine parameters [22, 39, 40], wind energy conversion optimization [41], control of 3-DOF helicopters [42], control of induction motors [43], manipulator fault diagnosis [18], control of fuel-cells [20] and fault tolerant control [44].

Probably the most popular SOSM algorithm is the super-twisting algorithm (STA). STA is an *absolutely continuous* SOSM algorithm [23], for relative degree one sliding variable, that achieves the main properties of first order SMC provided the matched uncertainties/disturbances are *Lipschitz continuous* with bounded gradients. Further implementation aspects of STA are studied in [19]. A multivariable extension of the super-twisting sliding mode structure by using fixed-constant gains and state feedback was proposed in [45].

The main motivation for adaptation is that the bounds of the unknown disturbances and uncertainties are often assumed known in SMC. However, overestimating perturbations increases chattering. Possible solutions are to consider control laws with

adaptive or varying gains. Adaptive versions of STA (for control and estimation) appear in [11, 13, 46–49]. Some problems in the current adaptation schemes are:

- *Monotonically increasing gains:* disturbances may be still overestimated and chattering increased since it goes against the key motivation of the algorithm which is to reduce control gain [49, 50];

- *Increasing and decreasing gains:* sliding modes may fail temporarily [48];

- *Certainty equivalence principle:* the convergence rate may become too slow [47];

- *Time-varying gains:* for global stability/convergence properties, it is needed to measure the plant state vector and/or apply strictly increasing gains (chattering!) [11, 13, 50];

- *Equivalent control:* known upper bounds for the disturbances derivatives are required [46].

In this sense, a variable gain STA (VGSTA) was presented in [51] with the promise of achieving exact compensation of smooth bounded uncertainties-disturbances with bounded derivatives, assuming knowledge of some functions providing the bounds dependents on the state variables. The VGSTA is a non homogeneous extension of the standard STA. A time-invariant non smooth Lyapunov function [52] is used in order to demonstrate convergence of the VGSTA.

The innovation of the Chapter 3 is to generalize the VGSTA results originally proposed in [51]. There, relative degree one plants were considered and the control law was designed under the assumption of the *full-state measurement*. In this Chapter, a more general class of nonlinear systems with arbitrary relative degree are handled and the control scheme is developed using only output feedback. Another important difference is that the exact tracking problem is now considered rather than the stabilization only. Exact tracking is specially difficulty if uncertain nonlinear systems are considered and the control design must follow the output-feedback paradigm. For instance, in reference [53], the authors have proposed an output-feedback control scheme which can only guarantee practical tracking, i.e., the output error remains within a non null prescribed residual set.

Our proposal is based on a (non) homogeneous exact differentiator with dynamic gains recently introduced in [54, 55]. Our contribution applies state-norm observers [56] to obtain the necessary information about the upper bound of the disturbances. This information is then used for updating the gains of the higher-order sliding mode (HOSM) differentiator and the controller gains of the VGSTA as well. In particular, the upper bounds for the state-dependent disturbances are growing with the unmeasured state, which makes the control and differentiation problems as well as the non local stability analysis more challenging since unknown upper bounds are being assumed due to the unmeasured plant state. It will be shown this class of disturbances is more general than some recent papers in the field. We present a complete and rigorous stability proof for the closed-loop system. A simulation example with an academic plant shows the convergence properties of the proposed output-feedback VGSTA. Experimental results verify the new adaptation method leads to control and differentiator gains which decrease together with the system states, improving tracking precision and reducing in practice the sensitivity of the overall scheme to measurement noise, unmodeled dynamics, switching delays and numerical discretization. For the experimental tests, we use a real-world scenario that consist in stabilizing the balance of a seesaw through the positioning of a linear servo cart mounted on the seesaw to travel freely along its length.

In Chapter 4, we introduce a global exact differentiator with dynamic gains and then apply it to the exact tracking problem via output-feedback for series of sliding modes controllers. Based on the conditions for the existence of time-varying gains presented in [11], we propose a new output-feedback methodology for disturbance domination and for differentiator gains adaptation based on state-norm observers which preserves the HOSM differentiation and accuracy of signals with unbounded higher derivatives. The general methodology is applicable to obtain a quite general family of output-feedback sliding mode controllers (including classical first-order SMC designs, finite-time controllers and (dis)continuous HOSM based SMC), as illustrated in our simulation examples.

Moreover, the model reference adaptive control (MRAC) is one of the main approaches to adaptive control. A reference model is chosen to generate the desired trajectory that the plant output has to follow. The closed-loop plant is made up of an ordinary feedback control law that contains the plant, a controller parametrized with respect to a vector of unknown parameters and a learning mechanism that generates in an online

fashion the controller parameter estimates [16].

MRAC schemes can be characterized as *direct* or *indirect* and with *normalized* or *unnormalized* adaptive laws [16, 57]. In both direct and indirect MRAC with normalized adaptive laws, the control law, motivated from the known parameter case, is kept unchanged. This design is based on the certainty equivalence principle [57], which allows the use of a wide class of online parameter estimation that includes gradient, least-squares and those based on Strictly Positive Real (SPR) Lyapunov design [16]. On the other hand, in the case of MRAC schemes with unnormalized adaptive laws, the control parametrization is modified to lead an error equation whose form allows the use of the SPR–Lyapunov design approach for generating the adaptive law.

The design of direct MRAC schemes with unnormalized adaptive laws can be obtained for plants with relative degree $\rho = 1, 2, 3$ (for more details, see [16, 58]). In such approaches, derivatives of the plant output were not required, but were replaced by filtered derivative signals. The case of $\rho > 3$ follows by using the same techniques as in the case of $\rho = 3$, but it is in general omitted or is not so popular because of the complexity of the control law that increases with the relative degree ρ of the plant [59]. The price of not using explicitly exact differentiators was the real obstacle to derive simple and attractive adaptive control schemes. As a result, it was not until the early 1990s (with the appearance of *backstepping* [60]) that the interest by adaptive schemes for plants with higher relative degrees were revived.

In the recent literature, $\mathcal{L}_1$ adaptive control [61] has risen as a modified and alternative MRAC architecture using an input-filtered control signal, a state-prediction loop and high-gain adaptation laws to provide fast adaptation with guaranteed transient properties. Despite several publications report successful applications of $\mathcal{L}_1$ adaptive control, some recent papers questioning the efficiency of that can be found in [62, 63]. Criticisms include the inability to track exactly an arbitrary time-varying reference, the use of excessively high adaptation gains to decrease the tracking error, and the impossibility of handling uncertain high-frequency gains [64]. Moreover, $\mathcal{L}_1$ adaptive control must be structurally redesigned becoming much more complex for output feedback under higher relative degrees [65, Chapter 4].

In Chapter 5, we introduce an output-feedback adaptive controller based on global exact differentiators with dynamic gains [54] and then apply it to address the global

and exact tracking problem for linear plants of arbitrary relative degree. For the first time, a HOSM based differentiator is combined to an adaptive control scheme, while guaranteeing global asymptotic stability when used in closed-loop feedback. Notice that previous HOSM differentiators with fixed gains [17] would lead only to local stability results. The construction of a global upper bound for the derivatives of the system states using only input-output data by means of a state-norm observer [15] is derived to compute the dynamic gains of the proposed differentiator. This general methodology is applicable to MRAC as well as to other adaptive designs based on parameter projection using switching σ–modification [16] or binary control concepts [66–68], allowing for *leakage* [16] but eliminating the deleterious effects of the *bursting phenomena* [69].

In contrast to previous MRAC results, the new solution does not involve any additional parametrization and filtering besides the global HOSM differentiator, being thus close in structure and complexity to conventional solutions for unitary relative degree. The simulation example illustrates the simplicity of our control design as well as its better transient responses and less control effort when compared to classical MRAC schemes for higher relative degrees.

At last, we present an application for the proposed output-feedback adaptive controller to bilateral teleoperation [70–72], where the actions of the master are transmitted to the slave system such that the latter has to behave as the former, according to the model reference paradigm.

In Chapter 6, we solve the *global* exact output tracking problem for a class of uncertain *multi-input-multi-output (MIMO)* nonlinear plants with *nonuniform* arbitrary relative degree and disturbances. For the sake of comparisons, the class considered here encompasses those in [3, 13, 26, 73, 74], with the benefit of guaranteeing global stability properties. The result is achieved by generalizing to a multivariable framework the global HOSM differentiation scheme originally proposed for SISO plants in [75–78]. The proposed approach applies for an output-feedback multivariable extension of the variable gain super-twisting algorithm (STA) – using norm-state observer for gain adaptation – to tackle a rather general class of matched nonlinear disturbances which grow with the measured and/or unmeasured states. This represents a significant extension of a recently proposed non decoupled multivariable super-twisting algorithm [79], based on state-feedback with fixed gains, to the case of output-feedback with variable gains. As a result, the error

system becomes uniformly globally exponentially stable and ultimately converges to zero.

Novel conditions must be assumed for the MIMO case, which make the problem hard to be solved. For example, it was assumed in [74] a known matrix multiplier S_p for the high-frequency gain (HFG) matrix K_p such that $K_p S_p + S_p^T K_p^T > 0$. Here, we consider a diagonally stable assumption for the HFG matrix which is a less restrictive assumption than the one raised in [74]. Furthermore, the hybrid switching scheme in [74] is restricted to linear plants and applies two set of estimators (lead filters plus HOSM differentiators with fixed gains) running in parallel, which is not necessary to obtain global stability. It requires at least the double of state variables when compared to our proposed method. Simulations show the simplicity of our solution.

Preliminaries: Throughout the text, all k's denote positive constants. The terms $\pi(t)$ denote exponentially decaying functions, *i.e.*, $|\pi(t)| \leq Ke^{-\lambda t}, \forall t$, where K possibly depends on the system initial conditions and λ is a generic positive constant. The notation $|\cdot|$ stands for the Euclidean norm for vectors, or the induced norm for matrices, whereas $||f_t||$ denotes the $\mathcal{L}_{\infty e}$ norm of a signal $f(t)$, *i.e.*, $\sup_{0 \leq \tau \leq t} |f(\tau)|$. Input-to-State Stability (Stable) – ISS definition as well as functions of class $\mathcal{K}$, $\mathcal{K}_\infty$ and $\mathcal{KL}$ are defined according to [80]. Here, Filippov's definition for the solution of discontinuous differential equations is assumed [81]. For the sake of simplicity, "s" will represent either the Laplace variable or the differential operator (d/dt), according to the context.

> To facilitate the reader's life, each chapter has its own assumptions list and it is presented at the beginning of each chapter :)

1 FIRST ORDER SLIDING MODE CONTROL

In this Chapter we introduce a global differentiator based on higher-order sliding modes (HOSM) and dynamic gains to solve the problem of trajectory tracking via output-feedback for a class of uncertain nonlinear plants with arbitrary relative degree and disturbances. Norm observers for the unmeasured state are employed to dominate the disturbances as well as to adapt the gains of the proposed differentiator since the nonlinearities may be state-dependent and time-varying. Uniform global stability and robust exact tracking are guaranteed employing the proposed HOSM based exact differentiator. The obtained results are not restricted to first-order sliding mode control feedback, but applies for second order sliding mode algorithms (twisting, super-twisting and variable gain super-twisting) as well as quasi-continuous HOSM finite-time controllers. Simulations with an aircraft pitch-control application illustrate the claimed properties, even in the presence of measurement noise.

1.1 Problem Statement

Consider an uncertain nonlinear plant described by:

$$\dot{x} = A_p x + B_p[u + d(x,t)] + \phi(t)\,, \qquad y = H_p x\,, \tag{1}$$

where $x \in \mathbb{R}^n$ is the state, $u \in \mathbb{R}$ is the input, $y \in \mathbb{R}$ is the output, $d(x,t) \in \mathbb{R}$ is a state dependent uncertain disturbance and $\phi(t)$ is a time-varying uncertain unmatched external disturbance. The term "unmatched" refers to $\phi(t)$ not contained in the range space of B_p, otherwise $\phi(t)$ could be directly incorporated into the "matched" disturbance $d(x,t)$. The uncertain matrices A_p, B_p and H_p belong to some compact set, such that the necessary uncertainty bounds to be defined later are available for design.

The following assumptions are made in this chapter:

(A1) The transfer function $G(s) = H_p(sI - A_p)^{-1}B_p$ is minimum phase.

(A2) The pairs (A_p, B_p) and (A_p, H_p) are controllable and observable, respectively.

(A3) The transfer function $G(s)$ has a known relative degree ρ and order n. The *high frequency gain* (HFG) $K_p \in \mathbb{R}$ satisfies $K_p = \lim_{s \to \infty} s^\rho G(s) = H_p A_p^{\rho-1} B_p$. Without loss of generality, we assume that $K_p > 0$.

(A4) The input disturbance $d(x,t)$ is assumed to be uncertain, locally integrable and norm bounded by $|d(x,t)| \leq k_x|x| + k_d$, $\forall x,t$, where $k_x, k_d \geq 0$ are *known* scalars. The unmatched disturbance $\phi(t)$ is assumed sufficiently smooth. Moreover, there exists a *known* constant $k_\phi \geq 0$ such that $|\phi^{(i)}(t)| \leq k_\phi$, $\forall i = 0, \ldots, \rho$.

Assumptions (A1)–(A3) are usual in model reference adaptive control (MRAC) [16]. From (A4), we note that the relative degree of (1) depends only on the linear part, being independent of the disturbances d and ϕ. In addition, the class of nonlinear disturbances are more general than those considered in [2, 4, 5, 14] and represents a challenge in the context of global output-feedback SMC.

Let the reference signal $y_m(t) \in \mathbb{R}$ be generated by the following reference model

$$y_m = W_m(s)\, r\,, \quad W_m(s) = (s + \gamma_m)^{-1} L_m^{-1}(s)\,, \quad \gamma_m > 0, \tag{2}$$

where $r(t) \in \mathbb{R}$ is an arbitrary uniformly bounded piecewise continuous reference signal and

$$L_m(s) = s^{(\rho-1)} + l_{\rho-2} s^{(\rho-2)} + \cdots + l_1 s + l_0\,, \tag{3}$$

with $L_m(s)$ being a Hurwitz polynomial. The transfer function matrix $W_m(s)$ has the same relative degree as $G(s)$ and its HFG is the unity.

The main objective is to find a control law u such that the output error

$$e(t) := y(t) - y_m(t) \tag{4}$$

is steered to zero, for arbitrary initial conditions.

The MRAC parametrization [16] using I/O filters is initially applied to obtain the *ideal matching control* [16] denoted by u^* and derive the dynamic error equations for the error system. However, we are not trying to recover any particular property from MRAC. In this sense, when the plant is known and $d(t) \equiv 0$, $\phi(t) \equiv 0$, a control law which achieves the matching between the closed-loop transfer function matrix and $W_m(s)$ is given by

$$u^* = \theta^{*T} \omega\,, \quad \theta^* = \begin{bmatrix} \theta_1^{*T} & \theta_2^{*T} & \theta_3^* & \theta_4^* \end{bmatrix}^T, \tag{5}$$

where θ^* is the parameter vector with $\theta_1^*, \theta_2^* \in \mathbb{R}^{(n-1)}$ and $\theta_3^*, \theta_4^* \in \mathbb{R}$. The regressor vector

$\omega = [\omega_u^T \ \omega_y^T \ y \ r]^T$, $w_u, w_y \in \mathbb{R}^{(n-1)}$ is obtained from I/O state variable filters given by:

$$\dot{\omega}_u = \Phi \omega_u + \Gamma u \,, \qquad \dot{\omega}_y = \Phi \omega_y + \Gamma y \,, \tag{6}$$

where $\Phi \in \mathbb{R}^{(n-1)\times(n-1)}$ is Hurwitz and $\Gamma \in \mathbb{R}^{(n-1)}$ is chosen such that the pair $(\Phi, \ \Gamma)$ is controllable. The matching conditions require that $\theta_4^* = K_p^{-1}$. Define the augmented state vector

$$X = [x^T, \omega_u^T, \omega_y^T]^T \,, \tag{7}$$

with dynamics described by $\dot{X} = A_0 X + B_0 u + B_0' d + B_\phi \phi$, and output $y = H_0 X$, where

$$A_0 = \begin{bmatrix} A_p & 0 & 0 \\ 0 & \Phi & 0 \\ (\Gamma H_p) & 0 & \Phi \end{bmatrix}, \ B_0 = \begin{bmatrix} B_p \\ \Gamma \\ 0 \end{bmatrix}, \ B_0' = \begin{bmatrix} B_p \\ 0 \\ 0 \end{bmatrix}, \tag{8}$$

$$B_\phi^T = \begin{bmatrix} I & 0 & 0 \end{bmatrix}, \quad H_0 = \begin{bmatrix} H_p & 0 & 0 \end{bmatrix}. \tag{9}$$

Then, adding and subtracting $B_0 \theta^{*T} \omega$ and noting that there exist matrices $\Omega_1 \in \mathbb{R}^{(2n-2)\times(3n-2)}$ and $\Omega_2 \in \mathbb{R}^{(2n-2)}$ such that [16]

$$\omega = \Omega_1 X + \Omega_2 r \,, \tag{10}$$

one has

$$\dot{X} = A_c X + B_c K_p [\theta_4^* r + u - u^*] + B_0' d + B_\phi \phi \,, \quad y = H_0 X \,, \tag{11}$$

where $A_c = A_0 + B_0 \theta^{*T} \Omega_1$ and $B_c = B_0 \theta_4^*$. Notice that (A_c, B_c, H_0) is a nonminimal realization of $W_m(s)$. For analysis purposes, the reference model can be described by

$$\dot{X}_m = A_c X_m + B_c K_p [\theta_4^* r - d_f] + B_0' d + B_\phi \phi \,, \quad y_m = H_0 X_m \,, \tag{12}$$

where the equivalent input disturbance $d_f = W_d(s) d + W_\phi(s) \phi$ with

$$W_d(s) \ = \ [W_m(s) K_p]^{-1} H_0 (sI - A_c)^{-1} B_0' \,, \tag{13}$$

$$W_\phi(s) \ = \ [W_m(s) K_p]^{-1} H_0 (sI - A_c)^{-1} B_\phi \,. \tag{14}$$

Note that $W_d(s)$ in (13) is a stable and proper transfer function and $W_\phi(s)$ in (14) is a stable and possibly improper transfer function, so that derivatives of $\phi(t)$ may appear in

the input channel. Following the steps given in [82], $[W_m(s)K_p]^{-1} = \bar{K}_\rho s^\rho + \bar{K}_{\rho-1}s^{\rho-1} + \ldots + \bar{K}_0$, where $\bar{K}_i \in \mathbb{R}$, $i = 0, \ldots, \rho$, are constants. By using the Markov parameters to represent $H_0(sI - A_c)^{-1}B_\phi = \frac{H_0 B_\phi}{s} + \frac{H_0 A_c B_\phi}{s^2} + \frac{H_0 A_c^2 B_\phi}{s^3} + \ldots$, the term $d_f(t)$ can be rewritten as

$$d_f := K_{\rho-1}\phi^{(\rho-1)} + \cdots + K_1\dot{\phi} + W_p(s) * \phi + W_d(s) * d \,, \tag{15}$$

where $*$ denotes the convolution operator, $K_j \in \mathbb{R}^{1 \times n}$ is given by

$$K_j = \sum_{i=j+1}^{\rho} \bar{K}_i H_0 A_c^{i-j-1} B_\phi \,, \quad j = 1, \ldots, \rho - 1 \,, \tag{16}$$

and $W_p(s)$ is a stable and proper transfer function matrix

$$W_p(s) = \sum_{i=1}^{\rho} \bar{K}_i H_0 A_c^{i-1} B_\phi + \sum_{i=0}^{\rho} \bar{K}_i H_0 A_c^i (sI - A_c)^{-1} B_\phi \,. \tag{17}$$

Thus, the error dynamics with state

$$X_e := X - X_m \tag{18}$$

can be written in the the state-space representation by

$$\dot{X}_e = A_c X_e + B_c K_p [u - \theta^{*T}\omega + d_f] \,, \tag{19}$$

$$e = H_0 X_e \,, \tag{20}$$

or in the I/O form as: $e = W_m(s)K_p\left[u - \theta^{*T}\omega + d_f\right]$.

The importance of considering the augmented dynamics (11) with state X including the I/O filters (6) is not only to derive the full-error equation (19), but to create an output-feedback framework which allow us to derive norm bounds for the unmeasured state of a possibly unstable plant (1) and for the equivalent disturbance $d_f(x,t)$, as discussed in the next section. As a bonus, we use (19) in the proof of the main theorem to state global stability by means of input-to-state properties of the closed-loop system, without appealing to Lyapunov based analysis.

1.2   State-Norm Observer

Considering Assumption (A4) and applying [8, Lemma 3] to (11), it is possible to find $k_x^* > 0$ such that, for $k_x \in [0, k_x^*]$, a norm bound for X and x can be obtained through stable *first order approximation filters* (FOAFs) (see details in [8]). Thus, one has

$$|x(t)|, |X(t)| \leq |\hat{x}(t)| + \hat{\pi}(t), \tag{21}$$

$$\hat{x}(t) := \frac{1}{s + \lambda_x}[c_1(k_d + k_\phi) + c_2|\omega(t)|], \tag{22}$$

with $c_1, c_2, \lambda_x > 0$ being appropriate constants that can be computed by the optimization methods mentioned in [8]. Regarding the parameter λ_x in (22), it is defined by $\lambda_x := \gamma_0 - |B_0'|k_x$, where $|B_0'|k_x > 0$ is a constant smaller than γ_0 computed with B_0' given in (8), k_x of Assumption (A4) and $\gamma_0 > 0$ being the stability margin of A_c in (11). Let $\{\lambda_i\}$ be the eigenvalues of A_c, the stability margin of A_c is defined by $\gamma_0 := \min_i[-\mathrm{Re}(\lambda_i)]$.

In this sense, inequality (21)–(22) establishes that the norm observer estimate $\hat{x}(t)$ provides a valid norm bound for the unmeasured state x of the uncertain and disturbed plant, *i.e.*, $|x| \leq |\hat{x}|$ except for exponentially decaying terms due to the system initial conditions, denoted here by $\hat{\pi}(t)$. From (21), we still can conclude the following norm bound

$$|x(t)|, |X(t)| \leq |\hat{x}(t)| + \delta_0, \quad \forall t \geq T_0,$$

valid after some finite time $T_0 > 0$, for any arbitrarily small positive constant δ_0 (independent of initial conditions) since $\hat{\pi}(t)$ is an exponentially decreasing term.

Since we assume sufficient differentiability for ϕ and uniform boundedness for its time derivatives, one can find a constant $\bar{k}_\phi > 0$ such that $|K_1\dot{\phi} + \ldots + K_{\rho-1}\phi^{(\rho-1)}| \leq \bar{k}_\phi$ and $|d_f| \leq \bar{k}_\phi + |W_p(s) * \phi| + |W_d(s) * d|$. Moreover, from (A4) and (22), one has $|d(x,t)| \leq k_x\hat{x}(t) + k_d$, *modulo* $\hat{\pi}$ term, and one can write $|d_f| \leq \hat{d}_f + \hat{\pi}_f$, where $\hat{\pi}_f$ is an exponentially decreasing term,

$$\hat{d}_f(t) := \bar{k}_\phi + \frac{c_f}{s + \lambda_f}[k_\phi + k_x\hat{x}(t) + k_d], \tag{23}$$

and $\frac{c_f}{s+\lambda_f}$ is a FOAF designed for $W_d(s)$ and $W_p(s)$, with adequate positive constants c_f and λ_f. At the price of some conservatism, we can simplify the FOAF design by choosing c_f sufficiently large and λ_f sufficiently small.

Remark 1 (Norm Observer Initialization)**.** *According to (21), we can rewrite the upper*

bound $|\hat{x}(t)| \geq |x(t)| - \hat{\pi}(t)$. *Let $\hat{x}$ be the state of the minimal state-space realization for the FOAF $1/(s + \lambda_x)$ in (22):*

$$\dot{\hat{x}} = -\lambda_x \hat{x} + [c_1(K_d + k_\phi) + c_2|\omega|].$$

For practical purposes, it is always possible to initialize the norm observer state with a positive value $\hat{x}(0) > 0$ in order to reduce the transient phase due to the term $\hat{\pi}(t)$ in (21), such that the upper bound $|x(t)| \leq \hat{x}(t)$ can be assured as soon as possible, i.e., $\forall t \geq T_0$ and some finite time $T_0 > 0$ arbitrarily small. It would be of particular interest in order to provide faster convergence properties for the differentiator to be introduced later on, although it is not needed to prove global stability for the overall closed-loop scheme. Although the norm state estimation cannot be globally obtained in a fixed-time, it is guaranteed after some finite time, which is unknown if no knowledge is assumed a priori about the plant initial conditions (global results). ⌟

1.3 Global Differentiator with Dynamic Gains

In what follows, a HOSM differentiator with coefficients being adapted using the estimate for the norm of the state x provided in (21) is proposed to achieve global exact estimation, *i.e.*, exact differentiation of signals with any initial conditions and unbounded higher derivatives.

Under the assumptions (A1)–(A4), the unmatched time-varying disturbance $\phi(t)$ cannot change the relative degree of the unperturbed linear system (1), thus it is easy to show that the nonlinear system (1) can be transformed into the *normal form* [80]:

$$\dot{\eta} = \mathcal{A}_0\eta + \mathcal{B}_0 y, \tag{24}$$

$$\dot{\xi} = \mathcal{A}_\rho\xi + \mathcal{B}_\rho K_p[u + d_e(x,t)], \quad y = \mathcal{C}_\rho\xi, \tag{25}$$

where $z^T = [\eta^T \ \xi^T] \in \mathbb{R}^n$ with $\eta \in \mathbb{R}^{(n-\rho)}$ being referred to the state of the inverse or zero dynamics and $\xi = [y \ \dot{y} \ \ldots \ y^{(\rho-1)}]^T$ the state of the external dynamics. The triple $(\mathcal{A}_\rho, \mathcal{B}_\rho, \mathcal{C}_\rho)$ is in the Brunovsky's controller form [80] and $\mathcal{A}_0$ is Hurwitz. The equivalent input disturbance $d_e(x,t) = d(x,t) + K_p^{-1} \left(H_p A_p^\rho x + \sum_{i=0}^{\rho-1} H_p A_p^{\rho-1-i} \phi^{(i)} \right)$ is affinely norm

bounded by

$$|d_e(x,t)| \leq \kappa_1|x| + \kappa_2\,, \tag{26}$$

where $\kappa_2 > k_d + K_p^{-1}\left|\sum_{i=0}^{\rho-1} H_p A_p^{\rho-1-i}\phi^{(i)}\right|$ and $\kappa_1 > k_x + K_p^{-1}\left|H_p A_p^\rho\right|$ are known constants. We can conclude the following state-dependent upper bound for higher derivative (order ρ) of the output signal

$$|y^{(\rho)}| \leq K_p\left[\kappa_1|x| + \kappa_2 + |u|\right]\,. \tag{27}$$

From (27) and (4), we can write

$$|e^{(\rho)}(t)| \leq L(x,t) = K_p\left[\kappa_1|x| + \kappa_2 + |u|\right] + |y_m^{(\rho)}(t)|\,. \tag{28}$$

Now, assume that the control input satisfies

$$|u| \leq k_\varrho \varrho(t) \leq \kappa_3||X_t|| + \kappa_4\,, \tag{29}$$

for constants $k_\varrho, \kappa_3, \kappa_4 > 0$ and an appropriate continuous *modulation function* $\varrho(t) \geq 0$, to be defined later on. Then, applying (21), we can obtain the following upper bound with the norm observer variable $\hat{x}(t)$ in (21)–(22):

$$|e^{(\rho)}(t)| \leq K_p\left[\kappa_1(|\hat{x}| + \delta_0) + \kappa_2 + k_\varrho \varrho(t)\right] + |y_m^{(\rho)}(t)|\,, \tag{30}$$

modulo exponential decaying terms due to initial conditions, which take into account the transient of the FOAF. By defining known positive constants k_1, k_2, k_3 and k_m satisfying $k_m \geq |y_m^{(\rho)}(t)|$, $k_1 \geq K_p\kappa_1$, $k_2 \geq K_p(\kappa_1\delta_0 + \kappa_2) + k_m$ and $k_3 \geq K_p k_\varrho$, we can define

$$\mathcal{L}(\hat{x},t) := k_1|\hat{x}| + k_2 + k_3\varrho(t)\,, \tag{31}$$

and state the following upper bound constructed only with measurable signals

$$|e^{(\rho)}(t)| \leq \mathcal{L}(\hat{x},t)\,, \quad \forall t \geq T\,, \tag{32}$$

for some finite time $T > 0$.

In light of (31)–(32), we can introduce the following HOSM differentiator based on dynamic gains for the output error $e \in \mathbb{R}$, with state $\zeta = [\zeta_0 \ \ldots \ \zeta_{\rho-1}]^T$ and order

$$p = \rho - 1: \qquad \dot{\zeta}_0 = v_0 = -\lambda_0 \mathcal{L}(\hat{x}, t)^{\frac{1}{p+1}} |\zeta_0 - e(t)|^{\frac{p}{p+1}} \operatorname{sgn}(\zeta_0 - e(t)) + \zeta_1,$$

$$\vdots$$

$$\dot{\zeta}_i = v_i = -\lambda_i \mathcal{L}(\hat{x}, t)^{\frac{1}{p-i+1}} |\zeta_i - v_{i-1}|^{\frac{p-i}{p-i+1}} \operatorname{sgn}(\zeta_i - v_{i-1}) + \zeta_{i+1}, \qquad (33)$$

$$\vdots$$

$$\dot{\zeta}_p = -\lambda_p \mathcal{L}(\hat{x}, t) \operatorname{sgn}(\zeta_p - v_{p-1}).$$

The dynamic gain of our differentiator must satisfy the same conditions for finite-convergence given in [11]: the global upper bound $\mathcal{L}(\hat{x}, t)$ must be absolutely continuous with bounded logaritmic derivative ($|\dot{\mathcal{L}}/\mathcal{L}| \leq M$, where $M > 0$ is some constant). It implies that $\mathcal{L}(\hat{x}, t)$ can grow at most exponentially as a result of $|\dot{\mathcal{L}}| \leq M|\mathcal{L}|$. Similar results can be obtained for non-homogeneous versions (with additional linear terms) of variable gains HOSM differentiators [83]. Our main advantage is that the differentiator gain is constructed using only input-output information, while the full-state measurement is assumed in [11].

According to the linear growth condition assumed in (A4) for the system nonlinearities and the *regularity condition* [57] assumed in (29) for the control signal, any finite-escape is precluded and only exponentially growing signals are possible in the closed-loop system, as it will be show in the proof of the main theorem. Thus, if the parameters λ_i are properly recursively chosen [17], the following equalities

$$\zeta_0 = e(t), \quad \zeta_i = e^{(i)}(t), \quad i = 1, \dots, p, \qquad (34)$$

are established in finite time [17], but with the theoretical advantage of being globally valid (for any initial conditions) since it is not required *a priori* that the signal $e^{(\rho)}(t)$ be uniformly bounded, as assumed in the HOSM differentiator with fixed gains [17].

Remark 2 (Impacts of the Measurement Noise)**.** *The inclusion of measurement noise and its impact on HOSM based differentiators (with constant or variable gains) was already discussed in the literature [11, 17]. Since our global HOSM differentiator follows the same philosophy, the existing uniformly ultimate boundedness (UUB) results are at least expected to be preserved. Due to space limitations, we could not add such existing knowledge here. However, the robustness of the overall control scheme to measurement noise will be illustrated in our numerical results. As a further remark, if $L(x, t)$ eventually decreases, $\mathcal{L}(\hat{x}, t)$ vanishes too. Consequently, less sensitivity to measurement noise, discretization*

and delays can be expected rather than the differentiator with necessarily high-constant gains used to prove semi-global stability. Thus, the globality is attained with advances in practical scenarios as well. ⌐

1.4 Global Tracking via Output-feedback

The next step is to proposed output-feedback control laws which satisfy (29) such that the global differentiator above can be indeed constructed and applied.

1.4.1 First Order SMC for Arbitrary Relative Degrees

The main idea of sliding mode control is to design the relative degree one sliding variable such that, when the motion is restricted to the manifold $\sigma = 0$, the reduced-order model has the required performance.

For higher relative degree plants, one could use the operator $L_m(s)$ defined in (3), to overcome the relative degree obstacle. The operator $L_m(s)$ is such that $L_m(s)G(s)$ and $L_m(s)W_m(s)$ have relative degree one. The ideal sliding variable $\sigma = L_m(s)e \in \mathbb{R}$ is given by

$$\sigma = e^{(\rho-1)} + \cdots + l_1\dot{e} + l_0 e \tag{35}$$

$$= \sum_{i=0}^{\rho-1} l_i H_0 A_c^i X_e = \bar{H} X_e \,,$$

where the second equality is derived from Assumption (A3) and (19). Notice that $\{A_c, B_c, \bar{H}\}$ is a nonminimal realization of $L_m(s)W_m(s)$. From (2)–(3), one has

$$\sigma = L_m(s)W_m(s)K_p \left[u - \theta^{*^T}\omega + d_f \right]$$

$$= \frac{K_p}{s + \gamma_m} \left[u - \theta^{*^T}\omega + d_f \right] \,. \tag{36}$$

If the first order SMC law was given by $u = -\varrho(t)\mathrm{sgn}(\sigma)$, with modulation function $\varrho(t) \geq 0$ satisfying

$$\varrho(t) \geq |-\theta^{*^T}\omega(t) + d_f(t)| + \delta \,, \quad \delta > 0 \,, \tag{37}$$

where the constant δ can be arbitrarily small, then the closed-loop error system (19) would be uniformly globally exponentially stable and the ideal sliding variable σ became

identically zero after some finite time, according to [84, Lemma 1]. Since A_p, B_p and H_p in (1) belong to some known compact set, an upper bound $\bar{\theta} \geq |\theta^*|$ can be obtained. Thus, a possible choice for the modulation function to satisfy (37) is given by

$$\varrho(t) = \bar{\theta}|\omega(t)| + \hat{d}_f(t) + \delta \,, \tag{38}$$

with $\hat{d}_f(t)$ defined in (23). However, σ is not directly available to implement the control law. Thus, using the proposed global HOSM differentiator, the following estimate for σ can be obtained:

$$\hat{\sigma} = \zeta_{\rho-1} + \cdots + l_1\zeta_1 + l_0\zeta_0 \,. \tag{39}$$

From (10), (22) and (23), it is easy to show that the following control signal

$$u = -\varrho(t)\mathrm{sgn}(\hat{\sigma}) \,, \tag{40}$$

with the modulation function $\varrho(t)$ in (38), satisfies inequality (29) for $k_\varrho = 1$. To show this property we just have to write $|\omega| \leq \kappa_5|X| + \kappa_6$ from (10), with $\kappa_5\,, \kappa_6 > 0$ and considering that $r(t)$ is an uniformly bounded reference signal. Then, from the ISS relation of the filtered signals in (22) and (23) with respect to ω, we conclude the norm bounds $|\hat{d}_f| \leq \kappa_a||X_t|| + \kappa_b$ and $|\hat{x}| \leq \kappa_c||X_t|| + \kappa_d$, for appropriate constants $\kappa_a\,, \kappa_b\,, \kappa_c\,, \kappa_d > 0$. Thus, the global differentiator with dynamic gains given in (33) can indeed be constructed and its state exactly surrogates the time derivatives of the signal $e(t)$ in the sliding variable $\hat{\sigma}$ (39), after some finite time.

1.4.2 Stability Analysis

The next theorem states the global stability results with ultimate exact tracking for the output-feedback scheme.

Theorem 1. *Consider the plant (1) and the reference model (2)–(3). The output-feedback control law u is given by (40) with modulation function ϱ defined in (38) satisfying (37) and the global exact estimate $\hat{\sigma}$ given by (39) and constructed with the state $\zeta = [\zeta_0 \ \ldots \ \zeta_{\rho-1}]^T$ of the proposed differentiator (33). Suppose that assumptions (A1) to (A4) hold. For $\lambda_i\,, i = 0, \ldots, \rho-1$, properly chosen and $\mathcal{L}(\hat{x}, t)$ in (33) satisfying (31), the estimation of the ideal sliding variable σ becomes exact after some finite time, i.e., $\hat{\sigma} \equiv \sigma$. Then, the*

closed-loop error system with dynamics (19) is uniformly globally exponentially stable in the sense that X_e and, hence, the output tracking error e converge exponentially to zero and all closed-loop signals remain uniformly bounded.

Proof 1. *In what follows, $k_i > 0$ are constants not depending on the initial conditions. The demonstration is divided in two steps. In the first one, it is necessary to show that no finite time escape in the closed-loop system signals is possible. By using the relations (10) and (18), one has that $X = X_e + X_m$ and the regressor vector*

$$\omega = \Omega_1 X_e + \Omega_1 X_m + \Omega_2 r \,. \tag{41}$$

Let $x_m := [y_m \ \dot{y}_m \ \ldots \ y_m^{(\rho-1)}]^T$ and $x_e := \xi - x_m$, with ξ in (25). From (19), it can be shown that $e^{(i)} = H_0 A^i X_e$, for $i = 0, \ldots, \rho-1$, hence $|x_e| \le k_0 |X_e|$. Therefore, since x_m is uniformly bounded, then $\xi = x_e + x_m$ can be affinely norm bounded in $|X_e|$. In addition, from (24), the η-dynamics is ISS with respect to $y = \mathcal{C}_\rho \xi$. Thus, one can conclude that $|x| \le k_1 \|\xi_t\| + k_2$, and consequently, $|x| \le k_3 \|(X_e)_t\| + k_4$. Due to assumption (A4) concerning the linear growth condition of the nonlinear disturbances with respect to the unmeasured state x, from (12) and (15), one has

$$|X_m| \le k_5 \|(X_e)_t\| + k_6 \,. \tag{42}$$

Finally, from (10), (41) and (42), we conclude ω, the term d_f in (19), and consequently the control input u with modulation function ϱ in (38) are all affinely norm bounded by X or X_e, i.e.,

$$|u|, |d_f|, |\omega| \ \le \ k_a \|X_t\| + k_b \,, \tag{43}$$

$$|u|, |d_f|, |\omega| \ \le \ k_c \|(X_e)_t\| + k_d \,. \tag{44}$$

Thus, the system signals will be regular and, therefore, can grow at most exponentially [57]. This fact lead us to the second step of the proof. There exist two finite-time instants $T_1 > 0$ and $T_2 > 0$ such that (32) and (37) are satisfied, $\forall t > \max\{T_1, T_2\}$. Then, the ideal sliding variable is exactly estimated, i.e., $\hat{\sigma} \equiv \sigma$ and the relative degree compensation is perfectly achieved. Moreover, from [84, Lemma 1], the ideal sliding mode $\hat{\sigma}(t) \equiv \sigma(t) \equiv 0$ is achieved in finite time. Since σ in (35) is the relative degree one output for (19), it is

possible to rewrite it into the normal form [80] such that the states of the error system are input-to-state stable (ISS) with respect to σ, for a particular exponential class-$\mathcal{KL}$ function. It can be shown reminding that $L_m(s)W_m(s) = 1/(s+\gamma_m)$. From (19) and (36), one gets $\dot{X}_e = A_c X_e + B_c(\dot{\sigma} + \gamma_m\sigma)$. Further, using the transformation $X_e := \bar{X}_e + B_c\sigma$, one has

$$\dot{\bar{X}}_e = A_c \bar{X}_e + (A_c B_c + \gamma_m B_c)\sigma \,, \tag{45}$$

which clearly implies an ISS relationship from σ to either X_e or $\bar{X}_e$ since A_c is Hurwitz. Thus, X_e and $e = H_0 X_e$ tends exponentially to zero as well as the state ζ of the differentiator, which is also driven by e. From (44), we conclude that all remaining signals are uniformly bounded. □

1.5 Application Example

The dynamic system used in this section is a *perturbed* version of a linearized model describing the vertical-plane motion used in [11]. The original system is perturbed with nonlinear terms $d(x,t)$ and $\phi(t)$ as in (1). This model for linear aircraft pitch-control loop will be made globally stable via the method proposed in the present chapter. In this sense, the terms in (1) are defined as follows:

$$A_p = \begin{bmatrix} -0.0121 & 0.0523 & -0.0001 & -31.9173 & -54.213 \\ -0.0722 & -0.7041 & 0.001 & -4.0242 & 433.03 \\ -0.12 & -0.9923 & 0 & 437.387 & 0 \\ 0 & 0 & 0 & 0 & 1 \\ 0.0062 & -0.0390 & 0 & -0.00001 & -0.596 \end{bmatrix},$$

$B_p = \begin{bmatrix} -2.062 & 46.2402 & 0 & 0 & 23.275 \end{bmatrix}^T$, $H_p = \begin{bmatrix} 0 & 0 & 0 & 1 & 0 \end{bmatrix}$. The system is perturbed by $d(x,t) = k_x x_3(t)\cos(x_1(t) + x_2(t))$ and $\phi(t) = \begin{bmatrix} 0 & 0 & 1 & 0 & 1 \end{bmatrix}^T (0.6\sin(3t) + 0.4\sin(0.8t))$. The states x_1, x_2 are the velocity components, x_3 is the altitude, $y = x_4$ is the pitch angle (the only available output of relative degree $\rho = 2$) and $x_5 = \dot{x}_4$.

The control goal is the tracking of $y_m = \frac{0.5}{(s+1)(s+0.5)}r$ with $r(t)$ being a bounded piecewise-continuous signal defined as $r = \sin(t)$ [rad] for $t \in [0, 12]$ [sec], $r = -0.4$ [rad] for $t \in (12, 20]$ [sec] and $r = 0$ [rad] for $t \in (20, 40]$ [sec]. The ideal sliding variable $\sigma = \dot{e} + l_0 e$, with $e = y - y_m$ and $l_0 = 7$, will be estimated using the robust global differentiator (33)
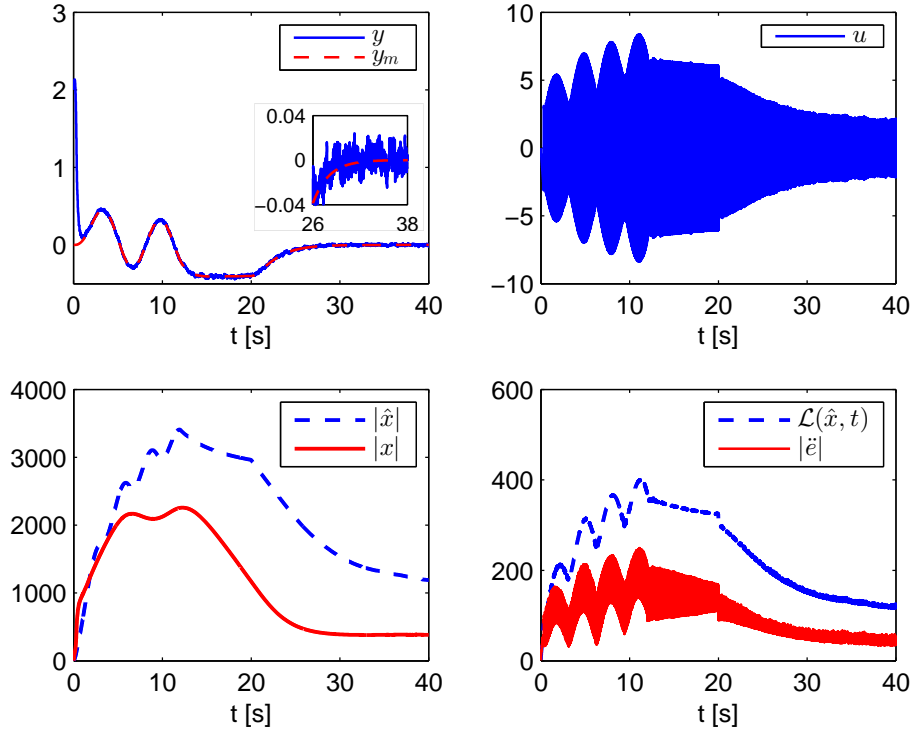
Figure 1 – Trajectory tracking (upper left), control signal (upper right), and estimated bounds (bottom).
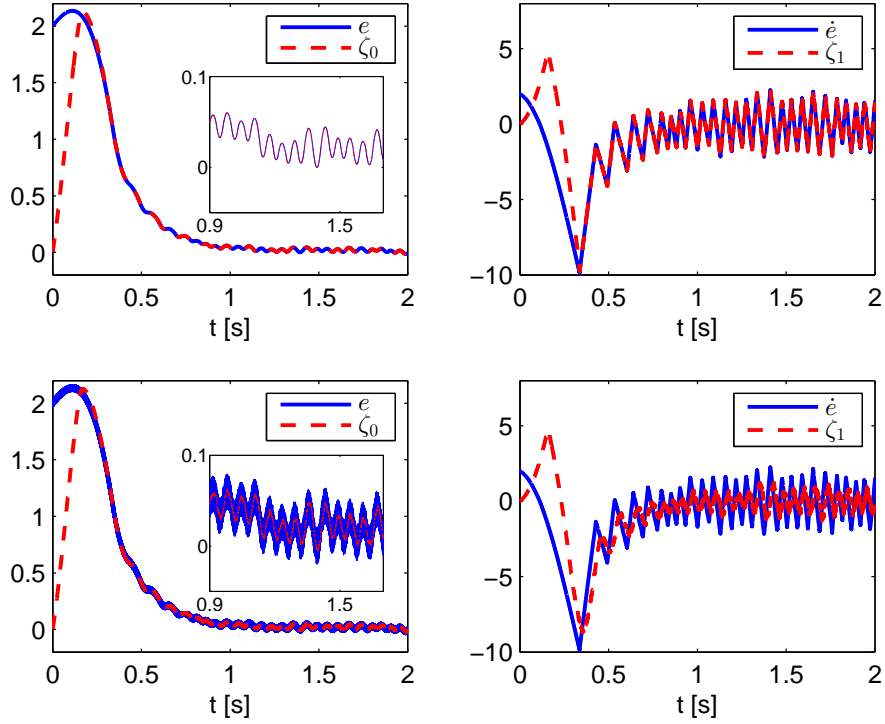
Figure 2 – Differentiator performance without noise (top) and with noise (bottom).

with $p = 1$, according to $\hat{\sigma}$ defined in (39). Such differentiator requires the upper bound for $\ddot{e}$. We have that $\ddot{y} = \dot{x}_5 = ax + K_p[u + d(x,t)] + H_p A_p \phi(t)$, where $a = H_p A_p^2 = [a_1, \ldots, a_5]$ is the fifth row of A_p and $K_p = H_p A_p B_p = 23.275$. Note that $|a_5| = \max |a_i|$ and $d(x,t) \leq k_x |x|$ ($k_x = 0.001$ for the simulations), then we may choose k_1 in Eq.(31) as $k_1 \geq 4|a_5| + |k_x|$, since $a_3 = 0$. However, by using the knowledge that the order of magnitude for the aircraft altitude variable is at least 100 times larger than the magnitude of the pitch angle derivatives, we propose the use of $k_1 \geq |a_1| + |a_2| + |a_4| + |a_5|/50 + k_x$ to obtain less conservative upper bounds when q is replaced by the full-state norm observer $\hat{x}$. Recalling that $|\ddot{y}_m| \leq k_m$ and $|H_p A_p \phi(t)| \leq 1$, one get the next missing parameters for Eq.(31): $k_2 \geq 2$ and $k_3 \geq 23.275$. Finally, one gets $\mathcal{L}(\hat{x}, t) = 0.1|\hat{x}| + 25\varrho(t) + 2$, which was used in our simulations. For the controller $u = -\varrho(t)\text{sgn}(\hat{\sigma})$ in (40), the modulation function (38) was applied as $\varrho(t) = 4|\omega| + \hat{d}_f(t) + 0.2$, with $\hat{d}_f(t) = \frac{1.6}{s+0.5}(0.001|\hat{x}|+6)$, $\bar{k}_\phi = k_d = 0$ in (23) and $|\hat{x}(t)| = \frac{1}{s+0.18}(180+720|\omega|)$ in (22). The regressor vector ω is constructed using the I/O filters given in (6) with $\Phi = \begin{bmatrix} 0 & I \\ -11 & -44.75 - 79.75 - 52.5 \end{bmatrix}$ and $\Gamma = \begin{bmatrix} 0 & 0 & 0 & 1 \end{bmatrix}^T$.

Figure 1 and Figure 2 depict the results obtained in the numerical tests with the same plant initial conditions used in [11], while the remaining initial values for the filters and the differentiator used to compute the control signal were set to zero. The measurement of the output y is contaminated by a zero-mean uniform noise with an amplitude of 0.02 [rad], the same level of noise used in [11]. As expected, after some finite time: **(a)** $|\hat{x}(t)| \geq |x(t)|$; **(b)** $\mathcal{L}(\hat{x}, t) \geq L(x, t) \geq |\ddot{e}(t)|$; **(c)** the global HOSM differentiator converges but the dynamic gain $\mathcal{L}(\hat{x}, t)$ is still large; **(d)** the controller with time-varying modulation function $\varrho(t)$ ensures the trajectory tracking; **(e)** the control signal $u(t)$ starts to converge with the state variables and the chattering intensity is reduced; **(f)** the bound $\mathcal{L}(\hat{x}, t)$ also decreases and the tracking precision grows, despite of the noisy scenario and the presence of nonlinear matched/unmatched perturbations.

In contrast to the design in [11], only I/O information is required to obtain the global controller. There, the other state variables were assumed to compute the time-varying gain of the differentiator applied to a continuous and *local* HOSM based controller. In our approach, the gains for the differentiator and controller are *globally* adapted so that chattering reduction is always allowed.

2 FIRST ORDER SLIDING MODE CONTROL WITH MONITORING FUNCTION

An algorithm for adaptation of the gains of higher-order sliding mode (HOSM) based exact differentiators is developed for the case where the upper bound for the ρth derivative of the tracking error signal exists but it is unknown. Unlikely other publications in the literature, the developed adaptive algorithm based on monitoring functions guarantees *global* and *exact* tracking when used in closed-loop output feedback. In the closed-loop scenario, a global-exact and finite-time estimate for the variables $\dot{e}(t), \ddot{e}(t), \dots, e^{(\rho-1)}(t)$ is applied to construct the sliding surface of the proposed sliding mode controller. The class of uncertain systems of arbitrary relative degree ($\rho \geq 1$) takes into account time-varying perturbations with unknown bounds and state-dependent nonlinearities satisfying a linear growth condition with any unknown rate. The norm of the unmeasured state is majorized by using a hybrid norm-state estimator. Numerical examples and an engineering application to wing rock control are presented in order to illustrate the properties and advantages of the novel adaptation approach for sliding mode control design.

2.1 Problem Statement

Consider the class of uncertain systems

$$\dot{x} = A_p x + B_p [u + d(x,t)], \qquad y = H_p x. \tag{46}$$

where $u \in \mathbb{R}$ is the input, $y \in \mathbb{R}$ is the measured output, $d(x,t) \in \mathbb{R}$ is a state dependent and time-varying nonlinear disturbance. The vector $x = [y \ \dot{y} \ \dots \ y^{(n-1)}]^T$ is the unmeasured state. The triple $(A_p, \ B_p, \ H_p)$ is in the Brunovsky's like-controller form [80]:

$$A_p = \begin{bmatrix} 0 & 1 & 0 & \dots & 0 \\ 0 & 0 & 1 & \dots & 0 \\ \vdots & \vdots & \vdots & \ddots & \vdots \\ 0 & 0 & 0 & \dots & 1 \\ 0 & 0 & 0 & \dots & 0 \end{bmatrix}, \qquad B_p = \begin{bmatrix} 0 \\ 0 \\ \vdots \\ 0 \\ K_p \end{bmatrix}, \qquad H_p = \begin{bmatrix} 1 & 0 & \dots & 0 & 0 \end{bmatrix}, \tag{47}$$

where the *high frequency gain* (HFG) $K_p \in \mathbb{R}$ as well as its sign, or also named control direction [29], are assumed to be **unknown** and the arbitrary relative degree is denoted by ρ. For the sake of simplicity, the zero dynamics [80] of the plant in (46) was dropped so that $\rho = n$.

We further assume that:

(A1) The uncertain input disturbance $d(x,t)$ is norm bounded by

$$|d(x,t)| \leq k_x|x| + k_d, \quad \forall x,t\,,$$

where $k_x, k_d \geq 0$ are **unknown** scalars.

Although this assumption restricts the class of disturbances to linear growing with respect to the unmeasured state, the problem remains quite challenging since unknown and arbitrary growth rate are considered. Simultaneously, global stability properties and perfect-exact tracking using output feedback are pursued.

We consider the following model for the reference signal $y_m(t) \in \mathbb{R}$:

$$y_m = W_m(s)\,r\,, \quad W_m(s) = (s + \gamma_m)^{-1} L_m^{-1}(s)\,, \quad \gamma_m > 0, \tag{48}$$

where $r(t) \in \mathbb{R}$ is an arbitrary uniformly bounded piecewise continuous reference signal and $L_m(s)$ is a Hurwitz polynomial defined as follows

$$L_m(s) = s^{(\rho-1)} + l_{\rho-2}s^{(\rho-2)} + \cdots + l_1 s + l_0. \tag{49}$$

The transfer function matrix $W_m(s)$ has the same relative degree ρ, as well as the plant, and its HFG is the unity.

The objective is to find u such that for arbitrary initial conditions, the output error

$$e(t) := y(t) - y_m(t) \tag{50}$$

tends to zero.

For $d \equiv 0$ and known plant, the ideal control signal $u^* = \theta^{*T}\omega$, with $\theta^* = \left[\theta_1^{*T}\; \theta_2^{*T}\; \theta_3^*\; \theta_4^*\right]^T$, $\theta_1^*, \theta_2^* \in \mathbb{R}^{(n-1)}, \theta_3^*, \theta_4^* \in \mathbb{R}$, achieves the matching between the closed-

loop transfer function matrix and $W_m(s)$, using the following regressor vector

$$\omega = [\omega_u^T \ \omega_y^T \ y \ r]^T, \tag{51}$$

with $w_u, w_y \in \mathbb{R}^{(n-1)}$ obtained from I/O state variable filters given by:

$$\dot{\omega}_u = \Phi\omega_u + \Gamma u, \qquad \dot{\omega}_y = \Phi\omega_y + \Gamma y, \tag{52}$$

where $\Phi \in \mathbb{R}^{(n-1)\times(n-1)}$ is Hurwitz and $\Gamma \in \mathbb{R}^{(n-1)}$ is chosen such that the pair $(\Phi, \ \Gamma)$ is controllable. The matching conditions require that $\theta_4^* = K_p^{-1}$. Define the augmented state vector

$$X = [x^T, \omega_u^T, \omega_y^T]^T, \tag{53}$$

with dynamics described by $\dot{X} = A_0 X + B_0 u + B_0' d$, $y = H_o X$. Then, by adding and subtracting $B_0 \theta^{*T} \omega$ and noting that there exist matrices Ω_1 and Ω_2 such that

$$\omega = \Omega_1 X + \Omega_2 r, \tag{54}$$

one has

$$\dot{X} = A_c X + B_c K_p [\theta_4^* r + u - u^*] + B_0' d, \quad y = H_o X, \tag{55}$$

where $A_c = A_0 + B_0 \theta^{*T} \Omega_1$, and $B_c = B_0 \theta_4^*$. We have that (A_c, B_c, H_o) is a nonminimal realization of $W_m(s)$. The reference model can be rewritten as

$$\dot{X}_m = A_c X_m + B_c K_p [\theta_4^* r - d_f] + B_0' d, \quad y_m = H_o X_m, \tag{56}$$

with the following filtered input disturbance

$$d_f = W_d(s) d, \tag{57}$$

where

$$W_d(s) = [W_m(s) K_p]^{-1} \bar{W}_d(s), \tag{58}$$

$$\bar{W}_d(s) = H_o (sI - A_c)^{-1} B_0'. \tag{59}$$

Therefore, $y_m = W_m(s)K_p\left[\theta_4^{*T}r - W_d(s)d\right] + \bar{W}_d(s)d$ and it is straightforward to conclude that $y_m = W_m(s)\,r$. Note that (58) is a stable and proper transfer function. In addition, $[W_m(s)K_p]^{-1} = \bar{K}_\rho s^\rho + \bar{K}_{\rho-1}s^{\rho-1} + \ldots + \bar{K}_0$, where $\bar{K}_i \in \mathbb{R}$, $i = 0, \ldots, \rho$ are constants. Thus, by defining the error state

$$X_e := X - X_m \tag{60}$$

the complete error dynamics can be obtained by subtracting (56) from (55), which leads to

$$\textbf{State Space:} \quad \dot{X}_e = A_c\, X_e + B_c K_p[u - \theta^{*T}\omega + d_f]\,, \tag{61}$$

$$e = H_o\, X_e,$$

$$\textbf{I/O Form:} \quad e = W_m(s)K_p\left[u - \theta^{*T}\omega + d_f\right]\,. \tag{62}$$

2.2 Switching Monitoring Function

In Section 2.5, it is described in details the proposed adaptive output-feedback SMC law which satisfies the control objectives. For the time being, we identify possible showstoppers in the design of an adequate control gain $\varrho(t)$ to dominate the unknown disturbance $d_f(x,t)$ in (61)–(62) and the appropriate sliding variable $\sigma(t)$ to guarantee the sliding mode existence for the disturbed system (46) with arbitrary relative degrees.

If $\text{sgn}(K_p)$ was *known*, the first-order SMC law could be defined by

$$u = -\text{sgn}(K_p)\varrho(t)\text{sgn}(\sigma)\,, \quad \sigma = L_m(s)e\,, \tag{63}$$

$L_m(s)$ is given in (49). According to (62), the control gain or *modulation function* $\varrho(t)$ is designed to overcome the ideal matching control $u^* := -\theta^{*T}\omega + d_f$, which is regarded as an input disturbance in (61). According to [84, Lemma 1], if we choose $\varrho(t)$ satisfying the inequality $\varrho(t) \geq |u^*(t)|$, one can conclude the σ-dynamics governed by

$$\dot{\sigma}(t) = -\gamma_m\sigma(t) + K_p[u + u^*(t)] + \pi(t)\,, \tag{64}$$

is at least exponentially stable, where $\pi(t)$ denotes a transient term due to initial conditions of the observable but not controllable subsystem of the nonminimal realization (A_c, B_c, H_o^T) of $W_m(s)$ in (61)–(62).

Since σ is the relative degree one output of the error system (61), it is possible to rewrite it into the *normal form* [80] such that the states of the error system are input-to-state stable (ISS) with respect to σ, for a particular exponential class-$\mathcal{KL}$ function. Thus, X_e and $e = H_o X_e$ tend exponentially to zero satisfying

$$|e(t)| \le e^{-\gamma_m(t-\bar{t}_0)}|e(\bar{t}_0)| + c_0 e^{-\lambda_0 t}, \quad \forall t \ge [\bar{t}_0, +\infty), \tag{65}$$

where $\bar{t}_0$ denotes some initial time, and $|\pi(t)| \le c_0 e^{-\lambda_0 t}$, for c_0 being an unknown positive constant depending on the initial conditions of the state variables and $\lambda_0 > 0$ being an unknown constant satisfying $0 < \lambda_0 < \min\{-\text{Re}(\lambda_i[A_c])\}$, with $\lambda_i[A_c]$ being the spectrum of A_c referred above [16, pp. 346].

The monitoring function is a hybrid operator which was first presented in [85]. The main idea is to construct a monitoring function to supervise the behavior of the tracking error and then, a switching scheme. As result, in closed-loop, after a finite number of switchings, the tracking error converges to zero at least exponentially [85]. Based on inequality (65), consider the auxiliary function φ_k defined as follows [29]:

$$\varphi_k(t) = e^{-\gamma_m(t-t_k)}|e(t_k)| + a(k)e^{-\frac{t}{a(k)+1}}, \tag{66}$$

$$t \in [t_k, \infty), \quad t_0 = 0, \quad k \in \mathbb{N},$$

where $a(k)$ is any positive monotonically increasing unbounded sequence.

The *monitoring function* φ_m can be defined as [29]:

$$\varphi_m(t) := \varphi_k(t), \quad \forall t \in [t_k, t_{k+1}) \ (\subset [0, +\infty)). \tag{67}$$

It is worth mention that the monitoring function (66) and (67) does not use the knowledge of the sign of K_p. Notice that equation (63) is presented previously just to guide us in the design of φ_m so that we can obtain a valid norm bound for the tracking error $e(t)$ when the control direction and $\varrho(t)$ are correct and, then, construct a monitoring signal which is always an upper bound for $e(t)$ and the latter eventually decreases with it.

Basically, the motivation behind the introduction of φ_m is that π in (64) is not available for measurement. Reminding that the inequality (65) holds if the inequality $\varrho(t) \ge |u^*|$ is satisfied, it seems natural to use the right-hand side of (65) as a benchmark

to detect if the sliding mode is being lost and the error is increasing so that k must be increased too. Since π is not available, one has (67) to invoke the switching of φ_m. Note that from (67), one always has $|e(t_k)| < \varphi_k(t_k)$ at $t = t_k$. Hence, the switching time t_k is well-defined (for $k \geq 0$):

$$t_{k+1} = \begin{cases} \min\{t > t_k : |e(t)| = \varphi_k(t)\}, & \text{if it exists}, \\ +\infty, & \text{otherwise}. \end{cases} \tag{68}$$

From this point of view, the monitoring function (66)–(67) is a hybrid operator [30], where the *jump variable* is the state of the monitoring function at the switching time t_k, the condition (68) defines the rule or *guard* of switching. The exponential behavior after the occurrence of a jump (that can be described by a differential equation) is referred to as *flow*. Figure 3 illustrates the tracking error norm $|e|$ and the monitoring function φ_m.
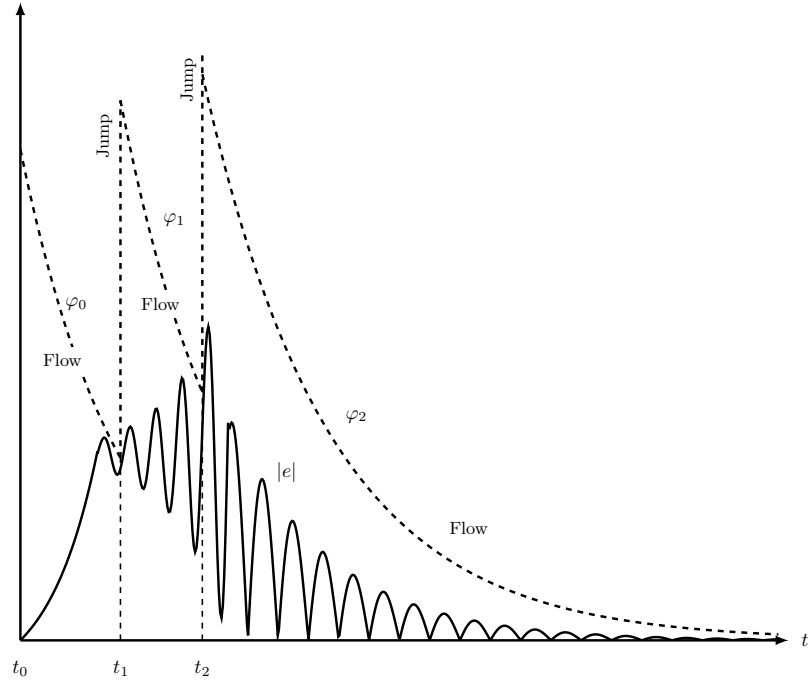
Figure 3 – The trajectories of φ_m (dashed line) and $|e(t)|$ (solid line). The monitoring function is a hybrid operator which jumps and flows.

Table 1 shows the pseudocode to get the main "global" switching variables k, t_k, $|e(t_k)|$ used in the computation of the monitoring function (66)–(67), being updated according to the switching rule (68). The control direction estimate (feedback sign) can

also be obtained simply by initializing such variable randomly with $+1$ or -1. After the switching process of the monitoring function φ_m stops the control direction is correctly estimated.

Table 1 – Pseudocode of the switching algorithm implemented on MATLAB (Mathworks, USA).

```
function [output] = switchingAlgorithm (input)

    global k % switching index
    global tk % switching time
    global moduloError % |e(tk)|
    global controlDirection % control direction

    error = input(1); % current value of error norm, |e(t)|
    phi = input(2); % current value of monitoring function, φm(t)
    time = input(3); % current value of time, t

    if (phi < error)
      tk = time;
      k = k+1;
      controlDirection = -controlDirection;
      moduloError =1*erro;
      output=[tk; k; controlDirection; moduloError];
    end

output=[tk; k; controlDirection; moduloError];
```

2.3 Hybrid State-Norm Observer

The importance of the calculations in Section 2.1 using the augmented state X, relies not only in deriving the full-error equation (61), but it yields also an output-feedback framework in which a norm bound for the unmeasured state can be obtained, as discussed in what follows. The main novelty is the introduction of a hybrid state-norm estimation scheme which flows through a continuous state space but also moves through different discrete switching modes, as defined in [30], according to the monitoring function introduced Section 2.2.

2.3.1 Known growth rate k_x and upper bound k_d

If k_x and k_d in assumption (A1) were assumed known as in previous publications [54, 55], by applying [8, Lemma 3] to (55), it would be possible to find $k_x^* > 0$ such that, for $k_x \in [0, k_x^*]$ a norm bound for X and x can be obtained through stable *first order approximation filters* (FOAFs). Thus, one could write

$$|x(t)|, |X(t)| \le |\hat{x}(t)| + \hat{\pi}(t), \tag{69}$$

$$\hat{x}(t) := \frac{1}{s + \lambda_x}[c_1 k_d + c_2|\omega(t)|], \tag{70}$$

where $c_1, c_2, \lambda_x > 0$ are appropriate constants that can be computed by the optimization methods described in [56]. In this sense, (69)–(70) state that the norm observer estimate $\hat{x}(t)$ provides a valid norm bound for the unmeasured state x of the uncertain and disturbed plant, *i.e.*, $|x| \le |\hat{x}|$ except for exponentially decaying terms due to the system initial conditions, denoted here by $\hat{\pi}(t)$.

Note that the parameter λ_x in (70) is defined by $\lambda_x := \gamma_0 - |B_0'|k_x$, where $|B_0'|k_x > 0$ is a constant smaller than γ_0 computed with B_0' given in (55), and $\gamma_0 > 0$ being the stability margin[1] of A_c in (55). Since the eigenvalues of A_c are the poles of the I/O filters (52) and the reference model (48), hence it is possible to consider an arbitrary scalar k_x by decreasing the time-constant of such filters. However, it would be necessary to know the exact value of k_x to choose the eigenvalues of Φ in (52) as well as γ_m and the roots of $L_m(s)$ in (48) to satisfy the condition $\lambda_x > 0$.

2.3.2 Unknown growth rate k_x and upper bound k_d

Now, we relax the restriction about the knowledge of the growth constant k_x and upper bound k_d by proposing a novel *hybrid state-norm observer* in the sense of [30]:

$$\dot{\hat{x}}(t) = -\underline{\lambda}_x(k)\hat{x}(t) + \bar{k}_\omega(k)[1 + |\omega(t)|], \tag{71}$$

where $\underline{\lambda}_x(k)$ is any positive monotonically decreasing sequence of the switching index k being lower bounded away from zero (*i.e.*, $\underline{\lambda}_x(+\infty) \ne 0$) and $\bar{k}_\omega(k)$ is a positive monotonically increasing unbounded sequence. By applying the *Comparison Theorem* [81] to

---

[1]Let $\{\lambda_i\}$ be the eigenvalues of A_c, the stability margin of A_c is defined by $\gamma_0 := \min_i[-\text{Re}(\lambda_i)]$.

(55) and (71), one obtain

$$|x(t)|, |X(t)| \leq |\hat{x}(t)| + \delta_0, \quad \forall t \geq T_0, \tag{72}$$

with $\delta_0 > 0$ being any arbitrary constant. Unlikely (69), inequality (72) guarantees a valid norm bound for the unmeasure state after some finite time $T_0 > 0$.

From (57), we can write $|d_f| \leq |W_d(s)d|$. Moreover, from (A1) and (70), one has $|d(x,t)| \leq k_x \hat{x}(t) + k_d$, *modulo* $\hat{\pi}$ term. Analogously to (72), at least one can write $|d_f| \leq \hat{d}_f + \hat{\pi}_f$, where $\hat{\pi}_f$ is an exponentially decaying term, and

$$\hat{d}_f(k,t) := \frac{c_f}{s + \lambda_f}[\bar{k}_x(k)\hat{x}(t) + \bar{k}_d(k)], \tag{73}$$

where $\frac{c_f}{s+\lambda_f}$ is a FOAF designed for $W_d(s)$, with adequate positive constants c_f and λ_f. At the price of some conservatism, we can simplify the FOAF design by choosing c_f sufficiently large and λ_f sufficiently small since the latter must satisfy $\lambda_f < \gamma_0$, where γ_0 is the known stability margin of A_c, and any uncertainty involving the computation of c_f could be encompassed in the switching terms $\bar{k}_x(k)$ and $\bar{k}_d(k)$. The unbounded increasing switching sequences $\bar{k}_x(k)$ and $\bar{k}_d(k)$ must (at least) ultimately satisfy $\bar{k}_x(k^*) > k_x$ and $\bar{k}_d(k^*) > k_d$, for some finite value $k^* < +\infty$, so that our hybrid system has an eventually continuous solution on the hybrid time domains [30] satisfying $|d_f(t)| \leq \hat{d}_f(k^*, t)$, after some finite time.

2.4 Global Adaptive HOSM Differentiator

The norm state estimation obtained with (69)–(70) was applied in [54] for the construction of a time-varying gain HOSM differentiator achieving exact differentiation of signals with any initial conditions. Here, we generalize the HOSM differentiator by adjusting adaptively the unknown gains of the differentiator through the hybrid norm-state estimation based on monitoring function introduced in Section 2.3.2.

From (46)–(47), assumption (A1) and using the augmented state X defined in (53), the following norm bound for $y^{(\rho)}$ is obtained

$$|y^{(\rho)}| \leq L(X,t) = k_1|X| + k_2 + k_3|u|, \tag{74}$$

where $k_1 \geq |K_p|k_x$, $k_2 \geq |K_p|k_d$ and $k_3 \geq |K_p|$ are **unknown** positive constants.

Now, from (74) and (50), we can write

$$|e^{(\rho)}(t)| \leq L(X, t) + |y_m^{(\rho)}(t)| . \tag{75}$$

The following upper bound involving the norm observer variable $\hat{x}(t)$, can be obtained using (69):

$$|e^{(\rho)}(t)| \leq L(\hat{x}, t) + |y_m^{(\rho)}(t)| , \tag{76}$$

$$= k_1|\hat{x}| + k_2 + k_3|u| + k_m, \tag{77}$$

modulo exponential decaying terms due to initial conditions which take into account the transient of the FOAF. The known positive constant k_m satisfies $|y_m^{(\rho)}(t)| \leq k_m$.

Our output-feedback generalization for SMC satisfies $|u| \leq \varrho(t)$, where $\varrho(t)$ is an absolutely continuous *modulation function* (to be defined later on) constructed with the signal $\hat{x}$ in (71)–(72). Thus, we can define the term

$$\mathcal{L}(\hat{x}, k, t) := \bar{k}_1(k)|\hat{x}| + \bar{k}_2(k) + \bar{k}_3(k)\varrho(t) + k_m , \tag{78}$$

with $\bar{k}_j(k)$, $\forall j = 1, 2, 3$, being monotonically increasing unbounded sequences of the switching index k such that $\bar{k}_1(k^*) > k_1$, $\bar{k}_2(k^*) > k_2$, $\bar{k}_3(k^*) > k_3$, for some finite value $k^* < +\infty$. Then, we can write the following norm bound

$$|e^{(\rho)}(t)| \leq \mathcal{L}(\hat{x}, k, t) , \quad \forall t \geq T , \tag{79}$$

for some finite time $T > 0$.

In light of (78)–(79), we can introduce the following HOSM based differentiator of

order $p = \rho - 1$ for the output error $e \in \mathbb{R}$:

$$\dot{\zeta}_0 = v_0 = -\lambda_0 \mathcal{L}(\hat{x}, k, t)^{\frac{1}{p+1}} |\zeta_0 - e(t)|^{\frac{p}{p+1}} \operatorname{sgn}(\zeta_0 - e(t)) + \zeta_1,$$

$$\vdots$$

$$\dot{\zeta}_i = v_i = -\lambda_i \mathcal{L}(\hat{x}, k, t)^{\frac{1}{p-i+1}} |\zeta_i - v_{i-1}|^{\frac{p-i}{p-i+1}} \operatorname{sgn}(\zeta_i - v_{i-1}) + \zeta_{i+1}, \qquad (80)$$

$$\vdots$$

$$\dot{\zeta}_p = -\lambda_p \mathcal{L}(\hat{x}, k, t) \operatorname{sgn}(\zeta_p - v_{p-1}).$$

Sufficient conditions for global finite-convergence of HOSM differentiators with variable gains were already given in [50]. Basically, the variable gain, denoted there by $L(t)$, may have an arbitrary growth so that $\dot{L}(t) \geq 0$ implies into faster convergence rates for the differentiator error. The faster is the growth of $L(t)$, the faster is the finite-time convergence of the differentiator error to zero. On the other hand, for the case $\dot{L}(t) < 0$, the differentiator gain $L(t)$ decreases, and at least local finite-time stability of the origin for arbitrary time-varying gains can be assured. If $|\dot{L}/L|$ is bounded, then the differentiator gain can grow in the worst case exponentially, and finite-escape time is not possible. The latter condition is the same introduced by [11], which results in locally convergence properties for homogeneous HOSM differentiators, but which is valid globally for non-homogeneous differentiators, as discussed in [28].

Since our differentiator gain $\mathcal{L}(\hat{x}, k, t)$ is constructed based on an upper bound $\hat{x}$ for the state vector $x(t)$ and the switching index k, hence $\mathcal{L}(\hat{x}, k, t)$ is always increasing when the plant state vector (and indirectly the differentiator error, which is driven by the tracking error $e(t)$) are not converging. Consequently, the differentiator errors are forced to ultimately achieve a compact set on which the local results for time-varying gains by [11] can be invoked when we use homogeneous HOSM differentiators such as (80). Thus, *global* convergence can be concluded. The convergence of the differentiator (80) is global since the upper estimation (79) holds independent of any initial condition of the closed-loop signals (the state trajectory must not be restricted a priori to any compact set $|e^{(\rho)}(t)| \leq D_R$, for some constant $D_R > 0$ sufficiently large).

The dynamic gain of our differentiator is the global upper bound $\mathcal{L}(\hat{x}, k, t)$ in (79) generated by continuous signals *almost everywhere* which can grow at most exponentially (there is no escape in finite time) due to the linear growth condition (A1). Thus, the logarithmic derivative $\dot{\mathcal{L}}/\mathcal{L}$ is bounded, except for a set of zero Lebesgue measure due to

the switching terms, and the following equalities

$$\zeta_0 = e(t)\,, \quad \zeta_i = e^{(i)}(t)\,, \quad i = 1\,,\ldots\,,\rho-1\,, \tag{81}$$

can be established in finite time according to [11, 28], provided the parameters λ_i are properly chosen. The boundedness of all closed-loop signals is presented in the proof of the main theorem.

Our main contribution is to show how to construct the differentiator gain for time-varying and state dependent terms in the signal $|e^{(\rho)}|$ using only input-output information in order to satisfy the conditions raised in [11, 50].

2.5 Output-Feedback Sliding Mode Control

The next step is to show in details the modulation function and sliding variable designs of the proposed first order output-feedback SMC law such that the adaptive HOSM differentiator above can be indeed constructed and applied. Then, the proof of convergence for the tracking error $e(t)$ with our output-feedback controller based on the estimate state of the HOSM differentiator is straightforward once the convergence of the differentiator (80) is already guaranteed and the separation principle is always fulfilled [11].

The proposed output-feedback SMC law can be written as

$$u = (-1)^{k+m}\varrho(t)\text{sgn}(\hat{\sigma})\,, \tag{82}$$

where $k \in \{0, 1, \ldots\}$ is the switching index generated by the monitoring function switching and $m \in \{0\,, 1\}$. Hence, depending on the choice of m (0 or 1), we can set the initial value for the estimate of the unknown control direction $(-1)^{k+m}$. The computation of $\varrho(t)$ and $\hat{\sigma}$ is presented in the next section.

The monitoring function (66) and (67) help us in detecting when a switching of the control gain $\varrho(t)$ as well as in the control direction is necessary. Inappropriate $\varrho(t)$ and the wrong control direction can cause a switching, and every time one of these two are violated, the monitoring function acts by increasing the switching index k in (82), so that our control objectives can be ultimately achieved.

2.5.1 Modulation function or control gain

As discussed at the beginning of Section 2.2, the modulation function or control gain $\varrho(t) \geq 0$ must dominate the equivalent input disturbance $u^*(t) := -\theta^{*^T}\omega(t) + d_f(t)$ in (61) so that:

$$\varrho(t) \geq |-\theta^{*^T}\omega(t) + d_f(t)| + \delta\,, \quad \delta > 0\,, \tag{83}$$

where the constant δ can be arbitrarily small. Regarding A_p, B_p and H_p in (46), since more precisely K_p in (47) belongs to some unknown compact set, an unknown upper bound $\Theta \geq |\theta^*|$ can be written, with θ^* being the ideal parameter vector for matching control given before equation (51). Thus, a possible choice for the modulation function to satisfy (83), at least after some finite time, is given by

$$\varrho(t) = \bar{\theta}(k)|\omega(t)| + \hat{d}_f(k,t) + \delta\,, \tag{84}$$

with $\hat{d}_f(k,t)$ defined in (73) and $\bar{\theta}(k)$ being any monotonically increasing unbounded sequence of the switching index k such that $\bar{\theta}(k^*) > \Theta$, for some finite value $k^* < +\infty$.

Of course, there is not an unique choice for $\varrho(t)$ due to the countless possibilities for the monotonically increasing sequences $\bar{\theta}(k)$. Basically, every modulation function $\varrho(t)$ which ultimately satisfies (83) serves as an appropriate selection. If more aggressive sequences in terms of growth with the switching index k are employed, less switchings may occur. However, the price to be paid is the obtainment of more conservative modulation functions $\varrho(t)$ in terms of larger control amplitudes. Thus, there is a trade-off between the choice of the switching sequences and its impact in the control signal.

The following condition

$$\varrho(t) \leq \kappa_a ||X_t|| + \kappa_b\,, \quad \kappa_a > 0\,, \quad \kappa_b > 0\,, \tag{85}$$

must be satisfied by $\varrho(t)$ to avoid finite-time scape in the closed-loop signals used to compute the variable gain (78) so that (81) can be verified for the adaptive differentiator (80). To show the modulation function $\varrho(t)$ in (84) indeed satisfies inequality (85), we just have to write $|\omega| \leq \kappa_c|X| + \kappa_d$ from (54), with $\kappa_c\,, \kappa_d > 0$ and considering that $r(t)$ is an uniformly bounded reference signal. Then, from the ISS relation of the filtered signals in (71) and (73) with respect to ω, we conclude the norm bounds $|\hat{d}_f| \leq \kappa_e||X_t|| + \kappa_f$

and $|\hat{x}| \leq \kappa_g ||X_t|| + \kappa_h$, for appropriate constants $\kappa_e, \kappa_f, \kappa_g, \kappa_h > 0$. Now, from (84), we conclude (85).

2.5.2 Sliding variable

The main idea of the sliding surface design is to obtain the relative degree one sliding variable such that, when the motion is restricted to the manifold $\sigma = 0$, the reduced-order model has the required performance.

For higher relative degree plants, one could use simply the operator $L_m(s)$ defined in (49), to overcome the relative degree obstacle. The operator $L_m(s)$ is such that $L_m(s)G(s)$ and $L_m(s)W_m(s)$ have relative degree one. The ideal sliding variable $\sigma = L_m(s)e \in \mathbb{R}$ is given by

$$\sigma = e^{(\rho-1)} + \cdots + l_1 \dot{e} + l_0 e. \tag{86}$$

More general (nonlinear) combinations of the variables $e^{(\rho-1)}, \ldots, \dot{e}$ and e, rather than the simple linear combination given in (86) could be envisaged. As an advantage, finite-time convergence for the tracking error $e(t)$ would be guaranteed instead of exponential convergence only.

Anyway, σ is not directly available to implement the control law. Thus, reminding (81) and using the proposed adaptive HOSM differentiator, the following estimate for σ can be obtained to replace (86):

$$\hat{\sigma} = \zeta_{\rho-1} + \cdots + l_1 \zeta_1 + l_0 \zeta_0. \tag{87}$$

Table 2 presents the complete equations for the proposed control scheme.

Table 2 – Complete equations for the control system.

Plant	$\dot{x} = A_p x + B_p[u + d(x,t)]$ $y = H_p x$
Model Reference	$y_m = W_m(s)r$ $W_m(s) = (s + \gamma_m)^{-1} L_m^{-1}(s), \ \gamma_m > 0$ $L_m(s) = s^{(\rho-1)} + l_{\rho-2} s^{(\rho-2)} + \cdots + l_1 s + l_0$
Error	$e = y - y_m$
Regressor Vector	$\omega = [\omega_u^T \ \omega_y^T \ y \ r]^T$ $\dot{\omega}_u = \Phi \omega_u + \Gamma u$ $\dot{\omega}_y = \Phi \omega_y + \Gamma y$
Switching Monitoring Function	$\varphi_m(t) := \varphi_m(t) = \mathrm{e}^{-\gamma_m(t-t_k)}|e(t_k)| + a(k)\mathrm{e}^{-\frac{t}{a(k)+1}}$ $\forall t \in [t_k, t_{k+1}) \ (\subset [0, +\infty)), \ k \in \mathbb{N}$ $t_{k+1} = \begin{cases} \min\{t > t_k : |e(t)| = \varphi_k(t)\}, & \text{if it exists,} \\ +\infty, & \text{otherwise.} \end{cases}$
Hybrid State-Norm Observer	$\dot{\hat{x}}(t) = -\underline{\lambda}_x(k)\hat{x}(t) + \bar{k}_\omega(k)[1 + |\omega(t)|]$ $\hat{d}_f(k,t) := \frac{c_f}{s+\lambda_f}[\bar{k}_x(k)\hat{x}(t) + \bar{k}_d(k)]$
Adaptive Differentiator Gain	$\mathcal{L}(\hat{x}, k, t) := \bar{k}_1(k)|\hat{x}| + \bar{k}_2(k) + \bar{k}_3(k)\varrho(t) + k_m$
Global Differentiator	$\dot{\zeta}_0 = v_0 = -\lambda_0 \mathcal{L}(\hat{x}, k, t)^{\frac{1}{p+1}} |\zeta_0 - e|^{\frac{p}{p+1}} \mathrm{sgn}(\zeta_0 - e) + \zeta_1,$ $\vdots$ $\dot{\zeta}_i = v_i = -\lambda_i \mathcal{L}(\hat{x}, k, t)^{\frac{1}{p-i+1}} |\zeta_0 - e|^{\frac{p-i}{p-i+1}} \mathrm{sgn}(\zeta_i - v_{i-1}) + \zeta_{i+1},$ $\vdots$ $\dot{\zeta}_p = -\lambda_p \mathcal{L}(\hat{x}, k, t) \mathrm{sgn}(\zeta_p - v_{p-1}).$
Sliding Variable	$\hat{\sigma} = \zeta_{\rho-1} + \cdots + l_1 \zeta_1 + l_0 \zeta_0$
Modulation Function	$\varrho(t) = \bar{\theta}(k)|\omega(t)| + \hat{d}_f(k,t) + \delta, \ \delta > 0$
Output-Feedback SMC Law	$u = (-1)^{k+m} \varrho(t) \mathrm{sgn}(\hat{\sigma})$

2.6 Stability Analysis

The stability results are summarized in the next theorem.

Theorem 2. *Consider the system (46) under assumption (A1) and the reference model in*

(48). The output-feedback SMC is given by (82), with modulation function ϱ in (84), $\hat{\sigma}$ in (87) constructed with the state $\zeta = [\zeta_0 \ldots \zeta_{\rho-1}]^T$ of the adaptive HOSM differentiator (80) with the variable gain $\mathcal{L}(\hat{x}, k, t)$ selected as (78) and $\hat{x}$ provided by the hybrid norm observer (71). Then, for any initial condition, the monitoring switching stops and the sliding surface $\hat{\sigma} = 0$ will be reached. Moreover, the closed-loop error system with dynamics (61) is globally exponentially stable in the sense that $X_e(t)$ and the output tracking error $e(t)$ converge exponentially to zero whereas all the remaining closed-loop signals are uniformly bounded.

Proof 2. *In what follows, $k_i > 0$ are constants not depending on the initial conditions. Let us assume a maximal time interval of definition for the existence of solution given by $[0, t_M)$, where t_M may be finite or infinite. The proof is divided into three steps.*

STEP 1: *In the first one, we need to show that the monitoring function switching stops. By contradiction, suppose that k switches without stopping $\forall t$. Then, $a(k)$ in (66); $\bar{k}_\omega(k)$ in (71); $\bar{k}_x(k)$ and $\bar{k}_d(k)$ in (73); $\bar{k}_1(k)$, $\bar{k}_2(k)$, $\bar{k}_3(k)$ in (78); $\bar{\theta}(k)$ in (84) increases unboundedly AND the term $\underline{\lambda}_x(k)$ in (71) decreases, as $k \to +\infty$. Thus, there is a finite value k^* such that: (a) the term $a(k^*)e^{-\frac{t}{a(k^*)+1}}$ will upper bound $c_0 e^{-\lambda_0 t}$ in (65); (b) the hybrid state-norm observer (71) satisfies $\hat{x} > |X|$; (c) consequently, the updated gain $\mathcal{L}(\hat{x}, k^*, t) > |e^{(\rho)}(t)|$ by verifying the condition (79); (d) the terms $\bar{\theta}(k^*)$ and $\hat{d}_f(k^*, t)$ in (84) are sufficiently large so that the modulation function $\varrho(t)$ satisfies (83) and (85); and (e) the control direction estimate in (82) verifies the following sign relation $sgn[(-1)^{k^*+m}] = -sgn[K_p]$.*

From (b), $\varphi_m(t) > RHS\{(65)\}$, $\forall t \in [t_{k^*}, t_{k^*+1})$, where $RHS\{\cdot\}$ denotes the right-hand side of some inequality. From (d) and (e), we can conclude $RHS\{(65)\}$ is a valid upper bound for $|e|$. Hence, no switching will occur after $t = t_{k^*}$, i.e., $t_{k^*+1} = t_M$, which leads to a contradiction. Therefore, φ_m has to stop switching after some finite time $k = N$ and $t_N \in [0, t_M)$.

STEP 2: *In the second step, it is shown that the closed-loop system signals cannot escape in finite time. By using the relations (54) and (60), one has that $X = X_e + X_m$ and the regressor vector*

$$\omega = \Omega_1 X_e + \Omega_1 X_m + \Omega_2 r. \tag{88}$$

Let $x_m := [y_m \ \dot{y}_m \ \ldots \ y_m^{(\rho-1)}]^T$ and $x_e := x - x_m$. From (61), it can be shown that $e^{(i)} = H_0 A^i X_e$, for $i = 0, \ldots, \rho-1$, hence $|x_e| \leq k_0 |X_e|$. Therefore, since x_m is uniformly bounded, then $x = x_e + x_m$ can be affinely norm bounded in $|X_e|$. Thus, one can conclude that $|x| \leq k_1 |X_e| + k_2$, and consequently, $|x| \leq k_3 \|(X_e)_t\| + k_4$. Due to assumption (A1) concerning the linear growth condition of the nonlinear disturbances with respect to the unmeasured state x, from (56) and (57), one has

$$|X_m| \leq k_5 \|(X_e)_t\| + k_6. \tag{89}$$

Finally, from (54), (88) and (89), we conclude ω, the term d_f in (61), and consequently the control input u with modulation function ϱ in (84), for $k = N$ (finite and fixed), are all affinely norm bounded by X or X_e, i.e.,

$$|u|, |d_f|, |\omega| \ \leq \ k_a \|X_t\| + k_b, \tag{90}$$

$$|u|, |d_f|, |\omega| \ \leq \ k_c \|(X_e)_t\| + k_d. \tag{91}$$

Thus, the system signals will be regular and, therefore, can grow at most exponentially [57], i.e., $t_M = +\infty$ by continuation of solutions [80].

STEP 3: This fact leads us to the third step of the proof. There exist two finite-time instants $T_1 > 0$ and $T_2 > 0$ such that (79) and (83) are satisfied, $\forall t > \max\{T_1, T_2\}$. Then, the ideal sliding variable is exactly estimated, i.e., $\hat{\sigma} \equiv \sigma$ and the relative degree compensation is perfectly achieved. Moreover, from [84, Lemma 1], the ideal sliding mode $\hat{\sigma}(t) \equiv \sigma(t) \equiv 0$ is achieved in finite time. Even if the monitoring function switching stops at a incorrect sign of the control direction and/or $\varrho(t) < |u^*|$ in (83), an exponentially convergent upper bound for $\sigma(t)$ is still obtained from (66)–(67) and (86) since $e(t) \to 0$ and $L_m(s)$ is a Hurwitz polynomial. Therefore, if the index k becomes constant in the monitoring function $\varphi_m(t)$ for all consecutive time interval, we can continue concluding that $\sigma(t)$ tends to zero at least exponentially.

As mentioned in Section 2.2, since σ in (86) is the relative degree one output for (61), it is possible to rewrite it into the normal form [80] such that the states of the error system are exponentially ISS with respect to σ. It can be shown reminding that

$L_m(s)W_m(s) = 1/(s + \gamma_m)$. *From (61) and*

$$\sigma = L_m(s)W_m(s)K_p \left[u - \theta^{*^T}\omega + d_f \right]$$
$$= \frac{K_p}{s + \gamma_m} \left[u - \theta^{*^T}\omega + d_f \right],$$

one gets $\dot{X}_e = A_c X_e + B_c(\dot{\sigma} + \gamma_m\sigma)$. Further, using the transformation $X_e := \bar{X}_e + B_c\sigma$, one has

$$\dot{\bar{X}}_e = A_c \bar{X}_e + (A_c B_c + \gamma_m B_c)\sigma, \tag{92}$$

which clearly implies an ISS relationship from σ to either X_e or $\bar{X}_e$ since A_c is Hurwitz. Thus, X_e and $e = H_0 X_e$ tends exponentially to zero as well as the state ζ of the differentiator, which is also driven by e. From (91), we conclude that all remaining signals are uniformly bounded. This completes the demonstration of the theorem. □

In fact, according to the results of Theorem 2, the monitoring function switching may stop at an *incorrect sign* of the control direction and/or $\varrho(t) < |u^*|$. However, two measures can be taken to force the monitoring function switching always stops at a *correct sign* of the control direction and satisfying $\varrho(t) \geq |u^*|$:

(i) the definition of a new upper bound Θ for the parameter vector θ used in (83)–(84) such that $\Theta \geq \max\{|\theta^*|, |\theta^\dagger|\}$, where $\theta^\dagger$ is the model matching vector with respect to an *unstable* reference model $M^\dagger(s) = \frac{1}{L_m(s)(s-a_m)}$, with $L_m(s)$ as in (49) and $a_m > 0$, so that equation (62) can be rewritten as $e = M^\dagger(s)K_p[u - u^\dagger]$, with $u^\dagger = \theta^{\dagger^T}\omega + d_f$;

(ii) the inclusion of a destabilizing term $u_d(t)$ in the control law (82) such that the equilibrium $e = 0$ is non attractive at least for some arbitrarily small neighborhood of it when the control direction is wrong and simultaneously $\varrho(t) < |u^\dagger|$. One possible choice would be $u = (-1)^{k+m}[\varrho(t) + u_d(t)]\text{sgn}(\hat{\sigma})$, where

$$u_d(t) = \begin{cases} k_\sigma |\hat{\sigma}(t)|^{-\frac{1}{2}}, & |\hat{\sigma}| > \varepsilon, \\ 0, & |\hat{\sigma}| \leq \varepsilon, \end{cases} \tag{93}$$

for constants $k_\sigma > 0$ and $0 < \varepsilon < 1$. Notice that the dead-zone operator is employed to avoid an unbounded control signal when $\hat{\sigma} = 0$, being uniformly bounded for all $\hat{\sigma}$

and such that the *regular* growth conditions in (90) and (91) are preserved. Then, the following corollary can be enunciated.

Thus, for ε sufficiently small, the switching process stops at $t = t_k = t_N$ with the sign of K_p correctly estimated and $\varrho(t) \geq |u^*|$ being always verified when the term $u_d(t)$ is added to the original modulation function (84) in the control law (82).

Corollary 1. *In addition to the results of Theorem 2, if we replace the control law (82) by*

$$u = (-1)^{k+m}[\varrho(t) + u_d(t)]\mathrm{sgn}(\hat{\sigma}) , \qquad (94)$$

with $u_d(t)$ defined as in (93) and $\varepsilon \in (0,1)$ sufficiently small, then, we can conclude that the switching process stops at $t = t_k = t_N < +\infty$ with the sign of K_p correctly estimated and $\varrho(t) \geq \max\{|u^*|, |u^\dagger|\}$. Consequently, the ideal sliding mode $\hat{\sigma} = \sigma = 0$ is always achieved in finite time.

Proof 1. *Since we have supposed that the monitoring function switching stopped with $k = N$ where $N < +\infty$, the tracking error $e(t)$ as well as the error state $X_e(t)$ and the augmented state X enter to a compact set where the exact differentiator will provide the exact estimate of the ideal sliding variable σ, i.e. $\hat{\sigma} = \sigma$. Now, suppose that we end up with an incorrect control direction estimate AND $\varrho(t) < |u^\dagger|$. Then, for all $|\hat{\sigma}| > \varepsilon$, the dynamic equation for σ can be written as $\dot{\sigma} = a_m\sigma + |K_p|[\varrho\,\mathrm{sgn}(\sigma) + k_\sigma|\sigma|^{-\frac{1}{2}}\,\mathrm{sgn}(\sigma) - u^\dagger] + \pi$, where π is an exponentially decaying term due to initial conditions. Consequently, the product $\sigma\dot{\sigma}$ is computed by*

$$\sigma\dot{\sigma} = a_m\sigma^2 + |K_p|[\varrho|\sigma| + k_\sigma|\sigma|^{\frac{1}{2}} - u^\dagger\sigma] + \pi\sigma , \quad |\sigma| > \varepsilon .$$

From the modulation function ϱ in (84) and the relationships for the regressor vector ω in (54) and (88), it is possible to state the difference $|\varrho - u^\dagger| \leq R$, for some constant $R > 0$, since $e(t)$ and $X_e(t)$ are converging to zero as $t \to +\infty$. So, there exists $t_d < +\infty$ such that $|\pi(t)| < \delta$ and, for ε sufficiently small, the term between brackets in $\sigma\dot{\sigma}$–equation becomes positive since the square-root function dominates the linear one in the neighborhood of the origin. Consequently, $\sigma\dot{\sigma} > 0$, $\forall t \geq t_d$. Hence, σ would diverge as $t \to \infty$ for all initial conditions if the control direction is incorrectly estimated, i.e., $\sigma(t)$ would not achieve the residual set where $|\sigma| \leq \varepsilon$, for ε sufficiently small. Since the error system with

state X_e is ISS with respect to σ, the tracking error $e := H_0 X_e$ must diverge as well. It generates a contradiction since $e(t)$ should converge to zero as $\varphi_m(t)$ converges when the switching process stops.

The same proof by contradiction/absurd can be derived considering that the control direction was correctly estimated BUT we still have $\varrho(t) < |u^*|$, where $u^* = \theta^{*^T}\omega + d_f$ as in (62). In this case, θ^* is the model matching vector with respect to the stable reference model $W_m(s) = \frac{1}{L_m(s)(s+\gamma_m)}$ in (48). Following the analogous steps performed before, we can write the dynamic equation $\dot{\sigma} = -\gamma_m\sigma - |K_p|[\varrho\,\text{sgn}(\sigma) + u_d(t)\,\text{sgn}(\sigma) - u^*] + \pi$. Since the monitoring function converges to zero when k is kept fix, we can conclude that $e(t)$ and $\sigma(t)$ tend exponentially to zero, according to (86). Thus, for t sufficiently large, we can guarantee the set $|\sigma| \leq \varepsilon$ is ultimately reached. Since $u_d(t) = 0$ for $|\sigma| \leq \varepsilon$, we can write:

$$\sigma\dot{\sigma} = -\gamma_m\sigma^2 - |K_p|[\varrho|\sigma| - u^*\sigma] + \pi\sigma\,, \quad |\sigma| \leq \varepsilon\,.$$

Finally, for $|\sigma| \leq \varepsilon < 1$ and ε sufficiently small, there exists $t_d < +\infty$ such that the linear term $u^*(t)\sigma(t)$ will dominate the remaining elements in the right-hand side of $\sigma\dot{\sigma}$ since $|u^*| > \varrho(t)$ by assumption. Again, we can conclude $\sigma\dot{\sigma} > 0$, $\forall t \geq t_d$.

Thus, for ε sufficiently small, the switching process stops at $t = t_k = t_N$ with the sign of K_p correctly estimated and $\varrho(t) \geq \max\{|u^*|, |u^\dagger|\}$ being always verified when the term $u_d(t)$ is added to the original modulation function (84) in the control law (82).

Remark 3 (*Tracking Control $\times$ Pure Differentiaton Problem*). *In the results of Theorem 2, we are interested in the global exact differentiation applied to tracking problem by means of output feedback, rather than pure differentiation simply. Reminding that ρ is the relative degree of the plant, the differentiator gain $\mathcal{L}(\hat{x}, k, t)$ must be an upper bound for the ρth derivative of the output error $e(t)$. Consequently, the implementation of $\mathcal{L}(\hat{x}, k, t)$ demands to dominate unknown terms with unknown bounds, which are time-varying and can grow with the unmeasured state variables as well. On the other hand, the pure differentiation of any exogenous signal $f(t)$ is a particular scenario, where the differentiator gain can be exclusively designed as a class $\mathcal{K}$ function of the switching index k in order to majorize the higher derivatives of $f(t)$, which are assumed uniformly bounded by unk-*

nown constants. As discussed in the introductory section, the latter problem has already been handled by [13]. The differentiation of signals with unbounded higher derivatives was introduced in [11] and, more recently, in [50]. However, in both publications, a known time-varying upper bound for the higher derivatives of $f(t)$ are assumed known to be applied as the differentiator gain.

2.7 Simulation Example

Consider the following perturbed linear system in normal form (46)–(47) with relative degree two:

$$\dot{x}_1 = x_2$$
$$\dot{x}_2 = -1.5x_2 + x_1 + 15\left[x_1^{2/3}x_2^{1/3} + 1\right]\sin(t) + u$$
$$y = x_1$$

where the state vector is $x = [x_1\ x_2]^T$. From (46), the nonlinear disturbance can be written as

$$d(x,t) = -1.5x_2 + x_1 + 15\left[x_1^{2/3}x_2^{1/3} + 1\right]\sin(t),$$

which satisfies (A1) for $k_x = 17.5$ and $k_d = 15$. The control aim is the trajectory tracking of $y_m = \frac{0.5}{(s+0.5)(s+1)}r$, with

$$r(t) = \begin{cases} 2.5\sin(3t), & t < 20, \\ 0, & t \geq 20. \end{cases} \tag{95}$$

The ideal sliding variable is chosen as $\sigma = \dot{e} + e$, which is estimated by $\hat{\sigma} = \zeta_1 + e$ using a first order robust differentiator (80) with $\rho = 2$.

The parameters of the adaptive modulation function $\varrho(t)$ in (84) are $\bar{\theta}(k) = k$, the small constant $\delta = 0.001$, and $\hat{d}_f(k,t)$ defined as in (73), with $c_f = 1$, $\lambda_f = 0.4$, $\bar{k}_x(k) = \bar{k}_d(k) = k$.

The following I/O filters (52) were used $\omega_u = \frac{1}{s+4}u$, $\omega_y = \frac{1}{s+4}y$. For the norm observer (71), the parameters are based on the positive monotonically sequences of the switching index k, such that: $\lambda_x(k) = 0.1 + \frac{4}{1+k}$ and $\bar{k}_\omega = k$.

The initial conditions of the plant and the differentiator were chosen as $x_1(0) =$

$3 \, , x_2(0) = -1 \, , \zeta_0(0) = 1 \, , \zeta_1(0) = 2$. Since $e = x_1 - y_m$, the variable gain $\mathcal{L}(\hat{x}, k, t)$ of the differentiator is computed as (78), where $\bar{k}_1(k) = \bar{k}_2(k) = \bar{k}_3(k) = k + 1$ and k_m must be an upper bound for $|\ddot{y}_m(t)| = |-1.5\dot{y}_m - 0.5y_m + 0.5r|$. The signals $y_m \, , \dot{y}_m$ can be directly implemented from the state-space representation of the reference model. The Euler integration method with fixed integration step of 10^{-5} s was used for the simulations.

The results obtained for the proposed SMC are shown in Figure 4(a) to Figure 4(f). In Figure 4(c), it can be seen how the norm observer state $\hat{x}$ overcomes after a finite time the actual value of the x-norm. Figure 4(b) shows the adaptive gain $\mathcal{L}(\hat{x}, k, t)$ applied to upper bound $|\ddot{e}(t)|$ used in the differentiator (80). Using the control signal of Figure 4(d), the exact tracking is achieved as shown in Figure 4(a), despite the disturbances and uncertainties. In Figure 4(e), the behavior of the error signal norm and the monitoring function are presented. As expected, every time instant (t_k) the monitoring function meets the tracking error, a jump is observed followed by an exponential decreasing profile.

(a) Exact tracking: output signals $y(t)$ and $y_m(t)$.

(b) Variable gain $\mathcal{L}(\hat{x}, k, t)$ (norm bound for $\ddot{e}(t)$) of the variable gain HOSM differentiator.

(c) Norm observer performance.

(d) Control signal $u(t)$.

(e) Monitoring function $\varphi_m(t)$ and output error norm $|e(t)|$.

(f) Estimate of $\dot{e}(t)$ given by the proposed global hybrid adaptive HOSM differentiator.

Figure 4 – Simulation results.
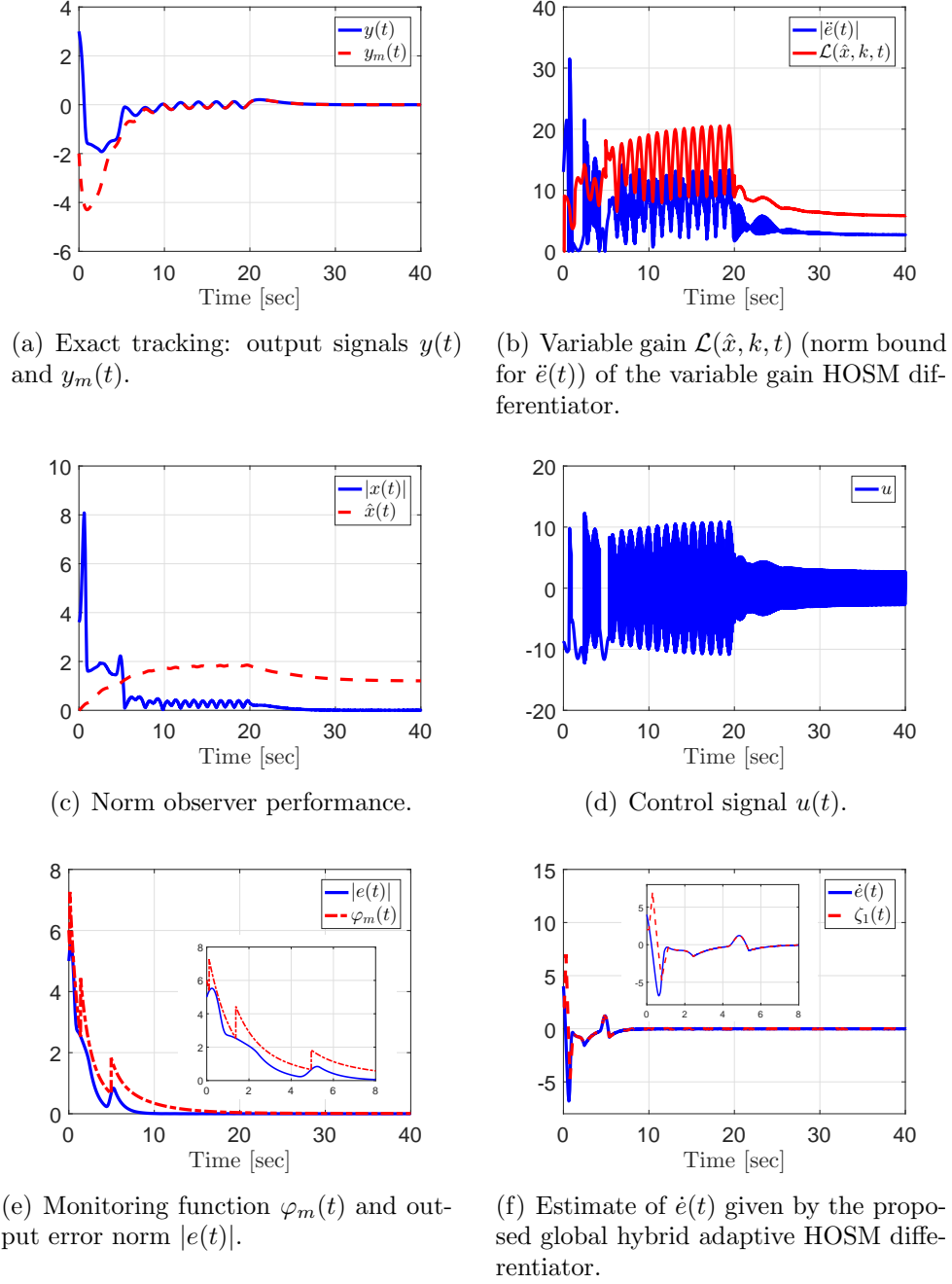
2.8 Application to Wing Rock Control

Wing rock is an undamped nonlinear oscillation phenomenon primarily in the roll axis that is exhibited by many combat aircraft at high angles of attack. Wing rock occurs due to asymmetric vortex shedding and vortex bursting and causes maneuver limitations ranging in severity from degradation in tracking effectiveness to loss of control [86]. The

oscillation is featured by a limit cycle which has a strong relationship to flow conditions, attack angle, and to aircraft setup.

In this application, according to [86, 87], the following model for a fighter aircraft with 80° swept back wing is employed:

$$\dot{x}_1 = x_2 \,, \tag{96}$$

$$\dot{x}_2 = d(x, t) + u \,, \tag{97}$$

$$d(x, t) = -\bar{\omega}^2 x_1 + \mu_1 x_2 + b_1 x_1^3 + \mu_2 x_1^2 x_2 + b_2 x_1 x_2^2 \,, \tag{98}$$

$$y = x_1 \,, \tag{99}$$

where $x = [x_1 \ x_2]^T$ is the state vector with roll angle x_1 and roll rate x_2, y is the output signal and u the control input. The parameter $\bar{\omega}$ is the wing rock limit cycle frequency, b_1, b_2, μ_1 and μ_2 are other system parameters, whose values dependent on the attack angle α and are shown in Table 3.

Table 3 – Variation of wing rock model parameters with angle of attack α.

α	$\bar{\omega}$	μ_1	b_1	μ_2	b_2
15.0^o	0.0603	-0.0085	-0.0502	0.3531	-0.2955
21.5^o	0.1220	0.0042	0.0167	-0.0658	0.0858
22.5^o	0.1287	0.0060	0.0201	-0.0803	0.2091
25.0^o	0.1419	0.0105	0.0260	-0.1273	0.5197

As a consequence of the limit cycle phenomenon, the amplitude of periodic oscillation is independent of initial conditions and the state x is bounded by an *unknown* scalar $\chi > 0$, *i.e.*, $|x(t)| < \chi$. This fact leads us to conclude that the input disturbance $d(x, t)$ can be affinely norm bounded by, $\forall |x(t)| < \chi$:

$$
\begin{aligned}
|d(x, t)| &\leq \bar{\omega}^2 |x_1| + |\mu_1||x_2| + |b_1||x_1|^3 + |\mu_2||x_1|^2|x_2| + |b_2||x_1||x_2|^2 \,, \\
&\leq \bar{\omega}^2 |x| + |\mu_1||x| + |b_1||x|^3 + |\mu_2||x|^3 + |b_2||x|^3 \,, \\
&\leq [\bar{\omega}^2 + |\mu_1| + (|b_1| + |\mu_2| + |b_2|)\chi^2]|x| \,, \\
&\leq k_x|x| + k_d \,, \tag{100}
\end{aligned}
$$

where $k_x > \bar{\omega}^2 + |\mu_1| + (|b_1| + |\mu_2| + |b_2|)\chi^2$ and $k_d \geq 0$ are *unknown* upper bounds, as in assumption (A1). The control objective is to ensure the system stabilization at $x = 0$.

In other words, forcing the output $y = x_1$ to track a reference model y_m with $r = 0$, we can also guarantee $x_2 = \dot{y} = 0$. Thus, according to (48), the following reference model is employed

$$y_m = \frac{1}{(s+5)^2} r . \tag{101}$$

Comparing (48) and (49) to (101), it is easy to obtain $\gamma_m = 5$ and $L_m(s) = s + 5$. Since $e = y - y_m$, the ideal sliding variable can be obtained as $\sigma = \dot{e} + 5e$. As discussed before, it can not be implemented since $\dot{e}$ is not available. Therefore, by using the proposed adaptive HOSM differentiator (80), with $\lambda_0 = 5$ and $\lambda_1 = 3$, the following estimate for σ can be obtained according to (87): $\hat{\sigma} = \zeta_1 + 5\zeta_0$.

For the construction of the time-varying gain $\mathcal{L}(\hat{x}, k, t)$ in (78), the switching sequences are computed by $\bar{k}_1(k) = \bar{k}_2(k) = \bar{k}_3(k) = k + 1$ and k_m being replaced by $|\ddot{y}_m| = |-10\dot{y}_m - 25y_m + r|$. The signals y_m, $\dot{y}_m$ can be implemented from the state-space representation of the reference model (101).

The regressor vector (51) is obtained with the I/O filters in (52), by setting $\Phi = -4$ and $\Gamma = 1$. The monitoring function φ_m in (66) is designed to perform jumps multiples of 0.0524 `rad` (three degrees), *i.e.*, $a(k) = 0.0524k$. The hybrid state-norm observer $\hat{x}(t)$ and the disturbance norm bound $\hat{d}_f(k, t)$ are calculated according to (71) and (73), respectively. In this application, their parameters were chosen as: $\underline{\lambda}_x(k) = 0.1 + \frac{1}{1+k}$, $\bar{k}_\omega = k + 1$, $\bar{k}_x(k) = 0.5k$, $\bar{k}_d(k) = 0.5k$, $c_f = 0.01$ and $\lambda_f = 1$. Finally, the proposed output-feedback SMC law (82) with modulation function (84) are designed considering $\bar{\theta}(k) = k$ and $\delta = 0.01$. In addition, the control direction was initialized with the incorrect sign ($m = 1$).

The results of control method are presented in Figure 5 and Figure 6. In particular, the phase portrait in Figure 5 shows the open-loop limit-cycle oscillation (in red) and the closed-loop behavior (in blue) of the aircraft system (96)–(99) with parameter $\alpha = 25.0^o$. It is remarkable how the proposed controller can suppress the wing rock oscillation, driving the system gracefully to the origin $x_1 = x_2 = 0$.
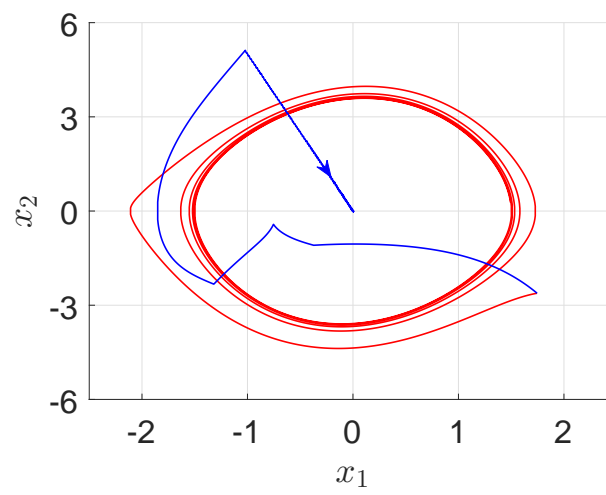
Figure 5 – Phase portrait of the open-loop system (red line) versus the closed-loop system (blue line).

(a) Monitoring function φ_m and the output error norm $|e(t)|$.

(b) Control direction signal.

(c) Time-history of the switching index k.

(d) Control signal $u(t)$.

(e) Norm observer performance.

(f) Control signal $u(t)$.

(g) Estimate of $e(t)$ given by the proposed global hybrid adaptive HOSM differentiator.

(h) Estimate of $\dot{e}(t)$ given by the proposed global hybrid adaptive HOSM differentiator.

Figure 6 – Suppression of the wing rock phenomenon.

3 VARIABLE GAIN SUPER-TWISTING ALGORITHM

This chapter presents an output-feedback control strategy based on the variable gain super-twisting algorithm. The proposal achieves robust global/semi-global exact tracking results for plants with arbitrary relative degree. This is ensured in spite of parametric uncertainties and disturbances that may be state-dependent and time-varying. The construction of such controller is based on a (non) homogeneous higher-order sliding mode differentiator with dynamic gains. The gain adaptation schemes for the controller and for the differentiator are based on norm observers to overcome the lack of state measurement. The continuous nature of the obtained control signal alleviates the chattering phenomenon. The stability properties of the proposed controller are demonstrated by means of a Lyapunov function based analysis. The theoretical results are verified through a simulation example, and experimentally tested on a seesaw module.

3.1 Problem Formulation

Consider the class of uncertain systems that can be transformed into the following *normal form* [80]:

$$\dot{\eta} = \mathcal{A}_0\eta + \mathcal{B}_0\xi \,, \tag{102}$$

$$\dot{\xi} = \mathcal{A}_\rho\xi + \mathcal{B}_\rho K_p[u + d(x,t)] \,, \tag{103}$$

$$y = \mathcal{C}_\rho\xi \,, \tag{104}$$

where $u \in \mathbb{R}$ is the input, $y \in \mathbb{R}$ is the measured output, $d(x,t) \in \mathbb{R}$ is a state dependent and time varying nonlinear disturbance. The vector $x^T = [\eta^T \ \xi^T] \in \mathbb{R}^n$ is the unmeasured state with $\eta \in \mathbb{R}^{(n-\rho)}$ being referred as the state of the inverse or zero dynamics and $\xi = [y \ \dot{y} \ \ldots \ y^{(\rho-1)}]^T$ being the external dynamics state. The triple $(\mathcal{A}_\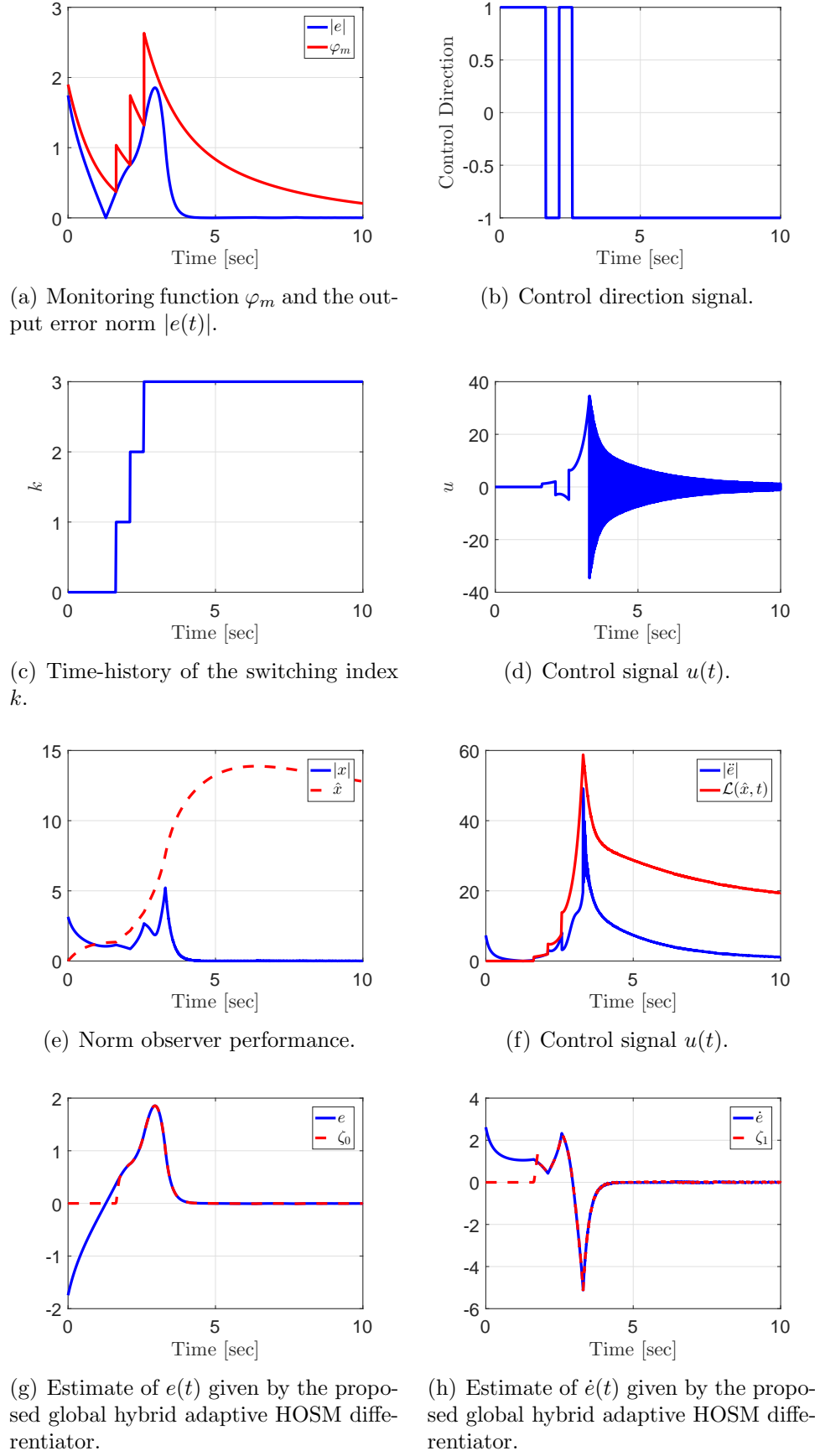rho, \ \mathcal{B}_\rho, \ \mathcal{C}_\rho)$ is in the Brunovsky's controller form [80], the pair $(\mathcal{A}_0, \ \mathcal{B}_0)$ is controllable, and $\mathcal{A}_0$ is Hurwitz in order to satisfy the minimum-phase condition. The *high frequency gain* (HFG) $K_p \in \mathbb{R}$ is assumed positive without loss of generality.

The nonlinear system (102)–(104) has *arbitrary relative degree* (denoted by $\rho \geq 1$) with respect to the measured output y, and it can be represented in the following compact

form:

$$\dot{x} = A_p x + B_p[u + d(x,t)], \qquad y = H_p x. \tag{105}$$

The uncertain matrices

$$A_p = \begin{bmatrix} \mathcal{A}_0 & \mathcal{B}_0 \\ 0 & \mathcal{A}_\rho \end{bmatrix}, \qquad B_p = \begin{bmatrix} 0 \\ \mathcal{B}_\rho K_p \end{bmatrix}, \qquad H_p = \begin{bmatrix} 0 & \mathcal{C}_\rho \end{bmatrix}, \tag{106}$$

belong to some compact set, such that the necessary uncertainty bounds to be defined later are available for design.

Notice that the relative degree relaxation is by itself a contribution with respect to [88]. There, an output-feedback generalization of the VGSTA by [51] is proposed under the condition of the plants having *relative degree one*. On the other hand, previous output-feedback version of fixed gains STA in [89] renders only local stability results and/or assumes uniformly bounded nonlinear disturbances, i.e., $|d(x,t)| \leq M = $ constant. Moreover, there are continuous finite-time controllers [90, 91] restricted to linear plants represented by a chain of integrators (without η–dynamics) at most perturbed by uniformly continuous exogenous functions of the time, i.e., no state-dependence for the disturbances are allowed. Finally, although "quasi-continuous"controllers by [92] can handle disturbances with variable bounds using state feedback, the control signal is ultimately discontinuous when sliding mode takes place, which deviates from the scope of the present contribution.

In order to alleviate the restrictions mentioned above, we further assume that:

(A1) The uncertain input disturbance $d(x,t)$ and its gradient are bounded by continuous functions almost everywhere, and in particular $d(x,t)$ is norm bounded by

$$|d(x,t)| \leq k_x|x| + k_d, \quad \forall x, t,$$

where $k_x, k_d \geq 0$ are *known* scalars.

The smoothness condition imposed on the unknown nonlinear disturbance $d(x,t)$ and its derivative was already assumed in earlier works about VGSTA, see [51]. As usual in the literature of continuous STA, it restricts the class of disturbances coped with to continuous functions. However, more general stability results (rather than only local stability) can be obtained when variable upper bounds such as $|d(x,t)| \leq k_x|x| + k_d$, with

$k_x > 0$ and $k_d > 0$ being known constants, are assumed instead of constant and more conservative upper bounds (e.g., $|d(x,t)| \leq k_d$) generally applied in earlier publications. The challenge here is to prove non local stability properties (global/semi-global) for the closed-loop system using only output feedback. Basically, we need to find a way to upper bound the state-dependent disturbance $d(x,t)$ using measured signals (the state x is unmeasured) while any possible finite-time escape is avoided. For this reason, we have introduced inequality $|d(x,t)| \leq k_x|x| + k_d$. The previous linear upper bound in x allows us to have system signals which are *regular* and that can grow at most exponentially [57]. It will be crucial to avoid finite-time escape for the system signals while perfect-exact tracking using output feedback is pursued.

We consider the following model for the reference signal $y_m(t) \in \mathbb{R}$:

$$y_m = W_m(s)\, r\,, \quad W_m(s) = (s + \gamma_m)^{-1} L_m^{-1}(s)\,, \quad \gamma_m > 0, \tag{107}$$

where $r(t) \in \mathbb{R}$ is an arbitrary uniformly bounded piecewise continuous reference signal and $L_m(s)$ is a Hurwitz polynomial defined as follows

$$L_m(s) = s^{(\rho-1)} + l_{\rho-2} s^{(\rho-2)} + \cdots + l_1 s + l_0. \tag{108}$$

The transfer function matrix $W_m(s)$ has the same relative degree ρ, as well as the plant, and its HFG is the unity.

The control problem is to find u such that for arbitrary initial conditions, the output error

$$e(t) := y(t) - y_m(t) \tag{109}$$

tends to zero.

For $d \equiv 0$ and known plant, the ideal control signal $u^* = \theta^{*T}\omega$, with $\theta^* = \left[\theta_1^{*T} \ \theta_2^{*T} \ \theta_3^* \ \theta_4^*\right]^T$, $\theta_1^*, \theta_2^* \in \mathbb{R}^{(n-1)}, \theta_3^*, \theta_4^* \in \mathbb{R}$, achieves the matching between the closed-loop transfer function matrix and $W_m(s)$, using the following regressor vector

$$\omega = [\omega_u^T \ \omega_y^T \ y \ r]^T\,, \tag{110}$$

with $w_u, w_y \in \mathbb{R}^{(n-1)}$ obtained from input–output (I/O) state variable filters given by [16]:

$$\dot{\omega}_u = \Phi\omega_u + \Gamma u\,, \qquad \dot{\omega}_y = \Phi\omega_y + \Gamma y\,, \tag{111}$$

where $\Phi \in \mathbb{R}^{(n-1)\times(n-1)}$ is Hurwitz and $\Gamma \in \mathbb{R}^{(n-1)}$ is chosen such that the pair $(\Phi,\ \Gamma)$ is controllable. The matching conditions require that $\theta_4^* = K_p^{-1}$. Define the augmented state vector

$$X = [x^T, \omega_u^T, \omega_y^T]^T\,, \tag{112}$$

with dynamics described by

$$\dot{X} = A_0 X + B_0 u + B_0' d, \quad y = H_0 X\,,$$

where

$$A_0 = \begin{bmatrix} A_p & 0 & 0 \\ 0 & \Phi & 0 \\ (\Gamma H_p) & 0 & \Phi \end{bmatrix}, \quad B_0 = \begin{bmatrix} B_p \\ \Gamma \\ 0 \end{bmatrix}, \quad B_0' = \begin{bmatrix} B_p \\ 0 \\ 0 \end{bmatrix}, \quad H_0 = \begin{bmatrix} H_p & 0 & 0 \end{bmatrix}.$$

Then, by adding and subtracting $B_0 {\theta^*}^T \omega$ and noting that there exist matrices Ω_1 and Ω_2 such that

$$\omega = \Omega_1 X + \Omega_2 r\,, \tag{113}$$

one has

$$\dot{X} = A_c X + B_c K_p [\theta_4^* r + u - u^*] + B_0' d\,, \quad y = H_0 X\,, \tag{114}$$

where $A_c = A_0 + B_0 {\theta^*}^T \Omega_1$, and $B_c = B_0 \theta_4^*$. We have that (A_c, B_c, H_0) is a non-minimal realization of $W_m(s)$. It is worth mention that the generalized augmented dynamics (114) is already different from those found in the usual Model Reference Adaptive Control (MRAC) literature [16, 57] since now disturbances are being considered. The reference model can be rewritten as

$$\dot{X}_m = A_c X_m + B_c K_p [\theta_4^* r - d_f] + B_0' d\,, \quad y_m = H_0 X_m\,, \tag{115}$$

with the following equivalent input disturbance

$$d_f = W_d(s)d\,, \tag{116}$$

where

$$W_d(s) \;=\; [W_m(s)K_p]^{-1}\,\bar{W}_d(s)\,, \tag{117}$$

$$\bar{W}_d(s) \;=\; H_0\,(sI - A_c)^{-1}\,B'_0\,. \tag{118}$$

Therefore, $y_m = W_m(s)K_p\left[\theta_4^{*T}r - W_d(s)d\right] + \bar{W}_d(s)d$ and it is straightforward to conclude that $y_m = W_m(s)\,r$. Note that (117) is a stable and proper transfer function. In addition, $[W_m(s)K_p]^{-1} = \bar{K}_\rho s^\rho + \bar{K}_{\rho-1}s^{\rho-1} + \ldots + \bar{K}_0$, where $\bar{K}_i \in \mathbb{R}$, $i = 0, \ldots, \rho$ are constants. Thus, by defining the state

$$X_e := X - X_m \tag{119}$$

the complete error dynamics can be obtained by subtracting (115) from (114), which leads to

$$\textbf{State Space:} \quad \dot{X}_e = A_c\,X_e + B_c K_p[u - \theta^{*T}\omega + d_f]\,, \tag{120}$$

$$e = H_0\,X_e,$$

$$\textbf{I/O Form:} \quad e = W_m(s)K_p\left[u - \theta^{*T}\omega + d_f\right]\,. \tag{121}$$

Remark 4. *The importance of using MRAC methodology by means of I/O filters is not to identify the unknown parameters, as in classical adaptive control. Moreover, it does not rely only in deriving the full-error equation (120) from the augmented state X, but it does yield a complete output-feedback framework on which a norm bound for the unmeasured state can be obtained through state-norm observers as follows.* ⌟

3.2 State-Norm Estimation

Considering assumption (A1) and applying [8, Lemma 3] to (114), it is possible to find $k_x^* > 0$ such that, for $k_x \in [0, k_x^*]$ a norm bound for X and x can be obtained through

stable *first order approximation filters* (FOAFs) (see details in [8]). Thus, one has

$$|x(t)| \leq |X(t)| \leq |\hat{x}(t)| + \hat{\pi}(t)\,, \tag{122}$$

$$\dot{\hat{x}}(t) = -\lambda_x \hat{x}(t) + [c_1 k_d + c_2 |\omega(t)|]\,, \tag{123}$$

with $c_1, c_2, \lambda_x > 0$ being appropriate constants that can be computed by the optimization methods described in [56]. In particular, the parameter λ_x in (123) is defined by $\lambda_x := \gamma_0 - |B_0'|k_x$, where $|B_0'|k_x > 0$ is a constant smaller than γ_0 computed with B_0' given in (114), and $\gamma_0 > 0$ being the stability margin[2] of A_c in (114). In a few words, k_x must be small enough to no break the ISS property of (114) from d to X. In this sense, (122)–(123) state that the norm observer estimate $\hat{x}(t)$ provides a valid norm bound for the unmeasured state x of the uncertain and disturbed plant, except for exponentially decaying terms due to the system initial conditions, denoted here by $\hat{\pi}(t)$.

From (116), we can write $|d_f| \leq |W_d(s)d|$. Moreover, from (A1) and (123), one has $|d(x,t)| \leq k_x \hat{x}(t) + k_d$, *modulo* $\hat{\pi}$ term, and one can write $|d_f| \leq \hat{d}_f + \hat{\pi}_f$, where $\hat{\pi}_f$ is an exponentially decaying term,

$$\dot{\hat{d}}_f(t) = -\lambda_f \hat{d}_f(t) + c_f[k_x \hat{x}(t) + k_d]\,, \tag{124}$$

and $\frac{c_f}{s+\lambda_f}$ is a FOAF designed for $W_d(s)$, with adequate positive constants c_f and λ_f. At the price of some conservatism, we can simplify the FOAF design by choosing c_f sufficiently large and λ_f sufficiently small.

In this section, assumption (A1) enable us to design the state-norm observer so that the following norm bound $|x(t)| < |X(t)| \leq \hat{x}(t)\,, \forall t > T_0$, can be achieved in some finite time $T_0 > 0$. Therefore, the disturbance can be ultimately dominated as desired (e.g., $|d(x,t)| \leq k_x \hat{x}(t) + k_d$) such that the variable gain $\mathcal{L}(\hat{x}, t)$ of the differentiator (in Section 3.3) as well as the gains $k_1(\hat{x}, t)$ and $k_2(\hat{x}, t)$ of the proposed output-feedback version of the VGSTA (in Section 3.4.2) can be finally constructed.

---

[2] Let $\{\lambda_i\}$ be the eigenvalues of A_c, the stability margin of A_c is defined by $\gamma_0 := \min_i[-\text{Re}(\lambda_i)]$.

3.3 HOSM Differentiator with Dynamic Gains

The state-norm estimation (122)–(123) was applied in [54] for the construction of a time-varying gain HOSM differentiator achieving exact differentiation of signals with any initial conditions. To this end, we need an upper bound for the *unknown* higher derivative $|e^\rho(t)|$.

From (103), assumption (A1) and using the augmented state X defined in (112), the following upper bound for $y^{(\rho)}$ is obtained

$$|y^{(\rho)}| \le L(X,t) = k_1|X| + k_2 + k_3|u|\,, \tag{125}$$

where $k_1 \ge K_p k_x$, $k_2 \ge K_p k_d$ and $k_3 \ge K_p$ are known positive constants.

Now, from (125) and (109), we can write

$$|e^{(\rho)}(t)| \le L(X,t) + |y_m^{(\rho)}(t)|\,. \tag{126}$$

The following upper bound involving the norm observer variable $\hat{x}(t)$, can be obtained using (122):

$$|e^{(\rho)}(t)| \le L(\hat{x},t) + |y_m^{(\rho)}(t)| = k_1|\hat{x}| + k_2 + k_3|u| + k_m\,, \tag{127}$$

modulo exponential decaying terms due to initial conditions which take into account the transient of the FOAF. The known positive constant k_m satisfies $|y_m^{(\rho)}(t)| \le k_m$.

Our output-feedback generalization for VGSTA is an absolutely continuous function u constructed with the signal $\hat{x}$ in (123). Thus, we can define the term

$$\mathcal{L}(\hat{x},t) := k_1|\hat{x}| + k_2 + k_3|u| + k_m\,, \tag{128}$$

using only continuous signals and write the following norm bound

$$|e^{(\rho)}(t)| \le \mathcal{L}(\hat{x},t)\,, \quad \forall t \ge T\,, \tag{129}$$

for some finite time $T > 0$.

In light of (128)–(129), we can introduce the following HOSM based differentiator

of order $p = \rho - 1$ for the output error $e \in \mathbb{R}$:

$$\dot{\zeta}_0 = v_0 = -\lambda_0 \mathcal{L}(\hat{x}, t)^{\frac{1}{p+1}} |\zeta_0 - e(t)|^{\frac{p}{p+1}} \operatorname{sgn}(\zeta_0 - e(t)) + \zeta_1,$$

$$\vdots$$

$$\dot{\zeta}_i = v_i = -\lambda_i \mathcal{L}(\hat{x}, t)^{\frac{1}{p-i+1}} |\zeta_i - v_{i-1}|^{\frac{p-i}{p-i+1}} \operatorname{sgn}(\zeta_i - v_{i-1}) + \zeta_{i+1}, \tag{130}$$

$$\vdots$$

$$\dot{\zeta}_p = -\lambda_p \mathcal{L}(\hat{x}, t) \operatorname{sgn}(\zeta_p - v_{p-1}).$$

According to the results in [93], the following non-homogeneous version of the proposed HOSM based differentiator (130) can also be derived

$$\dot{\zeta}_0 = v_0 = -\lambda_0 \mathcal{L}(\hat{x}, t)^{\frac{1}{p+1}} |\zeta_0 - e(t)|^{\frac{p}{p+1}} \operatorname{sgn}(\zeta_0 - e(t)) + \zeta_1 - \mu_0(\zeta_0 - e(t)),$$

$$\vdots$$

$$\dot{\zeta}_i = v_i = -\lambda_i \mathcal{L}(\hat{x}, t)^{\frac{1}{p-i+1}} |\zeta_i - v_{i-1}|^{\frac{p-i}{p-i+1}} \operatorname{sgn}(\zeta_i - v_{i-1}) + \zeta_{i+1} - \mu_i(\zeta_i - v_{i-1}), \tag{131}$$

$$\vdots$$

$$\dot{\zeta}_p = -\lambda_p \mathcal{L}(\hat{x}, t) \operatorname{sgn}(\zeta_p - v_{p-1}) - \mu_p(\zeta_p - v_{p-1}),$$

which may provide for faster convergence compared with (130) due to the additional linear terms with appropriate constants $\mu_i > 0$, for $i = 0, \dots, p$.

Since $\mathcal{L}(\hat{x}, t)$ in (129) is generated by signals which can grow exponentially at most (there is no escape in finite time) due to the linear growth condition (A1), then the logarithmic derivative $\dot{\mathcal{L}}/\mathcal{L}$ is bounded and the following equalities

$$\zeta_0 = e(t), \quad \zeta_i = e^{(i)}(t), \quad i = 1, \dots, \rho - 1, \tag{132}$$

can be established in finite time according to [11, 28, 50], provided the parameters λ_i (and μ_i) are properly chosen. The boundedness of all closed-loop signals is presented in the proof of the main theorem.

Unlikely conventional HOSM differentiators with fixed-constant gains [17, 23, 93], the convergence of the differentiators (130) and (131) with dynamic gains is non local, since the upper estimation (129) holds independent of any initial condition of the closed-loop signals. Thus, the state trajectory is NOT restricted a priori to any compact set such that $|e^{(\rho)}(t)| \leq C_\rho$, where $C_\rho > 0$ is a valid local upper bound for the higher-derivative

of $|e(t)|$. On the other hand, our main contribution with respect to [11, 28, 50] is to show how to construct the differentiator gain for time-varying and state dependent terms in the signal $|e^{(\rho)}(t)|$ using only input-output information in order to satisfy the conditions raised therein.

3.4   Output-Feedback Variable Gain Super-Twisting

In sliding mode control, the relative degree one sliding variable σ is designed to ensure that the reduced-order model meets the performance requirements, once the motion is restricted to the manifold $\sigma = 0$.

For higher relative degree plants, the operator $L_m(s)$ defined in (108) can be used to overcome the relative degree obstacle. The operator $L_m(s)$ is such that $L_m(s)W_m(s)$ have relative degree one. The ideal sliding variable $\sigma = L_m(s)e$ is given by

$$\sigma = e^{(\rho-1)} + \cdots + l_1\dot{e} + l_0 e \tag{133}$$

$$= \sum_{i=0}^{\rho-1} l_i H_0 A_c^{(i)} X_e = \bar{H} X_e \,,$$

where the second equality is derived from (120).

Remark 5. *Regarding the choice of a linear combination of the error derivatives for the ideal sliding variable σ in (133), we can point out two major advantages, as discussed in [94]: (a) simplicity when comparing to nonlinear functions which results in finite-time convergence; and (b) we can expect lower levels of chattering in practice caused by unmodelled dynamics. In addition, the obtainment of general nonlinear sliding surfaces which allow us to conclude finite-time convergence for the tracking error signal rather than exponential one seems to be a really hardy topic of research since only the existence of such general nonlinear sliding surfaces were proved in the current literature, but the design of them were not presented yet. Some advances were restricted to finite-time stabilization of linear plants represented by a chain of integrators. For more details, see [95].* ⌐

Note that $\{A_c, B_c, \bar{H}\}$ is a non-minimal realization of $L_m(s)W_m(s)$. From (107)–

(108), we have

$$\sigma = L_m(s)W_m(s)K_p \left[u - \theta^{*^T}\omega + d_f \right]$$

$$= \frac{K_p}{s + \gamma_m} \left[u - \theta^{*^T}\omega + d_f \right] . \qquad (134)$$

Then, the σ-dynamics can be expressed as

$$\dot{\sigma} = K_p u + f(X, \sigma, t) , \qquad (135)$$

with

$$f(X, \sigma, t) = -\gamma_m \sigma - K_p \left[\theta^{*^T}\omega - d_f \right] . \qquad (136)$$

The above equation can be rewritten as

$$f(X, \sigma, t) = \overbrace{f(X, \sigma, t) - f(X, 0, t)}^{g_1(X,\sigma,t)} + \overbrace{f(X, 0, t)}^{g_2(X,t)} , \qquad (137)$$

$$= g_1(X, \sigma, t) + g_2(X, t) \qquad (138)$$

where $g_1(X, \sigma, t) = 0$ if $\sigma = 0$. Therefore, it follows that

$$g_1(X, \sigma, t) = -\gamma_m \sigma , \qquad (139)$$

$$g_2(X, t) = -K_p \left[\theta^{*^T}\omega - d_f \right] . \qquad (140)$$

3.4.1   State-Feedback Variable-Gain STA

Consider the state-feedback VGSTA proposed in [51]:

$$u = -k_1 (X, t) \phi_1 (\sigma) - \int_0^t k_2 (X, \tau) \phi_2 (\sigma) \, d\tau , \qquad (141)$$

where

$$\phi_1 (\sigma) = |\sigma|^{\frac{1}{2}} \operatorname{sgn} (\sigma) + k_3 \sigma$$

$$\phi_2 (\sigma) = \tfrac{1}{2}\operatorname{sgn} (\sigma) + \tfrac{3}{2}k_3 |\sigma|^{\frac{1}{2}} \operatorname{sgn} (\sigma) + k_3^2 \sigma , \quad k_3 > 0 .$$

The standard STA is a particular case, where $k_3 = 0$ and the gains k_1 and k_2 are constants. The constant $k_3 > 0$ allows to deal with perturbations growing linearly in σ, *i.e.*, outside of the sliding surface, whereas the variable gains k_1 and k_2 enable to render the sliding

surface insensitive to perturbations growing with bounds given by known functions. Note that the VGSTA algorithm (141) is not homogeneous and the control variable is absolutely continuous, in contrast with the discontinuous nature of classical first order SMC.

The above continuous VGSTA is able to compensate perturbations $f(x,t)$ satisfying (almost everywhere) [51]:

$$|g_1(X,\sigma,t)| \leq \varrho_1(X,t)|\phi_1(\sigma)| = \varrho_1(X,t)\left[1 + k_3|\sigma|^{1/2}\right]|\sigma|^{1/2}, \tag{142}$$

$$\left|\frac{d}{dt}g_2(X,t)\right| \leq \varrho_2(X,t)|\phi_2(\sigma)| = \frac{1}{2}\varrho_2(X,t) + k_3\varrho_2(X,t)\left[\frac{3}{2} + k_3|\sigma|^{1/2}\right]|\sigma|^{1/2}, \tag{143}$$

where $\varrho_1(X,t) \geq 0$, $\varrho_2(X,t) \geq 0$ are known continuous functions.

3.4.2 Output-Feedback Variable-Gain STA

The controller (141) is implemented using the norm observer bound $\hat{x}$, see (122)–(123), instead of the unavailable X. Thus, from (142) and (143) we have that

$$\begin{aligned} |g_1(X,\sigma,t)| &\leq [\varrho_1(\hat{x},t) + |\pi_1(t)|]\,|\phi_1(\sigma)|\,, \\ \left|\tfrac{d}{dt}g_2(X,t)\right| &\leq [\varrho_2(\hat{x},t) + |\pi_2(t)|]\,|\phi_2(\sigma)|\,, \end{aligned} \tag{144}$$

where $\varrho_1(\hat{x},t) \geq 0$, $\varrho_2(\hat{x},t) \geq 0$ are known continuous functions satisfying

$$|\varrho_1(\hat{x},t)| \leq \Psi_1(|\hat{x}|) + \bar{k}_1\,, \tag{145}$$

$$|\varrho_2(\hat{x},t)| \leq \Psi_2(|\hat{x}|) + \bar{k}_2\,, \tag{146}$$

with $\Psi_{1,2} \in \mathcal{K}$, constants $\bar{k}_{1,2} > 0$, whereas $\pi_1(t)$ and $\pi_2(t)$ are exponential decaying terms due to the initial conditions of the norm observer.

The inequality $|g_1(X,\sigma,t)| \leq \gamma_m|\sigma|$ is straightforward obtained from (139). Moreover, from (140) it can be verified that $|g_2(X,t)| \leq \bar{\theta}|\omega(t)| + \hat{d}_f(t)$ with ω in (110) and $\hat{d}_f(t)$ defined in (124) and (123). The parameter $\bar{\theta}$ is a constant upper bound for $\bar{\theta} \geq |\theta^*|$, which can be computed due to the fact that A_p, B_p and H_p in (105) belong to some known compact. Regarding $\left|\frac{d}{dt}g_2(X,t)\right|$, similar upper bounds for $\dot{d}_f$ and $\dot{\omega}$ can be obtained from (107), (111) and (124), noting that ω and $\hat{d}_f$ are affinely norm bounded by $\hat{x}$.

Notice that g_1 and g_2 in (139)–(140) will always satisfy the conditions (144) since they are continuous functions in time generated by stable filters. At this point, we can

conclude that the restrictions assumed in (A1) are really necessary and smooth bounded disturbances $d(x,t)$ together with their time derivatives must be assumed according to (116), once $W_d(s)$ is a proper transfer function. This restrictions are in agreement with the disturbance smoothness assumption made for continuous SOSM based algorithms.

In this scenario with disturbances having bounded (time) derivatives, the functions g_1 and g_2 could be simpler to be obtained by using the normal form (102)–(103) rather than (120) for the σ-dynamics derivation. Reminding the σ-definition (133) and after some calculation, the final expression for σ would be given by:

$$\dot{\sigma} = K_p u + f_\sigma(x, \sigma, t) \,, \tag{147}$$

where $f_\sigma(x, \sigma, t) = \sum_{i=0}^{\rho-1} l_i e^{(i+1)}(t) - y_m^{(\rho)}(t) + K_p d(x,t)$ and $l_{\rho-1} = 1$, due to the monic polynomial in (108). Following an analogous procedure to the one previously described, new functions of $g_1(x, \sigma, t)$ and $g_2(x, t)$, depending on x and t, can be computed which also satisfy the conditions (144) due to assumption (A1) and the norm-observer bound (122).

Finally, the (non) homogeneous HOSM differentiator (130) or (131) can be applied to obtain an exact estimate for σ as follows:

$$\hat{\sigma} = \zeta_{\rho-1} + \cdots + l_1 \zeta_1 + l_0 e \,. \tag{148}$$

Then, the proposed output-feedback version for VGSTA can be written as

$$u = -k_1\left(\hat{x}, t\right) \phi_1\left(\hat{\sigma}\right) - \int_0^t k_2\left(\hat{x}, \tau\right) \phi_2\left(\hat{\sigma}\right) d\tau \,, \tag{149}$$

where
$$\begin{aligned}
\phi_1\left(\hat{\sigma}\right) &= |\hat{\sigma}|^{\frac{1}{2}} \operatorname{sgn}\left(\hat{\sigma}\right) + k_3 \hat{\sigma} \,, \\
\phi_2\left(\hat{\sigma}\right) &= \tfrac{1}{2}\operatorname{sgn}\left(\hat{\sigma}\right) + \tfrac{3}{2} k_3 |\hat{\sigma}|^{\frac{1}{2}} \operatorname{sgn}\left(\hat{\sigma}\right) + k_3^2 \hat{\sigma} \,, \ k_3 > 0 \,.
\end{aligned}$$

The stability results are summarized in the next theorem.

Theorem 3. *Consider the system (105) under assumptions (A1). The output-feedback VGSTA based controller is given by (149) with $\hat{\sigma}$ in (148) constructed with the state $\zeta = [\zeta_0 \ \ldots \ \zeta_{\rho-1}]^T$ of the HOSM differentiator (130) (or (131)) and $\hat{x}$ provided by the norm observer (122)–(123). Suppose that for some known continuous functions $\varrho_1\left(\hat{x}, t\right) \geq 0$,*

$\varrho_2(\hat{x},t) \geq 0$ *the inequalities (144) are satisfied. Then, for any initial condition, the sliding surface* $\hat{\sigma} = 0$ *will be reached in finite time if the variable gains in (149) are selected as*

$$
\begin{aligned}
k_1(\hat{x},t) &= \delta + \tfrac{1}{\beta}\left\{\tfrac{1}{4\epsilon}\left[2\epsilon\varrho_1 + \varrho_2\right]^2 + 2\epsilon\varrho_2 + \epsilon + \left[2\epsilon + \varrho_1\right]\left(\beta + 4\epsilon^2\right)\right\}, \\
k_2(\hat{x},t) &= \beta + 4\epsilon^2 + 2\epsilon k_1(\hat{x},t),
\end{aligned}
\tag{150}
$$

where $\beta > 0$, $\epsilon > 0$, $\delta > 0$ *are arbitrary positive constants. Moreover, the closed-loop error system with dynamics (120) is globally/semi-globally exponentially stable in the sense that* $X_e(t)$ *and the output tracking error* $e(t)$ *converge exponentially to zero whereas all the remaining closed-loop signals are uniformly bounded.* ⌐

Proof 3. *The demonstration is divided into four steps.*

– *STEP 1 – Global/Semi-global stability and finite-time escape avoidance*

First of all, let us assume a maximal time interval of definition for the existence of solution given by $[0, t_M)$, *where* t_M *may be finite or infinite. For the sake of clarity, we define the vector*

$$
z^T := [X_e^T, \zeta^T].
\tag{151}
$$

By continuity, given any $R > 0$, *if* $|z(0)| \leq R/2$, $\exists t^* \in [0, t_M)$ *such that* $|z(t)| < R$, $\forall t \in [0, t^*)$. *Hence,* $\forall t \in [0, t^*)$, *any class-$\mathcal{K}$ function* $\Psi_i(a)$ *can be norm bounded by* $\Psi_i(a) \leq k^R a$, *with* $k^R > 0$ *constant and possibly depending on* R. *On the other hand, all* κ's *and* k's *without the R-indexation denote positive constants independent on* R.

From (145), (146) and (150), one has $\forall t \in [0, t^*)$:

$$
|k_1(\hat{x},t)| \leq \kappa_1^R|\hat{x}| + \kappa_1,
\tag{152}
$$

$$
|k_2(\hat{x},t)| \leq \kappa_2^R|\hat{x}| + \kappa_2,
\tag{153}
$$

where $\kappa_{1,2}^R > 0$ *and* $\kappa_{1,2} > 0$ *are appropriate constants.*

Reminding that ζ *is assumed bounded* $\forall t \in [0, t^*)$ *and* $k_{1,2}(\hat{x},t)$ *satisfy (152)–(153), it is easy to show that* u *defined as in (149), with* $\hat{\sigma}$ *in (148), is norm bounded by*

$$
|u| \leq (\kappa_3^R + t^*)\|\hat{x}_t\| + (\kappa_3 + t^*), \quad \forall t \in [0, t^*).
\tag{154}
$$

From (123), we know that $|\hat{x}| \le \kappa_4 \|\omega_t\| + \kappa_5$. By using the relations (113) and (119), one has that $X = X_e + X_m$ and the regressor vector

$$\omega = \Omega_1 X_e + \Omega_1 X_m + \Omega_2 r. \tag{155}$$

Let $x_m := [y_m \ \dot{y}_m \ \dots \ y_m^{(\rho-1)}]^T$ and $x_e := \xi - x_m$, with ξ in (103). From (120), it can be shown that $e^{(i)} = H_0 A^i X_e$, for $i = 0, \dots, \rho-1$, hence $|x_e| \le \kappa_6 |X_e|$. Therefore, since x_m is uniformly bounded, then $\xi = x_e + x_m$ can be affinely norm bounded in $|X_e|$. In addition, from (102), the η-dynamics is ISS with respect to $y = \mathcal{C}_\rho \xi$. Thus, one can conclude that $|x| \le \kappa_7 \|\xi_t\| + \kappa_8$, and consequently, $|x| \le \kappa_9 \|(X_e)_t\| + \kappa_{10}$. Due to assumption (A1) concerning the linear growth condition of the nonlinear disturbances with respect to the unmeasured state x, from (115) and (116), one has

$$|X_m| \le \kappa_{11} \|(X_e)_t\| + \kappa_{12}. \tag{156}$$

Finally, from (113), (155) and (156), we conclude ω, the term d_f in (120), and consequently the control input u in (154) are all affinely norm bounded by X or X_e such that, $\forall t \in [0, t^*)$:

$$|u|, |d_f|, |\omega| \le k_a \|X_t\| + k_b, \tag{157}$$

$$|u|, |d_f|, |\omega| \le k_c \|(X_e)_t\| + k_d, \tag{158}$$

for some appropriate constants $k_a, k_b, k_c, k_d > 0$. Thus, the system signals will be regular and, therefore, they can grow at most exponentially [57] during the interval $[0, t^*)$. Thus, the solution of (120) can diverge according to

$$|X_e(t)| \le e^{k_L t} |X_e(0)| + k_e, \quad \forall t \in [0, t^*), \tag{159}$$

for some positive constants k_L and k_e, or equivalently $|X_e(t)| \le \Psi_e(|X_e(0)|) + k_e$, for some appropriate $\Psi_e(\cdot) \in \mathcal{K}$. Finally, given any $R > k_e$, for $|X_e(0)| \le R_0$, with $R_0 \le \Psi_e^{-1}(R - k_e)$, then $|X_e(t)|$ is bounded away from R as $t \to t^*$. Taking into account (151) and (158), this implies that $z(t)$ as well as any other signal of the closed-loop system are uniformly bounded and cannot escape in finite time, i.e., $t_M = +\infty$ by continuation of solutions [80]. Hence, semi-global stability with respect to any ball of radius

k_e is guaranteed $\forall X_e(0)$ since R and R_0 can be chosen arbitrarily large. Moreover, if $k_1(\hat{x}, t)$ and $k_2(\hat{x}, t)$ are such that u is a globally Lipschitz function of $\hat{x}$ such that κ_1^R, κ_2^R, in (152)–(153) can be replaced by constants independents of initial conditions and/or the relative degree is one ($\rho = 1$), then the stability properties become global.

– STEP 2 – The ideal sliding variable is exactly estimated

This fact lead us to the next step of the proof. There exist two finite time instants $T_1 > 0$ and $T_2 > 0$ such that (129) and (144) are satisfied, $\forall t > \max\{T_1, T_2\}$. From the regularity condition in (157), one can conclude that (128) grows at most exponentially so that the logarithmic derivative ($\dot{\mathcal{L}}/\mathcal{L}$) of the variable gain $\mathcal{L}(\hat{x}, t)$ of the differentiator is always bounded [11], [28]. Since the gain is increasing when the plant state is not converging, the differentiator errors are forced to ultimately achieve a compact set on which the sufficient conditions given by [11], [28] and [50] can be invoked and conclude that (132) is satisfied. After that, the ideal sliding variable (of relative degree one) in (133) is indeed exactly estimated by (148), i.e., $\hat{\sigma} = \sigma$.

– STEP 3 – Finite-time convergence of the sliding variable to zero

Thus, equation (135) driven by the output-feedback VGSTA (149) can be written as

$$
\begin{aligned}
\dot{\sigma} &= -K_p k_1 (\hat{x}, t) \phi_1 (\sigma) + z + g_1 (X, \sigma, t) , \\
\dot{z} &= -K_p k_2 (\hat{x}, t) \phi_2 (\sigma) + \tfrac{d}{dt} g_2 (X, t) .
\end{aligned}
\tag{160}
$$

In the next, we show that the quadratic form [51]

$$
V (\sigma, z) = \chi^T P \chi ,
\tag{161}
$$

where

$$
\chi^T = \left[|\sigma|^{\frac{1}{2}} \, sign (\sigma) + k_3 \sigma , \quad z \right] ,
\tag{162}
$$

$$
P = \begin{bmatrix} p_1 & p_3 \\ p_3 & p_2 \end{bmatrix} = \begin{bmatrix} \beta + 4\epsilon^2 & -2\epsilon \\ -2\epsilon & 1 \end{bmatrix} ,
\tag{163}
$$

with arbitrary positive constants $\beta > 0$, $\epsilon > 0$, is a (strict) Lyapunov function for the subsystem (σ, z) of (160), showing finite time convergence. Function (161) is positive definite, everywhere continuous and differentiable everywhere except on the set $\mathcal{S} = \{(\sigma, z) \in \mathbb{R}^2 \mid \sigma = 0\}$.

The inequalities (142)–(143) can be rewritten as $g_1(X, \sigma, t) = \alpha_1(X, t)\phi_1(\sigma)$ and $\frac{d}{dt}g_2(X, t) = \alpha_2(X, t)\phi_2(\sigma)$ for some functions $|\alpha_1(X, t)| \leq \varrho_1(\hat{x}, t)$ and $|\alpha_2(X, t)| \leq \varrho_2(\hat{x}, t)$. Using these functions and noting that $\phi_2(\sigma) = \phi_1'(\sigma)\phi_1(\sigma)$ one can show that

$$
\begin{aligned}
\dot{\chi} &= \begin{bmatrix} \phi_1'(\sigma)\{-K_p k_1(\hat{x}, t)\phi_1(\sigma) + z + g_1(X, t)\} \\ -K_p k_2(\hat{x}, t)\phi_2(\sigma) + \frac{d}{dt}g_2(X, t) \end{bmatrix} \\
&= \phi_1'(\sigma) \begin{bmatrix} -(K_p k_1(\hat{x}, t) - \alpha_1(X, t)) & 1 \\ -(K_p k_2(\hat{x}, t) - \alpha_2(X, t)) & 0 \end{bmatrix} \chi \\
&= \phi_1'(\sigma)\, \mathcal{A}(t, X, \hat{x})\, \chi \,,
\end{aligned}
$$

for every point in $\mathbb{R}^2 \backslash \mathcal{S}$, where this derivative exists. For the sake of simplicity we will consider $K_p = 1$. For the case of uncertain HFG, it is sufficient to consider the knowledge of a lower bound $0 < \underline{k}_p \leq K_p$ to normalize the equations in what follows. Similarly one can calculate the derivative of $V(\sigma, z)$ on the same set $\mathbb{R}^2 \backslash \mathcal{S}$ as

$$
\begin{aligned}
\dot{V}(\sigma, z) &= \phi_1'(\sigma)\chi^T \left[\mathcal{A}^T(t, X, \hat{x})P + P\mathcal{A}(t, X, \hat{x}) \right] \chi \\
&= -\phi_1'(\sigma)\chi^T Q(t, X, \hat{x})\chi,
\end{aligned}
$$

where (the arguments of the functions were left out)

$$
Q = \begin{bmatrix} 2(k_1 - \alpha_1)p_1 + 2(k_2 - \alpha_2)p_3 & \bigstar \\ (k_1 - \alpha_1)p_3 + (k_2 - \alpha_2)p_2 - p_1 & -2p_3 \end{bmatrix},
$$

and $\bigstar$ is used to indicate a symmetric element. Selecting P as in (163) and the gains as

in (150), we have

$$Q - 2\epsilon\mathbb{I}=$$

$$= \begin{bmatrix} 2\beta k_1 + 4\epsilon\left(2\epsilon k_1 - k_2\right) - 2\left(\beta + 4\epsilon^2\right)\alpha_1 + 4\epsilon\alpha_2 - 2\epsilon & \bigstar \\ k_2 - 2\epsilon k_1 - \left(\beta + 4\epsilon^2\right) + 2\epsilon\alpha_1 - \alpha_2 & 2\epsilon \end{bmatrix}$$

$$= \begin{bmatrix} 2\beta k_1 - \left(\beta + 4\epsilon^2\right)\left(4\epsilon + 2\alpha_1\right) + 4\epsilon\alpha_2 - 2\epsilon & \bigstar \\ 2\epsilon\alpha_1 - \alpha_2 & 2\epsilon \end{bmatrix}$$

being positive definite for every value of $(t, X, \hat{x})$. Thus,

$$\begin{aligned} \dot{V} &= -\phi_1'(\sigma)\chi^T Q\left(t, X, \hat{x}\right)\chi \\ &\leq -2\epsilon\phi_1'(\sigma)\chi^T\chi = -2\epsilon\left(\frac{1}{2\left|\sigma\right|^{\frac{1}{2}}} + k_3\right)\chi^T\chi \ . \end{aligned}$$

By applying Rayleigh-Ritz inequality $\lambda_{\min}\{P\}\left|\chi\right|^2 \leq \chi^T P\chi \leq \lambda_{\max}\{P\}\left|\chi\right|^2$, where $\left|\chi\right|^2 = \chi_1^2 + \chi_2^2 = \left|\sigma\right| + 2k_3\left|\sigma\right|^{\frac{3}{2}} + k_3^2\sigma^2 + z^2$ is the Euclidean norm of χ, and

$$\left|\chi_1\right| \leq \left|\chi\right| \leq \frac{V^{\frac{1}{2}}(\sigma, z)}{\lambda_{\min}^{\frac{1}{2}}\{P\}},$$

we can conclude that

$$\dot{V} \leq -\gamma_1 V^{\frac{1}{2}}(\sigma, z) - \gamma_2 V(\sigma, z) \ ,$$

$$\gamma_1 = \frac{\epsilon\lambda_{\min}^{\frac{1}{2}}\{P\}}{\lambda_{\max}\{P\}} \ , \quad \gamma_2 = \frac{2\epsilon k_3}{\lambda_{\max}\{P\}} \ . \tag{164}$$

Note that the trajectories of the STA cannot stay on the set $\mathcal{S} = \{(\sigma, z) \in \mathbb{R}^2 \mid \sigma = 0\}$. This means that $V(\sigma, z)$ is a continuously decreasing function and using the generalized Lyapunov's theorem in [96, Proposition 14.1, p. 205] for differential inclusions we can conclude that the equilibrium point $(\sigma, z) = 0$ is reached in finite time from every initial condition. The key property that allows our conclusion is that [96, Proposition 14.1, p. 205] requires only continuity and not differentiability of the Lyapunov function candidate.

Since the solution of the differential equation

$$\dot{v} = -\gamma_1 v^{\frac{1}{2}} - \gamma_2 v \ , \quad v(T_3) = v_0 \geq 0$$

is given by

$$v(t) = e^{-\gamma_2(t-T_3)} \left[v_0^{\frac{1}{2}} + \frac{\gamma_1}{\gamma_2} \left(1 - e^{\frac{\gamma_2}{2}(t-T_3)} \right) \right]^2,$$

where $T_3 > \max\{T_1, T_2\}$. Invoking the comparison principle, it follows that $V(t) \leq v(t)$ and, consequently, $(\sigma(t), z(t))$ converges to zero in finite time and reaches that value at most after a finite time given by

$$T = T_3 + \frac{2}{\gamma_2} \ln \left(\frac{\gamma_2}{\gamma_1} V^{\frac{1}{2}} (\sigma(T_3), z(T_3)) + 1 \right). \tag{165}$$

– *STEP 4 – Exponential convergence of the complete error system*

From the Lyapunov analysis developed above, the existence of the ideal sliding mode $\hat{\sigma}(t) \equiv \sigma(t) \equiv 0$ in finite time could be demonstrated. Since σ is the relative degree one output for the original closed-loop error system (120) with state X_e, it is possible to rewrite it into the normal form [80] such that the states of the transformed error system $\bar{X}_e := [\eta_e^T \ \sigma]^T$ are ISS with respect to σ, for a particular exponential class-$\mathcal{KL}$ function, where σ is treated as the "input" of the η_e–dynamics of this transformed system obtained from the linear similarity transformation $X_e = T\bar{X}_e$. Thus, X_e and $e = H_0 X_e$ tend exponentially to zero as well as the state ζ of the differentiator, which is also driven by e. This completes the proof of the theorem. $\qquad \square$

The main challenge in the stability analysis is to guarantee that the closed-loop system signals cannot escape in finite time, without invoking uniform boundedness of the signals (and disturbances) as is usually done in SMC literature. Note that our nonlinear disturbances are state dependent, and the state cannot be uniformly bounded by constants over all the stability domain, otherwise only local stability could be obtained or the fixed upper bounds would become unnecessarily large with quite conservative constants (which would also compromise the controller performance in practice).

Corollary 2 (*Stabilization for Multi-Output Systems*)**.** *Consider the following perturbed minimum-phase linear system*

$$\dot{x} = Ax + B[u + d(x,t)], \quad y = Cx, \tag{166}$$

where A, B, C are constant matrices of appropriate dimensions, $x \in \mathbb{R}^n$ is the unmeasured

state vector, $u \in \mathbb{R}$ is the control input, $y \in \mathbb{R}^m$ is the measured output vector and $d(x,t)$ is an absolutely continuous disturbance satisfying (A1). Assume that (166) is in some particular canonical form such that the state vector can be written as $x =: [x_1^T \ \xi^T]^T$, where $x_1 \in \mathbb{R}^{n-m-q}$ and the partition $\xi = [y^T \ \dot{y}^T]^T \in \mathbb{R}^{m+q}$ contains the measured portion of the state ($y \in \mathbb{R}^m$) and all of its needed derivatives ($\dot{y} \in \mathbb{R}^q$). Under the mentioned conditions, there exist a relative degree one variable $\sigma = S\xi$ for the system (166) and a linear transformation $\bar{x} = \bar{T}x$, with $\bar{x} := [\eta^T \ \sigma]^T$, such that (166) can be put into the form

$$\dot{\eta} = A_{11}\eta + A_{12}\sigma, \tag{167}$$

$$\dot{\sigma} = A_{21}\eta + A_{22}\sigma + K_p[u + \bar{d}(\eta, \sigma, t)], \tag{168}$$

where A_{11} is Hurwitz and $\bar{d}(\eta, \sigma, t)$ also continues satisfying (A1). If the control law of Theorem 3 is applied to (167)–(168), or (166), with $\hat{\sigma} = S\hat{\xi}$, the matrix S being constructed using the Ackermann-Utkin formula [97] and $\hat{\xi}$ being the estimate for ξ provided by the HOSM differentiator with dynamic gains in (130), we can guarantee that the sliding surface $\hat{\sigma} = \sigma = 0$ will be reached in finite time. Moreover, from the ISS property of (167), the state η tends to zero exponentially as $\sigma = 0$. Thus, by applying the inverse transformation $x = \bar{T}^{-1}\bar{x}$, one can conclude at least exponential convergence to zero for the original state vector x of (166). ⌟

Summarizing, Theorem 3 and Corollary 2 propose non local methodologies for tracking and stabilization using only output or partial-state feedback, and leading to an absolutely continuous control signal provided by a scalar or multivariable VGSTA controller. Such strategy ensures establishment of the sliding motion $\hat{\sigma} = 0$, with $\hat{\sigma}$ defined in (148). The continuity of the control signal can substantially reduce the chattering in comparison with the discontinuous first order SMC [54], as illustrated in the following academic example and experimental tests.

3.5   Simulation Example

Consider the following perturbed linear system in normal form (102)–(104) with relative degree two ($\rho = 2$) and second-order internal dynamics:

$$\dot{\eta}_1 = -\eta_1 + \xi_1\,,$$

$$\dot{\eta}_2 = -\eta_2 + \eta_1\,,$$

$$\dot{\xi}_1 = \xi_2\,,$$

$$\dot{\xi}_2 = -\xi_2 + \frac{1}{6}\xi_1 + \frac{1}{6}\sin\left(\eta_1 + \eta_2\right) + 2\cos\left(t\right) + u\,,$$

$$y = \xi_1\,,$$

where $x = [\eta^T,\ \xi^T]^T \in \mathbb{R}^4$, being the η and ξ the internal and external dynamics, respectively. The system is unstable in open-loop. The control aim is the trajectory tracking of $y_m = \frac{1}{(s+1)^2}r$, with

$$r(t) = \begin{cases} \sin\left(t\right)\,, & t \leq 20 \\ 0\,, & t > 20\,. \end{cases} \tag{169}$$

From (105), the nonlinear disturbance can be written as $d(x,t) = -\xi_2 + \frac{1}{6}\xi_1 + \frac{1}{6}\sin\left(\eta_1 + \eta_2\right) + 2\cos\left(t\right)$. The parameters $k_x = 7/6$ and $k_d = 13/6$ are chosen to satisfy the norm bound in (A1). Choosing the ideal sliding variable as $\sigma = \dot{e} + e$, we have:

$$\dot{\sigma} = \frac{1}{6}y + \frac{1}{6}\sin\left(\eta_1 + \eta_2\right) + 2\cos\left(t\right) + \dot{y}_m + y_m - r + u\,. \tag{170}$$

which is estimated by $\hat{\sigma} = \zeta_1 + e$ using a first order robust differentiator (130) with $\rho = 2$. In this case, $g_1(X,\sigma,t) = 0$, $g_2(X,t) = \frac{1}{6}y + \frac{1}{6}\sin\left(\eta_1 + \eta_2\right) + 2\cos\left(t\right) + \dot{y}_m + y_m - r$ and $\frac{d}{dt}g_2(X,t) = \frac{1}{6}\xi_2 + \frac{1}{6}\cos\left(\eta_1 + \eta_2\right)\left[y - \eta_2\right] - 2\sin\left(t\right) - y_m - \dot{y}_m + r - \dot{r}$. Thus, the controller (149) is implemented with $k_1(\hat{x},t)$ and $k_2(\hat{x},t)$ using $\varrho_1(\hat{x},t) = 0$ and $\varrho_2(\hat{x},t) = |\hat{x}| + 4 + 2|y_m| + 2|\dot{y}_m| + 2|r| + 2|\dot{r}|$. The other controller gains were: $k_3 = 1$, $\epsilon = 0.25$, $\delta = 0.01$, and $\beta = 7$. The following I/O filters were used $\omega_u = \frac{1}{(s+5)^3}u$, $\omega_y = \frac{1}{(s+5)^3}y$. For the norm observer, the parameters were selected as: $\gamma_x = 0.8$, $k_d = 13/6$, $c_1 = 0.05$, $c_2 = 1.4$. The initial conditions were chosen as $\eta_1(0) = -0.5$, $\eta_2(0) = 1$, $\xi_1(0) = 1$, $\xi_2(0) = 0.5$. Since $e = y - y_m$, the upper bound for $\ddot{e}$ is computed as $\mathcal{L}(\hat{x},t) = 7/6|\hat{x}| + |u| + 13/6 + |\ddot{y}_m(t)|$, where $|\ddot{y}_m(t)| = |-2\dot{y}_m - y_m + r|$ and the signals y_m, $\dot{y}_m$ can be implemented from the

state-space representation of the reference model.

The Euler integration method with fixed integration step of 10^{-5} s was used for the simulations. The results obtained for the proposed VGSTA are shown in Figs. Figure 7(a) to Figure 7(d). In Figure 7(c), it can be seen how, after a finite time, the norm observer state $\hat{x}$ overcomes the actual value of the x-norm and the upper bound $\mathcal{L}(\hat{x}, t)$ for $|\ddot{e}(t)|$ applied to the differentiator (130) is valid as well – see Figure 7(b). The successful achievement of exact tracking despite disturbances is shown in Figure 7(a) using a continuous control signal (Figure 7(d)). In Figure 7(e), the same tracking objective is pursued and achieved by means of an output-feedback first order sliding mode controller, as proposed in [54]. Nevertheless, the drawbacks of larger and discontinuous control signal appear, see Figure 7(f).
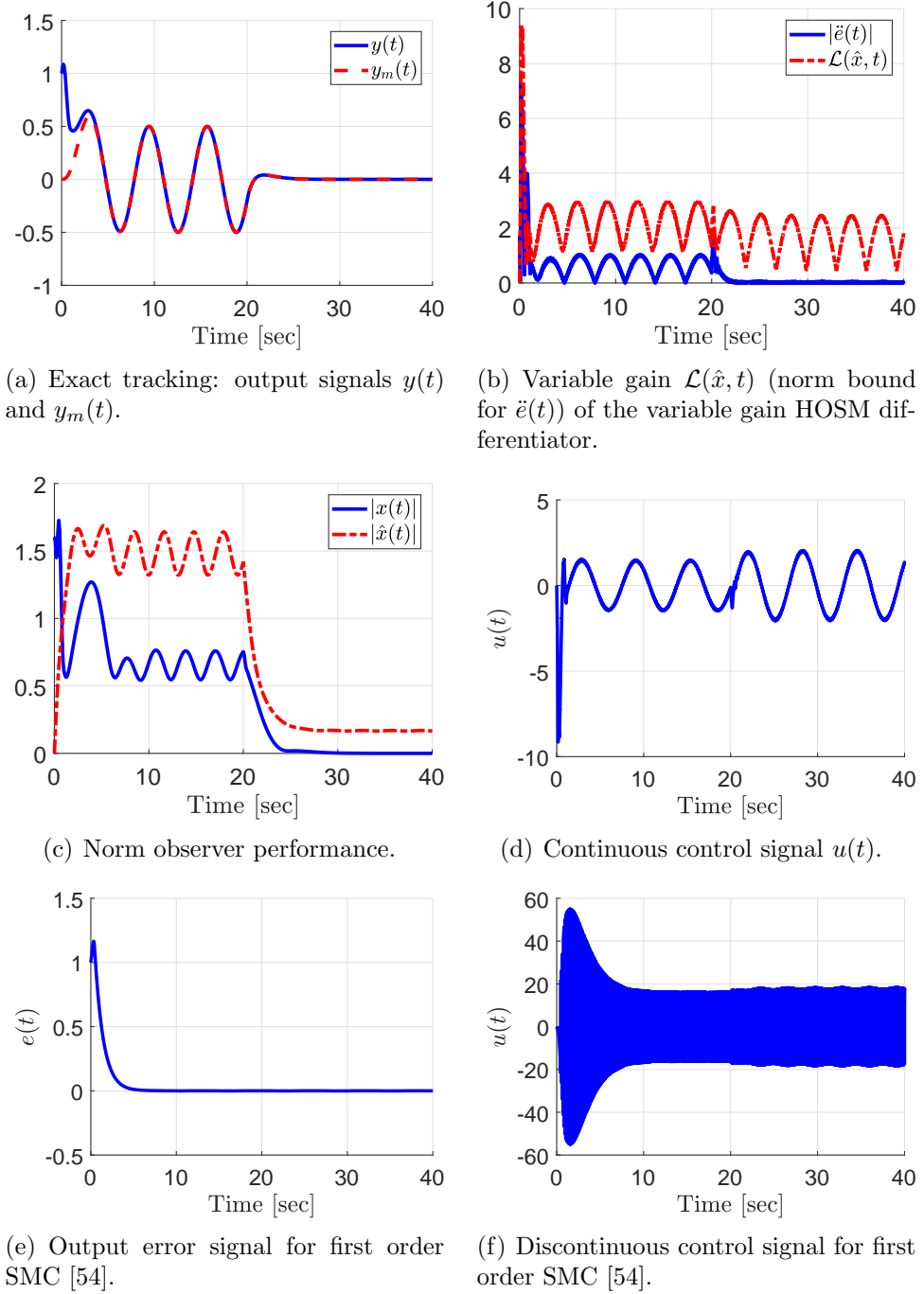
(a) Exact tracking: output signals $y(t)$ and $y_m(t)$.

(b) Variable gain $\mathcal{L}(\hat{x}, t)$ (norm bound for $\ddot{e}(t)$) of the variable gain HOSM differentiator.

(c) Norm observer performance.

(d) Continuous control signal $u(t)$.

(e) Output error signal for first order SMC [54].

(f) Discontinuous control signal for first order SMC [54].

Figure 7 – Simulation Results

3.6 Application Example

3.6.1 Model Description

To illustrate the application of our output-feedback VGSTA using the proposed adaptive HOSM differentiator, let us consider a seesaw experiment illustrated in Figure 8. The seesaw is free to rotate about the pivot in the center and the objective is to position

the cart on the track to balance the system. One possible real-world application of this system is the roll control of an airplane [98].

In this example, the output signals are the cart position $p(t)$ and the seesaw's tilt angle $\theta(t)$. The cart is driven by a DC motor which the armature voltage $u(t)$ is the only control signal. The system parameters are: constant motor torque $K_m = 0.00767$ V/(rad/sec), armature resistance $R_a = 2.6\ \Omega$, internal gear ratio $K_g = 3.7 : 1$, motor gear radius $r = 0.635$ cm, cart mass $m = 0.455$ Kg, seesaw mass $M = 3.3$ Kg, seesaw inertia $J_M = 0.42$ Kgm^2, center of gravity $c = 5.8$ cm and height of the track $h = 14$ cm.
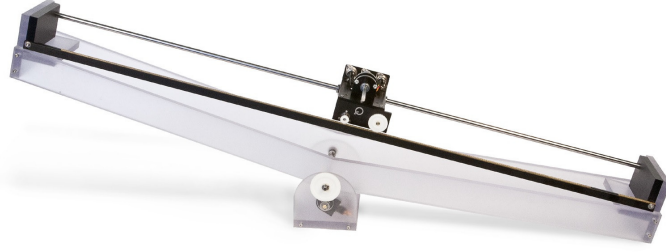

Figure 8 – Seesaw module and linear servo base unit of Quanser Consulting Inc.

From Figure 9, the cart position is described by the coordinate pair $(x_m, y_m) = (h\sin(\theta)+p\cos(\theta)\, , h\cos(\theta)-p\sin(\theta))$ and the gravity center of the seesaw is in $(x_M, y_M) = (c\sin(\theta)\, , c\cos(\theta))$. By considering kinetic energy $E_k = \frac{m}{2}\left(\sqrt{\dot{x}_m^2 + \dot{y}_m^2}\right)^2 + \frac{J_M}{2}\dot{\theta}^2$ and potential energy $E_p = Mg\ y_M + mg\ y_m$, the Lagrange function is given by $L = E_k - E_p$. Taking into account the Lagrangian mechanics, one can obtain the dynamic equations which govern the system by computing

$$\frac{\partial}{\partial t}\left(\frac{\partial L}{\partial \dot{q}}\right) - \frac{\partial L}{\partial q} = Q_q\,,$$

where q is a generalized coordinate and Q_q is the sum of nonconservatives forces that act in the q axis. In the example, $q = \{p, \theta\}$ with $Q_p = F - b_m\dot{p}$ and $Q_\theta = -b_M\dot{\theta}$, where F is the force that acts in the cart through the DC motor, b_m and b_M are viscous frictions related to the cart and seesaw, respectively. The modeling of the electrical phenomena together with the equations of the mechanical part, derived by Lagrange approach, allow us to describe the system by a complete state-space representation. The state vector is assigned as $x := [p\ \theta\ \dot{p}\ \dot{\theta}]^T$, so that the complex nonlinear system $\dot{x} = f(x, u)$ representing

the set formed by the DC motor–cart–seesaw is simply

$$\dot{x}_1 = x_3 \,, \tag{171}$$

$$\dot{x}_2 = x_4 \,, \tag{172}$$

$$\dot{x}_3 = \frac{2mhx_1x_3x_4 - Mgch\sin(x_2) - mghx_1\cos(x_2)}{J_M + mx_1^2}$$
$$+ \frac{mh^2x_1x_4^2 - h^2b_mx_3 + hb_Mx_4}{J_M + mx_1^2} + x_1x_4^2 + g\sin(x_2)$$
$$- \frac{(mh^2 + J_M + mx_1^2)}{m(J_M + mx_1^2)}\left(\frac{K_mK_g}{r}\right)^2\frac{1}{R_a}x_3$$
$$- \frac{b_m}{m}x_3 + \frac{(mh^2 + J_M + mx_1^2)}{m(J_M + mx_1^2)}\frac{K_mK_g}{rR_a}u \,, \tag{173}$$

$$\dot{x}_4 = \frac{-2mx_1x_3x_4 + Mgc\sin(x_2) + mgx_1\cos(x_2)}{J_M + mx_1^2}$$
$$+ \frac{-mhx_1x_4^2 + hb_mx_3 - b_Mx_4}{J_M + mx_1^2}$$
$$+ \frac{h}{J_M + mx_1^2}\left(\frac{K_mK_g}{r}\right)^2\frac{1}{R_a}x_3 - \frac{h}{J_M + mx_1^2}\frac{K_mK_g}{rR_a}u \,, \tag{174}$$

$$y = [x_1 \; x_2]^T \,. \tag{175}$$

There is no problem in considering a simplified (linear) model of the plant when a robust control strategy is implemented. Essentially in practice, this is exactly the main reason to choose a sliding mode controller robust to unmodelled dynamics, parametric uncertainties and nonlinear disturbances rather than a linear control, which is not robust in this general sense. In order to facilitate the control design for the local stabilization problem, it is more attractive to appreciate the linearized version of the nonlinear system described by (171)–(174) in the form (105), such that one can write

$$\dot{x}(t) = Ax(t) + Bu(t) \,,$$
$$y(t) = Cx(t) \,,$$

where $A = \partial f(x, u)/\partial x$ and $B = \partial f(x, u)/\partial u$ are the Jacobian matrices in the equilibrium. Therefore, the linearization of the nonlinear system around $x = 0$ yields:
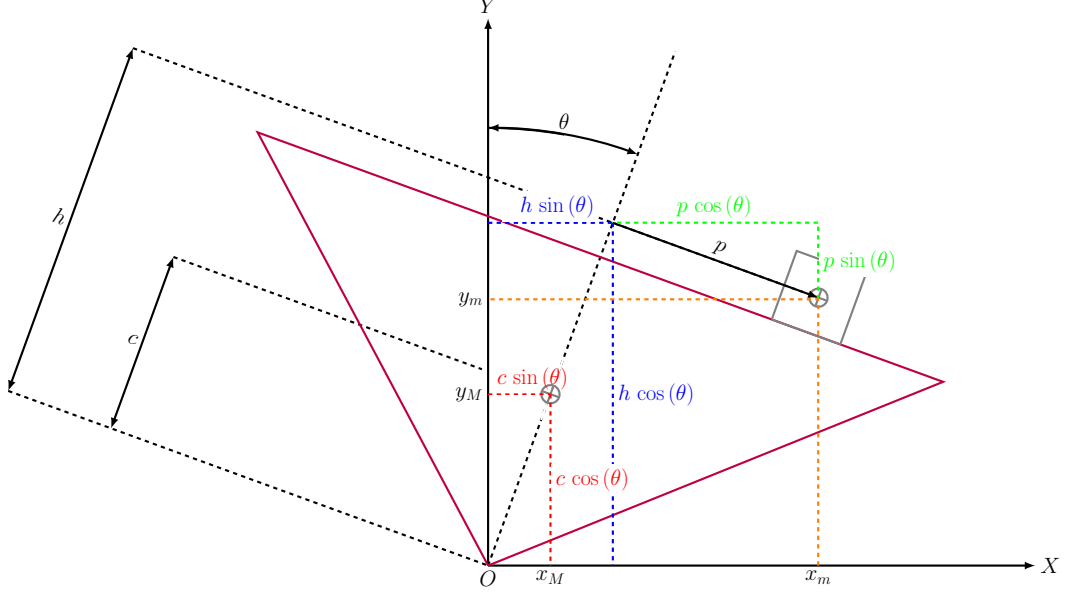
Figure 9 – Diagram of the seesaw-cart scheme.

$$A = \begin{bmatrix} 0 & 0 & 1 & 0 \\ 0 & 0 & 0 & 1 \\ \dfrac{-mgh}{J_M} & \dfrac{(J_M - Mhc)g}{J_M} & -\dfrac{\left(mr^2 R_a h^2 b_m + b_m r^2 R_a J_M + K_m^2 K_g^2 \left(J_M + mh^2\right)\right)}{mr^2 R_a J_M} & \dfrac{b_M h}{J_M} \\ \dfrac{mg}{J_M} & \dfrac{Mgc}{J_M} & \dfrac{r^2 R_a b_m h + K_m^2 K_g^2 h}{r^2 R_a J_M} & -\dfrac{b_M}{J_M} \end{bmatrix}, \qquad (176)$$

$$B = \begin{bmatrix} 0 \\ 0 \\ \dfrac{K_m K_g \left(J_M + mh^2\right)}{mr R_a J_M} \\ -\dfrac{K_m K_g h}{r R_a J_M} \end{bmatrix}, \qquad C = \begin{bmatrix} 1 & 0 & 0 & 0 \\ 0 & 1 & 0 & 0 \end{bmatrix}. \qquad (177)$$

Numerically, for $b_m = 0$ and $b_M = 0$, it can be noted that

$$A = \begin{bmatrix} 0 & 0 & 1 & 0 \\ 0 & 0 & 0 & 1 \\ -1.4495 & 9.2002 & -17.2327 & 0 \\ 10.3538 & 4.3554 & 2.4947 & 0 \end{bmatrix}, B = \begin{bmatrix} 0 \\ 0 \\ 3.8559 \\ -0.5582 \end{bmatrix}.$$

The linear approximation has output signals $y_1 = x_1 = p$ and $y_2 = x_2 = \theta$, it is controllable, observable and has eigenvalues $\lambda_i \in \{2.6854, -1.4153 \pm j0.4587, -17.0875\}$, $i = 1, \ldots, 4$.

3.6.2   Control Design

For designing the sliding variable σ it is employed the Ackermann-Utkin formula [97], such that the closed-loop eigenvalues are assigned as $\lambda_{1,2} = -2 \pm j2$, $\lambda_3 = -8.5$ and $\lambda_4 = -11$. According to Corollary 2, by driving σ to zero then the state vector x goes to zero. Thus, it is obtained the ideal sliding variable

$$\sigma = 54.9063 x_1 + 52.5038 x_2 + 4.2986 x_3 + 18.4658 x_4 \,,$$

that can be estimated by

$$\hat{\sigma} = 54.9063 x_1 + 52.5038 x_2 + 4.2986 \zeta_1^p + 18.4658 \zeta_1^\theta \,, \tag{178}$$

where ζ_1^p and ζ_1^θ are the state variables of two exact differentiators in the form (130), with $\rho = 2$, which estimate $x_3 = \dot{p}$ and $x_4 = \dot{\theta}$, respectively.

A state-norm observer $\hat{x}_3$ is applied to estimate an upper bound for the norm of the unmeasurable state variable x_3 by using only known upper/lower bounds for the system parameters and available signals. The norm observer applied here is given by

$$\dot{\hat{x}}_3 = -15\hat{x}_3 + 1.5\,|x_1| + 10\,|x_2| + 4\,|u| \,. \tag{179}$$

This approach guarantees a less conservative estimate for the dynamic gains $\mathcal{L}(\hat{x}, t)$ since it is possible to construct a norm bound for $\dot{x}_3$ and $\dot{x}_4$ to be used in the exact differentiators taking into account the state vector upper bound

$$\hat{x} := [x_1 \ x_2 \ \hat{x}_3]^T.$$

Using the output signals x_1, x_2 and the norm observer variable $\hat{x}_3$, the gains of the differentiators are given by

$$\mathcal{L}_p\,(\hat{x}, t) = 2\,|x_1| + 10\,|x_2| + 20\,|\hat{x}_3| + 4\,|u| \,, \tag{180}$$

$$\mathcal{L}_\theta\,(\hat{x}, t) = 11\,|x_1| + 5\,|x_2| + 3\,|\hat{x}_3| + |u| \,. \tag{181}$$

Therefore, the exact differentiators (182)–(185) can be implemented and (178) be obtai-

ned:

$$\dot{\zeta}_0^p = v_0^p = -5\mathcal{L}_p\left(\hat{x}, t\right)^{\frac{1}{2}} \left|\zeta_0^p - y_1\right|^{\frac{1}{2}} \operatorname{sgn}\left(\zeta_0^p - y_1\right) + \zeta_1^p, \tag{182}$$

$$\dot{\zeta}_1^p = -3\mathcal{L}_p\left(\hat{x}, t\right) \operatorname{sgn}\left(\zeta_1^p - v_0^p\right), \tag{183}$$

$$\dot{\zeta}_0^\theta = v_0^\theta = -5\mathcal{L}_\theta\left(\hat{x}, t\right)^{\frac{1}{2}} \left|\zeta_0^\theta - y_2\right|^{\frac{1}{2}} \operatorname{sgn}\left(\zeta_0^\theta - y_2\right) + \zeta_1^\theta, \tag{184}$$

$$\dot{\zeta}_1^\theta = -3\mathcal{L}_\theta\left(\hat{x}, t\right) \operatorname{sgn}\left(\zeta_1^\theta - v_0^\theta\right). \tag{185}$$

3.6.3   Experimental Results

In this application example, we have considered $d(x, t) = 0$ in (105) and the controller parameters were chosen simply as $\varrho_1(\hat{x}, t) = 0$, $\varrho_2(\hat{x}, t) = 0$, $k_3 = 1$, $\delta = 0.01$, $\beta = 5$, and $\epsilon = 1$, for the purpose of local stabilization of the linearized model in (176)–(177).

In what follows, simulations and experimental results of balancing control using the proposed output-feedback VGSTA for the seesaw are presented in the right column of Figures 4, 5 and 6. The $\mathcal{L}$ gains of differentiators computed based on the norm observer signal allow the automatic adjustment of their amplitudes when demanded. Thereby the control action in closed-loop system, such dynamic gains $\mathcal{L}_p$ and $\mathcal{L}_\theta$ tend to decrease as the norm observer variable $\hat{x}_3$ vanishes, as shown in Figure 11(d), Figure 11(f), and Figure 10(f), respectively. The VGSTA has a smooth control action which decays as long as the closed-loop system is stabilized, see Figure 10(h). Its performance can be evaluated from Figure 10(b), Figure 10(d), Figure 12(b) and Figure 12(d), where $x_1 = p$ and $x_2 = \theta$ are the measured signals whereas ζ_1^p and ζ_1^θ are constructed by means of the proposed variable-gain differentiators, to overcome the lack of the state variables x_3 and x_4.

The continuous control signal u is able to guarantee the convergence of sliding variable $\hat{\sigma}$ in Figure 11(b) to a neighborhood of zero in finite time in spite of the clear adverse effects provoked by measurement noise, unmodeled dynamics, switching delays and numerical discretization with lower sampling frequency (integration step of 10^{-3}) noted in the collected signals.

The left column of Figures 4, 5 and 6 also presents the experiments for classical FOSMC so that a more clear comparison can be portrayed with the proposed generalization of VGSTA. From this plots it is possible to realize the advantages achieved by our

output-feedback VGSTA in terms of smaller residual sets in the stabilization error and considerable reduction of switching amplitude and frequency of the control signal when compared to FOSMC. Moreover, in [94] and [99], a detailed and fair study is performed highlighting the conditions where one strategy is potentially better than the other.

We carried out experimental comparisons of the proposed output-feedback generalization for VGSTA only with the classical FOSMC. However, we suggest to the readers the publication [100] for a wider discussion about such various SMC controllers available in the literature for arbitrary order systems. There, the authors have focused the discussion on: (a) first-order sliding mode control, (b) non-singular terminal sliding modes, (c) second-order sliding mode (SOSM) algorithms (twisting and super-twisting) as well as (d) quasi-continuous HOSM finite-time controllers.

As a general rule, the discontinuities in control lead to chattering – an unacceptable phenomenon in some applications. The major advantage of VGSTA when compared with other nonlinear sliding surface based controllers like Twisting Algorithm, Non-Singular Terminal, Nested SMC and Quasi-Continuous SMC is to ensure a continuous control signal. Despite the chapter contribution focus on VGSTA generalization using variable-gains based HOSM differentiators, it can be also extended to this class of sliding mode controllers. At this point the reader could argument that a possible solution for control signal discontinuity would be evident: the control signal being generated by the output of an auxiliary integrator with a discontinuous function of the state and time derivative of σ as an output. Of course, this modification remains in the framework of the conventional sliding mode control, but applies an extra artificial derivative of the signal σ which is not needed for STA or VGSTA.

(a) FOSMC: Plant state variable x_1.   (b) VGSTA: Plant state variable x_1.

(c) FOSMC: Plant state variable x_2.   (d) VGSTA: Plant state variable x_2.

(e) FOSMC: Norm observer $\hat{x}$.   (f) VGSTA: Norm observer $\hat{x}$.

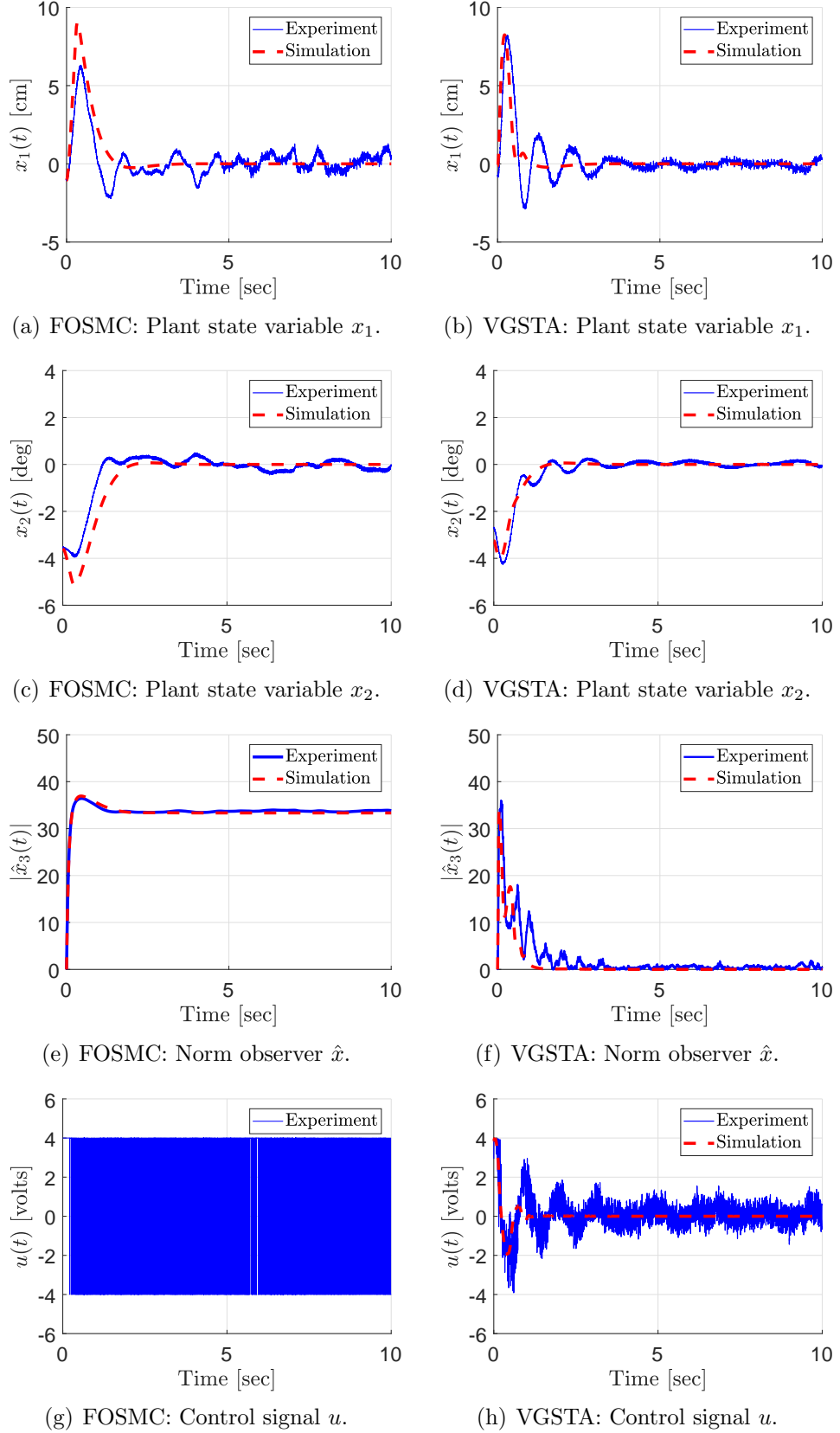(g) FOSMC: Control signal u.   (h) VGSTA: Control signal u.

Figure 10 – Experimental Results: First-Order Sliding Mode Control (FOSMC) × Variable Gain Super-Twisting Algorithm (VGSTA).

(a) FOSMC: Sliding variable $\hat{\sigma}$.
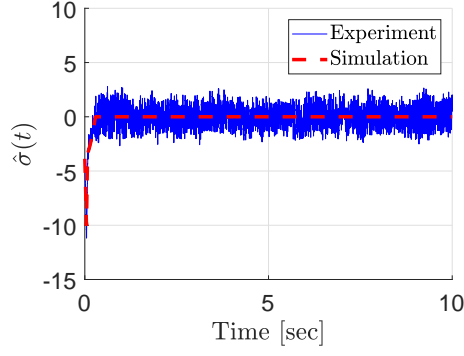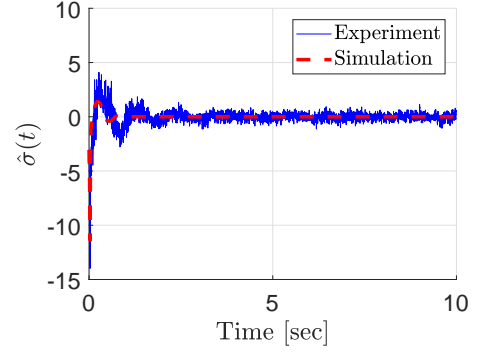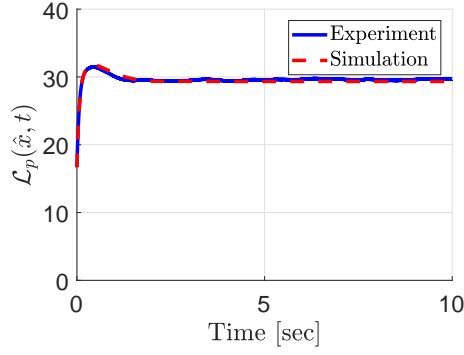
(b) VGSTA: Sliding variable $\hat{\sigma}$.

(c) FOSMC: Gain of the exact differentiator $\mathcal{L}_p$.

(d) VGSTA: Gain of the exact differentiator $\mathcal{L}_p$.

(e) FOSMC: Gain of the exact differentiator $\mathcal{L}_\theta$.
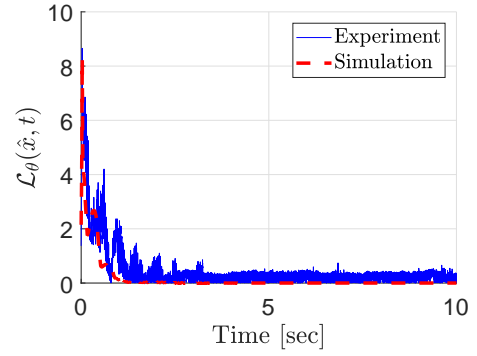
(f) VGSTA: Gain of the exact differentiator $\mathcal{L}_\theta$.

Figure 11 – Experimental Results: First-Order Sliding Mode Control (FOSMC) $\times$ Variable Gain Super-Twisting Algorithm (VGSTA).
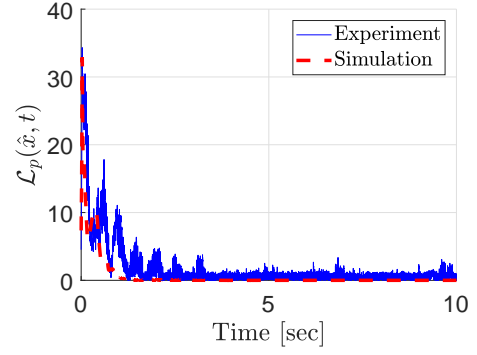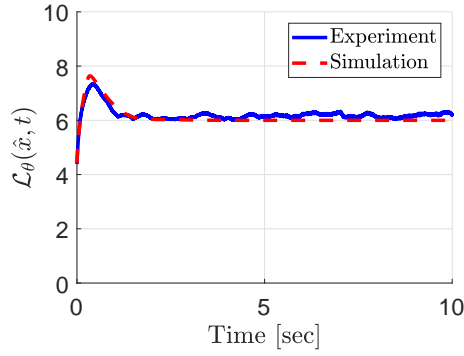
(a) FOSMC: Differentiator state variable ζ_1^p.

(b) VGSTA: Differentiator state variable ζ_1^p.

(c) FOSMC: Differentiator state variable ζ_1^θ.

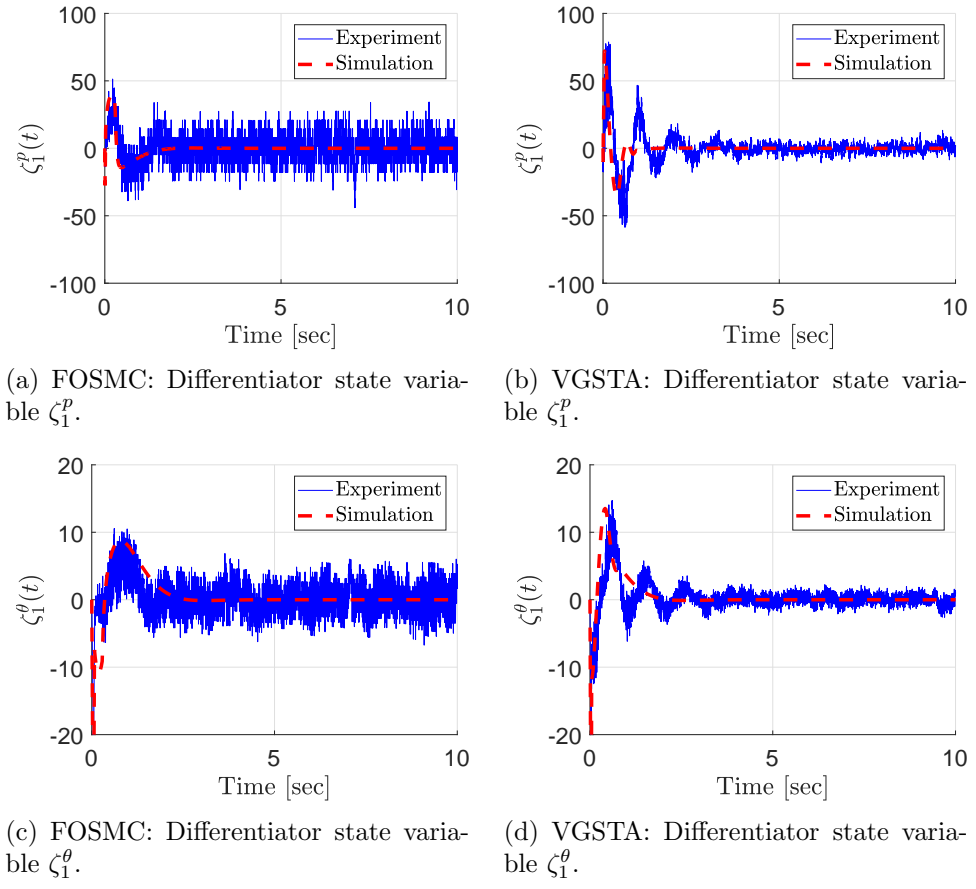(d) VGSTA: Differentiator state variable ζ_1^θ.

Figure 12 – Experimental Results: First-Order Sliding Mode Control (FOSMC) $\times$ Variable Gain Super-Twisting Algorithm (VGSTA).

4 OTHER SLIDING MODES CONTROLLERS

This chapter develops a higher-order sliding mode (HOSM) based global differentiator with adaptive gains to address the tracking control problem using only input-output information of a wider class of nonlinear systems with disturbances and parametric uncertainties. The complete state of the plant is assumed unmeasured so that a norm state estimator is constructed to norm bound the state-dependent disturbances and dynamically update the gains of the proposed differentiator. Stability properties and robust exact tracking can be achieved when the proposed adaptive HOSM based differentiator is applied to output-feedback purposes. Numerical simulations are presented for different sliding mode control designs, such as: (a) first-order sliding mode control, (b) terminal sliding modes, (c) second order sliding mode algorithms (twisting and super-twisting), (d) nested sliding mode control as well as (e) quasi-continuous HOSM finite-time controllers.

4.1 Problem Formulation

Consider an uncertain nonlinear plant described by:

$$\dot{x} = A_p x + B_p[u + d(x,t)] + \phi(t), \qquad y = H_p x, \qquad (186)$$

where $x \in \mathbb{R}^n$ is the state, $u \in \mathbb{R}$ is the input, $y \in \mathbb{R}$ is the output, $d(x,t) \in \mathbb{R}$ is a state dependent uncertain disturbance and $\phi(t)$ is a time-varying uncertain unmatched external disturbance. The term "unmatched" refers to $\phi(t)$ not contained in the range space of B_p, otherwise $\phi(t)$ could be directly incorporated into the "matched" disturbance $d(x,t)$. The uncertain matrices A_p, B_p and H_p belong to some compact set, such that the necessary uncertainty bounds to be defined later are available for design. The following assumptions are made in the chapter:

(A1) $G(s) = H_p(sI - A_p)^{-1}B_p$ is minimum phase.

(A2) The pair (A_p, B_p) is controllable and observable.

(A3) The transfer function $G(s)$ has a known relative degree ρ and order n. The *high frequency gain* (HFG) $K_p \in \mathbb{R}$ satisfies $K_p = \lim_{s \to \infty} s^\rho G(s) = H_p A_p^{\rho-1} B_p$. Without loss of generality, we assume that $K_p > 0$.

(A4) The input disturbance $d(x,t)$ is assumed to be uncertain, locally integrable and norm bounded by $|d(x,t)| \leq k_x|x| + k_d$, $\forall x, t$, where $k_x, k_d \geq 0$ are *known* scalars. The unmatched disturbance $\phi(t)$ is assumed sufficiently smooth. Moreover, there exists a *known* constant $k_\phi \geq 0$ such that $|\phi^{(i)}(t)| \leq k_\phi$, $\forall i = 0, \ldots, \rho$.

Assumptions (A1)–(A3) are usual in model reference adaptive control (MRAC) [16]. From (A4), we note that the relative degree of (186) depends only on the linear part, being independent of the disturbances d and ϕ. In addition, the class of nonlinear disturbances are more general than those considered in $[2, 4, 5, 14]$ and represents a challenge in the context of global output-feedback SMC.

Let the reference signal $y_m(t) \in \mathbb{R}$ be generated by the following reference model

$$y_m = W_m(s)\, r\,, \quad W_m(s) = (s + \gamma_m)^{-1} L_m^{-1}(s)\,, \quad \gamma_m > 0, \tag{187}$$

where $r(t) \in \mathbb{R}$ is an arbitrary uniformly bounded piecewise continuous reference signal and

$$L_m(s) = s^{(\rho-1)} + l_{\rho-2} s^{(\rho-2)} + \cdots + l_1 s + l_0\,, \tag{188}$$

with $L_m(s)$ being a Hurwitz polynomial. The transfer function matrix $W_m(s)$ has the same relative degree as $G(s)$ and its HFG is the unity. The main objective is to find a control law u such that the output error

$$e(t) := y(t) - y_m(t) \tag{189}$$

is steered to zero, for arbitrary initial conditions.

The MRAC parametrization [16] using I/O filters is initially applied to obtain the *ideal matching control* [16] denoted by u^* and derive the dynamic error equations for the error system. However, we are not trying to recover any particular property from MRAC. In this sense, when the plant is known and $d(t) \equiv 0$, $\phi(t) \equiv 0$, a control law which achieves the matching between the closed-loop transfer function matrix and $W_m(s)$ is

$$u^* = \theta^{*T} \omega\,, \quad \theta^* = \begin{bmatrix} \theta_1^{*T} & \theta_2^{*T} & \theta_3^* & \theta_4^* \end{bmatrix}^T, \tag{190}$$

where θ^* is the parameter vector with $\theta_1^*, \theta_2^* \in \mathbb{R}^{(n-1)}$ and $\theta_3^*, \theta_4^* \in \mathbb{R}$. The regressor vector

$\omega = [\omega_u^T \ \omega_y^T \ y \ r]^T$, $w_u, w_y \in \mathbb{R}^{(n-1)}$ is obtained from I/O state variable filters given by:

$$\dot{\omega}_u = \Phi\omega_u + \Gamma u, \qquad \dot{\omega}_y = \Phi\omega_y + \Gamma y, \tag{191}$$

where $\Phi \in \mathbb{R}^{(n-1)\times(n-1)}$ is Hurwitz and $\Gamma \in \mathbb{R}^{(n-1)}$ is chosen such that the pair $(\Phi, \ \Gamma)$ is controllable. The matching conditions require that $\theta_4^* = K_p^{-1}$. Define the augmented state vector

$$X = [x^T, \omega_u^T, \omega_y^T]^T, \tag{192}$$

with dynamics described by $\dot{X} = A_0 X + B_0 u + B_0' d + B_\phi \phi$, and output $y = H_0 X$, where

$$A_0 = \begin{bmatrix} A_p & 0 & 0 \\ 0 & \Phi & 0 \\ (\Gamma H_p) & 0 & \Phi \end{bmatrix}, \ B_0 = \begin{bmatrix} B_p \\ \Gamma \\ 0 \end{bmatrix}, \ B_0' = \begin{bmatrix} B_p \\ 0 \\ 0 \end{bmatrix}, \tag{193}$$

$$B_\phi^T = \begin{bmatrix} I & 0 & 0 \end{bmatrix}, \quad H_0 = \begin{bmatrix} H_p & 0 & 0 \end{bmatrix}. \tag{194}$$

Then, adding and subtracting $B_0 \theta^{*T} \omega$ and noting that there exist matrices Ω_1 and Ω_2 such that [16]

$$\omega = \Omega_1 X + \Omega_2 r, \tag{195}$$

one has

$$\dot{X} = A_c X + B_c K_p [\theta_4^* r + u - u^*] + B_0' d + B_\phi \phi, \quad y = H_0 X, \tag{196}$$

where $A_c = A_0 + B_0 \theta^{*T} \Omega_1$ and $B_c = B_0 \theta_4^*$. Notice that (A_c, B_c, H_0) is a nonminimal realization of $W_m(s)$. For analysis purposes, the reference model can be described by

$$\dot{X}_m = A_c X_m + B_c K_p [\theta_4^* r - d_f] + B_0' d + B_\phi \phi, \quad y_m = H_0 X_m, \tag{197}$$

where the equivalent input disturbance $d_f = W_d(s)d + W_\phi(s)\phi$ with

$$W_d(s) = [W_m(s)K_p]^{-1} H_0 (sI - A_c)^{-1} B_0', \tag{198}$$

$$W_\phi(s) = [W_m(s)K_p]^{-1} H_0 (sI - A_c)^{-1} B_\phi. \tag{199}$$

Note that $W_d(s)$ in (198) is a stable and proper transfer function and $W_\phi(s)$ in (199) is a stable and possibly improper transfer function, so that derivatives of $\phi(t)$ may ap-

pear in the input channel. Now, remind that $[W_m(s)K_p]^{-1} = \bar{K}_\rho s^\rho + \bar{K}_{\rho-1} s^{\rho-1} + \ldots + \bar{K}_0$, where $\bar{K}_i \in \mathbb{R}$, $i = 0, \ldots, \rho$, are constants. By using the Markov parameters to represent $H_0 (sI - A_c)^{-1} B_\phi = \frac{H_0 B_\phi}{s} + \frac{H_0 A_c B_\phi}{s^2} + \frac{H_0 A_c^2 B_\phi}{s^3} + \ldots$, the term $d_f(t)$ can be rewritten as

$$d_f := K_{\rho-1} \phi^{(\rho-1)} + \cdots + K_1 \dot{\phi} + W_p(s) * \phi + W_d(s) * d, \tag{200}$$

where $*$ denotes the convolution operator, $K_j \in \mathbb{R}^{1 \times n}$ is given by

$$K_j = \sum_{i=j+1}^{\rho} \bar{K}_i H_0 A_c^{i-j-1} B_\phi, \quad j = 1, \ldots, \rho - 1, \tag{201}$$

and $W_p(s)$ is a stable and proper transfer function matrix

$$W_p(s) = \sum_{i=1}^{\rho} \bar{K}_i H_0 A_c^{i-1} B_\phi + \sum_{i=0}^{\rho} \bar{K}_i H_0 A_c^i (sI - A_c)^{-1} B_\phi. \tag{202}$$

Thus, the error dynamics with state

$$X_e := X - X_m \tag{203}$$

can be written in the the state-space representation by

$$\dot{X}_e = A_c X_e + B_c K_p [u - \theta^{*T} \omega + d_f], \tag{204}$$

$$e = H_0 X_e, \tag{205}$$

or in the I/O form as: $e = W_m(s)K_p \left[u - \theta^{*T} \omega + d_f \right]$. The importance of considering the augmented dynamics (196) with state X including the I/O filters (191) is not only to derive the full-error equation (204), but to create an output-feedback framework which allow us to derive norm bounds for the unmeasured state of a possible unstable plant (186) and for the equivalent disturbance $d_f(x, t)$, as discussed in the next section. As a bonus, we use (204) in the proof of the main theorem to state global stability by means of input-to-state properties of the closed-loop system, without appealing to Lyapunov based analysis.

4.2   State-Norm Observer

Considering Assumption (A4) and applying [8, Lemma 3] to (196), it is possible to find $k_x^* > 0$ such that, for $k_x \in [0, k_x^*]$, a norm bound for X and x can be obtained through stable *first order approximation filters* (FOAFs) (see details in [8]). Thus, one has

$$|x(t)|, |X(t)| \leq |\hat{x}(t)| + \hat{\pi}(t), \tag{206}$$

$$\hat{x}(t) := \frac{1}{s + \lambda_x}[c_1(k_d + k_\phi) + c_2|\omega(t)|], \tag{207}$$

with $c_1, c_2, \lambda_x > 0$ being appropriate constants that can be computed by the optimization methods mentioned in [8]. In this sense, (206)–(207) state that the norm observer estimate $\hat{x}(t)$ provides a valid norm bound for the unmeasured state x of the uncertain and disturbed plant, *i.e.*, $|x| \leq |\hat{x}|$ except for exponentially decaying terms due to the system initial conditions, denoted here by $\hat{\pi}(t)$.

Since we assume sufficient differentiability for ϕ and uniform boundedness for its time derivatives, one can find a constant $\bar{k}_\phi > 0$ such that $|K_1 \dot{\phi} + \ldots + K_{\rho-1} \phi^{(\rho-1)}| \leq \bar{k}_\phi$ and $|d_f| \leq \bar{k}_\phi + |W_p(s) * \phi| + |W_d(s) * d|$. Moreover, from (A4) and (207), one has $|d(x,t)| \leq k_x \hat{x}(t) + k_d$, *modulo* $\hat{\pi}$ term, and one can write $|d_f| \leq \hat{d}_f + \hat{\pi}_f$, where $\hat{\pi}_f$ is an exponentially decreasing term,

$$\hat{d}_f(t) := \bar{k}_\phi + \frac{c_f}{s + \lambda_f}[k_\phi + k_x \hat{x}(t) + k_d], \tag{208}$$

and $\frac{c_f}{s+\lambda_f}$ is a FOAF designed for $W_d(s)$ and $W_p(s)$, with adequate positive constants c_f and λ_f. At the price of some conservatism, we can simplify the FOAF design by choosing c_f sufficiently large and λ_f sufficiently small.

4.3   Global Differentiator with Adaptive Gains

In what follows, a HOSM differentiator with coefficients being adapted using the estimate for the norm of the state x provided in (206) is proposed to achieve global exact estimation, *i.e.*, exact differentiation of signals with any initial conditions and unbounded higher derivatives.

Under the assumptions (A1)–(A4), the unmatched time-varying disturbance $\phi(t)$ cannot change the relative degree of the unperturbed linear system (186), thus it is easy

to show that the nonlinear system (186) can be transformed into the *normal form* [80]:

$$\dot{\eta} \;=\; \mathcal{A}_0\eta + \mathcal{B}_0 y\,, \tag{209}$$

$$\dot{\xi} \;=\; \mathcal{A}_\rho\xi + \mathcal{B}_\rho K_p[u + d_e(x,t)]\,, \quad y = \mathcal{C}_\rho\xi\,, \tag{210}$$

where $z^T = [\eta^T\ \xi^T] \in \mathbb{R}^n$ with $\eta \in \mathbb{R}^{(n-\rho)}$ being referred to the state of the inverse or zero dynamics and $\xi = [y\ \dot{y}\ \ldots\ y^{(\rho-1)}]^T$ the state of the external dynamics. The triple $(\mathcal{A}_\rho,\ \mathcal{B}_\rho,\ \mathcal{C}_\rho)$ is in the Brunovsky's controller form [80] and $\mathcal{A}_0$ is Hurwitz. The equivalent input disturbance $d_e(x,t) = d(x,t) + K_p^{-1}\left(H_p A_p^\rho x + \sum_{i=0}^{\rho-1} H_p A_p^{\rho-1-i}\phi^{(i)}\right)$ is affinely norm bounded by

$$|d_e(x,t)| \le \kappa_1|x| + \kappa_2\,, \tag{211}$$

where $\kappa_2 > k_d + K_p^{-1}\left|\sum_{i=0}^{\rho-1} H_p A_p^{\rho-1-i}\phi^{(i)}\right|$ and $\kappa_1 > k_x + K_p^{-1}\left|H_p A_p^\rho\right|$ are known constants. We can conclude the following state-dependent upper bound for higher derivative (order ρ) of the output signal

$$|y^{(\rho)}| \le K_p\left[\kappa_1|x| + \kappa_2 + |u|\right]\,. \tag{212}$$

From (212) and (189), we can write

$$|e^{(\rho)}(t)| \le L(x,t) = K_p\left[\kappa_1|x| + \kappa_2 + |u|\right] + |y_m^{(\rho)}(t)|\,. \tag{213}$$

Now, assume that the control input satisfies

$$|u| = k_\varrho\varrho(t) \le \kappa_3\|X_t\| + \kappa_4\,, \tag{214}$$

for constants $k_\varrho,\kappa_3,\kappa_4 > 0$ and an appropriate continuous *modulation function* $\varrho(t) \ge 0$, to be defined later on. Then, applying (206), we can obtain the following upper bound with the norm observer variable $\hat{x}(t)$ in (206)–(207):

$$|e^{(\rho)}(t)| \le K_p\left[\kappa_1|\hat{x}| + \kappa_2 + \varrho(t)\right] + |y_m^{(\rho)}(t)|\,, \tag{215}$$

modulo exponential decaying terms due to initial conditions, which take into account the transient of the FOAF. By defining known positive constants k_1, k_2, k_3 and k_m satisfying

$k_m \geq |y_m^{(\rho)}(t)|$, $k_1 \geq K_p\kappa_1$, $k_2 \geq K_p\kappa_2 + k_m$ and $k_3 \geq K_p$, we can define

$$\mathcal{L}(\hat{x}, t) := k_1|\hat{x}| + k_2 + k_3\varrho(t),\tag{216}$$

and state the following upper bound constructed only with measurable signals

$$|e^{(\rho)}(t)| \leq \mathcal{L}(\hat{x}, t), \quad \forall t \geq T,\tag{217}$$

for some finite time $T > 0$.

In light of (216)–(217), we can introduce the following HOSM differentiator of order $p = \rho - 1$ with dynamic gains for the output error $e \in \mathbb{R}$:

$$\dot{\zeta}_0 = v_0 = -\lambda_0 \mathcal{L}(\hat{x}, t)^{\frac{1}{p+1}} |\zeta_0 - e(t)|^{\frac{p}{p+1}} \mathrm{sgn}(\zeta_0 - e(t)) + \zeta_1,$$

$$\vdots$$

$$\dot{\zeta}_i = v_i = -\lambda_i \mathcal{L}(\hat{x}, t)^{\frac{1}{p-i+1}} |\zeta_i - v_{i-1}|^{\frac{p-i}{p-i+1}} \mathrm{sgn}(\zeta_i - v_{i-1}) + \zeta_{i+1},\tag{218}$$

$$\vdots$$

$$\dot{\zeta}_p = -\lambda_p \mathcal{L}(\hat{x}, t)\mathrm{sgn}(\zeta_p - v_{p-1}).$$

Sufficient conditions for finite-convergence of HOSM differentiators with variable gains were already formulated in [11]. The main difference is that there the authors assume the measurement of the state vector. In the proposed differentiator (218), the global upper bound $\mathcal{L}(\hat{x}, t)$ must be absolutely continuous and its logarithmic derivative $\dot{\mathcal{L}}/\mathcal{L}$ must be bounded, that is, $|\dot{\mathcal{L}}/\mathcal{L}| \leq M$, where $M > 0$ is some constant. It implies that $\mathcal{L}(\hat{x}, t)$ can grow at most exponentially.

According to the linear growth condition assumed in (A4) for the system non-linearities and the *regularity condition* [57] assumed in (214) for the control signal, any finite-escape is precluded and only exponentially growing signals are possible in the closed-loop system, as it will be show in the proof of the main theorem. Thus, if the parameters λ_i are properly recursively chosen[3], the following equalities

$$\zeta_0 = e(t), \quad \zeta_i = e^{(i)}(t), \quad i = 1, \ldots, p,\tag{219}$$

---

[3]In particular, the following choice is valid for $p \leq 3$: $\lambda_0 = 5, \lambda_1 = 3, \lambda_2 = 1.5, \lambda_3 = 1.1$. For more details, see [17].

are established in finite time [17], but with the theoretical advantage of being globally valid (for any initial conditions) since it is not required *a priori* that the signal $e^{(\rho)}(t)$ be uniformly bounded, as assumed in the HOSM differentiator with fixed gains [17].

4.4 Output-feedback via Adaptive HOSM Differentiator

The next step is to proposed output-feedback control laws which satisfy (214) such that the global differentiator above can be indeed constructed and applied. Then, the proof of convergence for the tracking error $e(t)$ with our output-feedback controller based on the estimate state of the HOSM differentiator is straightforward once the convergence of the differentiator (218) is already guaranteed and the separation principle is always fulfilled [11, 92].

(a) Modulation function or control gain:

A common feature of the family of output-feedback controllers described in the following is the use of a modulation function or control gain $\varrho(t) \geq 0$ which dominates the equivalent input disturbance in (204) so that:

$$\varrho(t) \geq |-\theta^{*^T}\omega(t) + d_f(t)| + \delta, \quad \delta > 0, \tag{220}$$

where the constant δ can be arbitrarily small. Since A_p, B_p and H_p in (186) belong to some known compact set, an upper bound $\bar{\theta} \geq |\theta^*|$ can be obtained. Thus, a possible choice for the modulation function to satisfy (220) is given by

$$\varrho(t) = \bar{\theta}|\omega(t)| + \hat{d}_f(t) + \delta, \tag{221}$$

with $\hat{d}_f(t)$ defined in (208).

To show the modulation function $\varrho(t)$ in (221) satisfies inequality (214) we just have to write $|\omega| \leq \kappa_5|X| + \kappa_6$ from (195), with $\kappa_5, \kappa_6 > 0$ and considering that $r(t)$ is an uniformly bounded reference signal. Then, from the ISS relation of the filtered signals in (207) and (208) with respect to ω, we conclude the norm bounds $|\hat{d}_f| \leq \kappa_a||X_t|| + \kappa_b$ and $|\hat{x}| \leq \kappa_c||X_t|| + \kappa_d$, for appropriate constants $\kappa_a, \kappa_b, \kappa_c, \kappa_d > 0$.

(b) Ideal sliding variable:

The main idea of sliding mode control is to design the relative degree one sliding

variable and such that, when the motion is restricted to the manifold $\sigma = 0$, the reduced-order model has the required performance.

For higher relative degree plants, one could use simply the operator $L_m(s)$ defined in (188), to overcome the relative degree obstacle. The operator $L_m(s)$ is such that $L_m(s)G(s)$ and $L_m(s)W_m(s)$ have relative degree one. The ideal sliding variable $\sigma = L_m(s)e \in \mathbb{R}$ is given by

$$\sigma = e^{(\rho-1)} + \cdots + l_1\dot{e} + l_0 e = \sum_{i=0}^{\rho-1} l_i H_0 A_c^i X_e = \bar{H}X_e \,, \tag{222}$$

where the second equality is derived from Assumption (A3) and (204). Notice that $\{A_c, B_c, \bar{H}\}$ is a nonminimal realization of $L_m(s)W_m(s)$. From (187)–(188), one has

$$\begin{aligned}
\sigma &= L_m(s)W_m(s)K_p \left[u - \theta^{*T}\omega + d_f \right] \\
&= \frac{K_p}{s + \gamma_m} \left[u - \theta^{*T}\omega + d_f \right] \,.
\end{aligned} \tag{223}$$

More general (nonlinear) combinations of the variables $e^{(\rho-1)}, \dots, \dot{e}$ and e, rather than the simple linear combination given in (222) could be envisaged. As an advantage, finite-time convergence for the tracking error $e(t)$ would be guaranteed instead of exponential convergence only, as will be discussed in the next sections.

Anyway, σ is not directly available to implement the control law. Thus, reminding (219) and using the proposed adaptive HOSM differentiator, the following estimate for σ can be obtained to replace (222):

$$\hat{\sigma} = \zeta_{\rho-1} + \cdots + l_1\zeta_1 + l_0\zeta_0 \,. \tag{224}$$

(c) Numerical Simulation:

To show the wide range of global differentiators presented in this article, simulation results are presented for distinct control designs. Such controllers are: first order sliding mode, non-singular terminal sliding mode, twisting algorithm, super-twisting algorithm, nested sliding mode and quasi-continuous sliding mode. For all simulations the follows

perturbed plant is used,

$$\dot{x}_1 = x_2 \,,$$

$$\dot{x}_2 = -1.5x_2 + x_1 + u + 0.5x_1^{2/3}x_2^{1/3}\sin(t) \,,$$

where the perturbation is represented by the term $d(x,t) = 0.5x_1^{2/3}x_2^{1/3}\sin(t)$ and the output is given by

$$y = x_1 \,.$$

The smooth reference signal is

$$r(t) = 0.25\sin(0.5t) + 0.8\sin(6t)$$

and it is nulled after $t = 20$ to show the dynamic differentiator gains behavior. For tracking problem a reference model is employed, its transfer function is

$$y_m = \frac{0.5}{s^2 + 1.5s + 0.5}r \,.$$

Furthermore, to build the regressor vector $\omega := [\omega_u \ \omega_y \ y \ r]^T$, the I/O filtered signals are obtained by

$$\dot{\omega}_u = -2\omega_u + u \,,$$

$$\dot{\omega}_y = -2\omega_y + y \,.$$

The norm observer $\hat{x}(t)$, obtained through regressor vector ω, provide an upper bound to state norm $|x|$ that allows the design of global differentiators based on dynamic gain $\mathcal{L}(\hat{x},t)$, the major $d_f(\hat{x},t)$ for the modulo of perturbation $d(x,t)$ and the modulation function $\varrho(t)$ employed in controllers. The norm observer (206), the disturbance norm bound (208), the modulation function (221) and the differentiartor gain (216) are used with parameters: $\lambda_x = 0.1$, $c_1 = 0.06$, $c_2 = 0.2$, $k_d = 1$, $k_\phi = 1$, $\lambda_f = 2$, $k_x = 1$, $\bar{k}_\phi = 1$, $c_f = 0.001$, $\bar{\theta} = 3$, $\delta = 0.001$, $k_1 = 2$, $k_2 = 0$ and $k_3 = 3$. The initial conditions are $x_1(0) = 2$, $x_2(0) = 1$, $\omega_u(0) = 0$, $\omega_y(0) = 0$, $\zeta_0(0) = 1$ and $\zeta_1(0) = 2$.

4.4.1 First Order Sliding Mode Control

If the first order SMC law was given by $u = -\varrho(t)\text{sgn}(\sigma)$, with modulation function $\varrho(t)$ in (221), then the closed-loop error system (204) would be uniformly globally exponentially stable and the ideal sliding variable σ in (223) became identically zero after some finite time, according to [84, Lemma 1].

From (195), (207) and (208), it is easy to show that the following control signal

$$u = -\varrho(t)\text{sgn}(\hat{\sigma}), \tag{225}$$

with sliding variable $\hat{\sigma}$ in (224), satisfies inequality (214) for $k_\varrho = 1$. Thus, the global differentiator with dynamic gains given in (218) can indeed be constructed and its state exactly surrogates the time derivatives of the signal $e(t)$ in the sliding variable $\hat{\sigma}$ after some finite time.
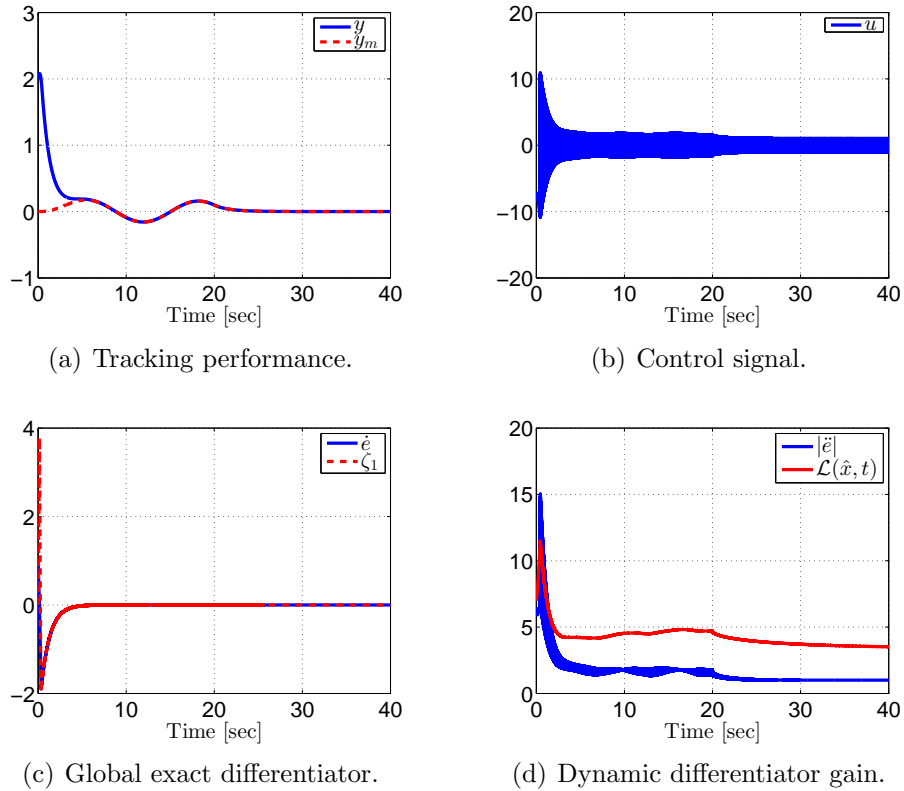

(a) Tracking performance.

(b) Control signal.

(c) Global exact differentiator.

(d) Dynamic differentiator gain.

Figure 13 – First order sliding mode - simulation results

4.4.2   Terminal Sliding Mode Control

The Non-Singular Terminal Sliding Mode differs from standard sliding mode basically by two reasons. First, the sliding surface is as nonlinear function of state variables. Second, while the asymptotically convergence is guaranteed when the closed loop systems stay in standard sliding surface, its non-singular terminal version is able to do the state reaches the origin in finite time. The controller presented here follows the steps given by [101]. The nonlinear surface is

$$\hat{\sigma} = \zeta_0 + \frac{1}{2}\zeta_1^{5/3},$$
(226)

and the controller is

$$u = -\left(3\zeta_0 + \frac{6}{5}\zeta_1^{1/3} + \varrho\left(t\right)\operatorname{sgn}\left(\hat{\sigma}\right)\right).$$
(227)

(a) Tracking performance.

(b) Control signal.

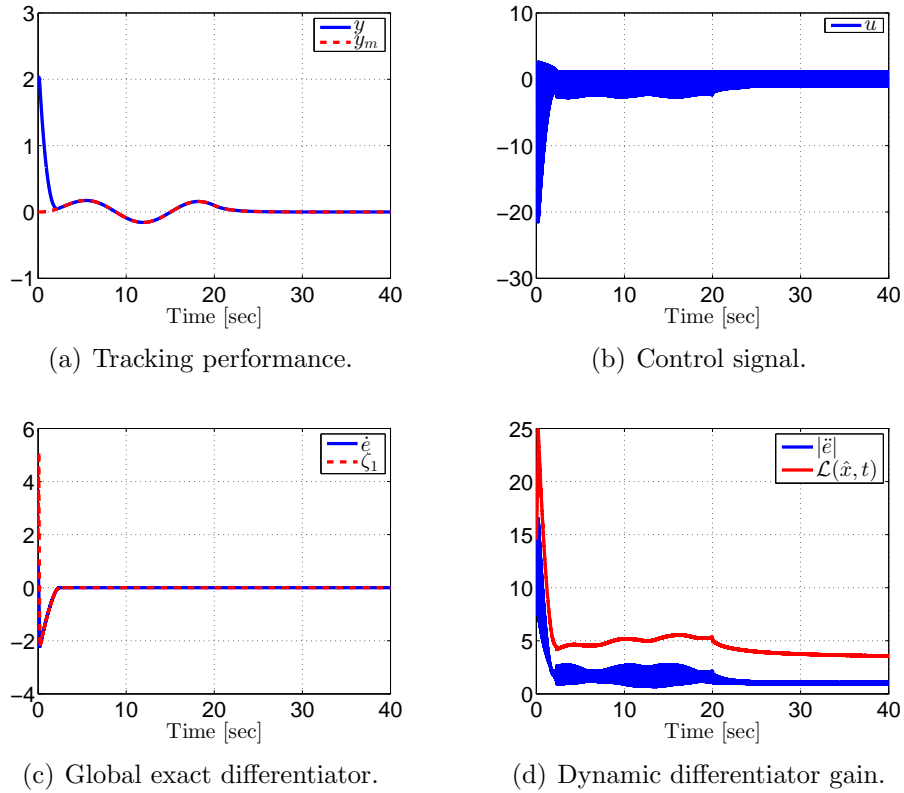(c) Global exact differentiator.

(d) Dynamic differentiator gain.

Figure 14 – Non-singular terminal sliding mode - simulation results

4.4.3 Twisting Algorithm

The first and simplest second order sliding mode (SOSM) algorithm is the so-called "twisting algorithm (TA)" [51]. For a error system (204)–(205) with relative degree $\rho = 2$, our global output-feedback version of the TA is given by:

$$u = -a(t)\mathrm{sgn}(\zeta_1) - b(t)\mathrm{sgn}(\zeta_0)\,, \quad b(t) \geq 2a(t)\,, \tag{228}$$

where $a(t) = \varrho(t)$ in (221) is defined analogously to satisfy (220). The TA ensures the finite-time exact convergence of both $\zeta_0 = e$ and $\zeta_1 = \dot{e}$, *i.e.*, there exists $T > 0$ such that $e(t) = \dot{e}(t) = 0$, $\forall t > T$.
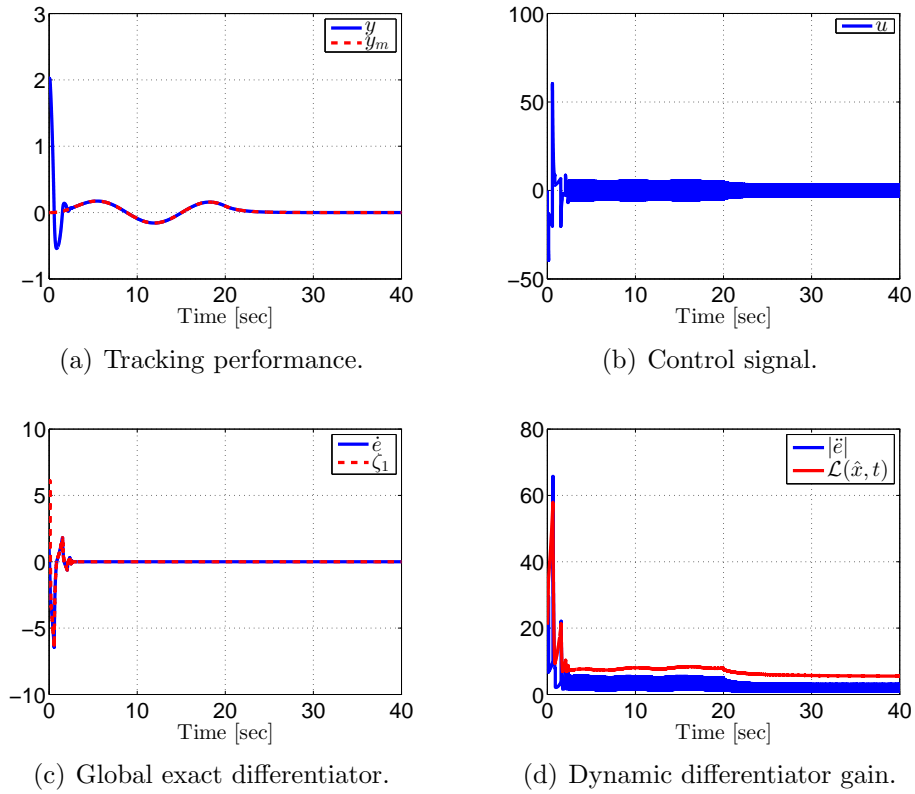

(a) Tracking performance.

(b) Control signal.

(c) Global exact differentiator.

(d) Dynamic differentiator gain.

Figure 15 – Twisting sliding mode - simulation results

4.4.4 Super-Twisting Algorithm

HOSM based control is effective for arbitrary relative degrees and it is well-known that the chattering effect is significantly attenuated since the high-frequency switching is hidden in the higher derivative of the sliding variable. The proposed global HOSM differentiator (218) can be applied to provide the output-feedback generalization for all

the existing HOSM control schemes, substituting the *discontinuous* control variable from the first order SMC (225) by an *absolutely continuous* control, while preserving global stability properties.

For instance, the proposed output-feedback version of the original state-feedback "variable gain super-twisting algorithm (VGSTA)" [51] can be written as:

$$u = -k_1 \phi_1(\hat{\sigma}) - k_2 \int_0^t \phi_2(\hat{\sigma}) \, dt, \quad k_1, k_2 > 0, \tag{229}$$

where $\hat{x}$ is given in (207), $\hat{\sigma}$ in (224) and

$$
\begin{aligned}
\phi_1(\hat{\sigma}) &= |\hat{\sigma}|^{\frac{1}{2}} \operatorname{sgn}(\hat{\sigma}) + k_3 \hat{\sigma} \\
\phi_2(\hat{\sigma}) &= \tfrac{1}{2}\operatorname{sgn}(\hat{\sigma}) + \tfrac{3}{2}k_3 |\hat{\sigma}|^{\frac{1}{2}} \operatorname{sgn}(\hat{\sigma}) + k_3^2 \hat{\sigma}, \ k_3 > 0.
\end{aligned}
$$

The variable gains in (229) are selected as

$$
\begin{aligned}
k_1(\hat{x},t) &= \delta + \tfrac{1}{\beta}\left\{\tfrac{1}{4\epsilon}\left[2\epsilon\varrho_1 + \varrho_2\right]^2 + 2\epsilon\varrho_2 + \epsilon + \left[2\epsilon + \varrho_1\right](\beta + 4\epsilon^2)\right\}, \\
k_2(\hat{x},t) &= \beta + 4\epsilon^2 + 2\epsilon k_1(\hat{x},t),
\end{aligned}
\tag{230}
$$

where $\varrho_1(\hat{x},t) \geq 0$, $\varrho_2(\hat{x},t) \geq 0$ are known continuous functions and $\beta > 0$, $\epsilon > 0$, $\delta > 0$ are arbitrary positive constants. For more details, see [51]. The continuity of the control (229) can substantially reduce the chattering level of the second-order VGSTA [51] in practice.

4.4.5 Nested-Sliding Mode Control

The nested-sliding-mode controller are designed by using a recursive process of finite time stabilization of sliding surface σ and its $\rho - 1$-derivatives. This controller is based on a complicated switching motion. Let $p \geq \rho$, $i = 1, \ldots, \rho - 1$, $\beta_1, \ldots, \beta_{\rho-1}$ be some positive numbers. Denote

$$N_{1,\rho} = |\sigma|^{(\rho-1)/\rho}, \tag{231}$$

$$N_{i,\rho} = \left(|\sigma|^{p/\rho} + |\dot{\sigma}|^{p/(\rho-1)} + \ldots + \left|\sigma^{(i-1)}\right|^{p/(\rho-i+1)}\right)^{(\rho-i)/p}, \tag{232}$$

$$\psi_{0,r} = \operatorname{sgn}(\sigma), \tag{233}$$

$$\Psi_{i,\rho} = \operatorname{sgn}\left(\sigma^{(i)} + \beta_i N_{i,\rho} \Psi_{i-1,\rho}\right). \tag{234}$$

(a) Tracking performance.

(b) Control signal.

(c) Global exact differentiator.
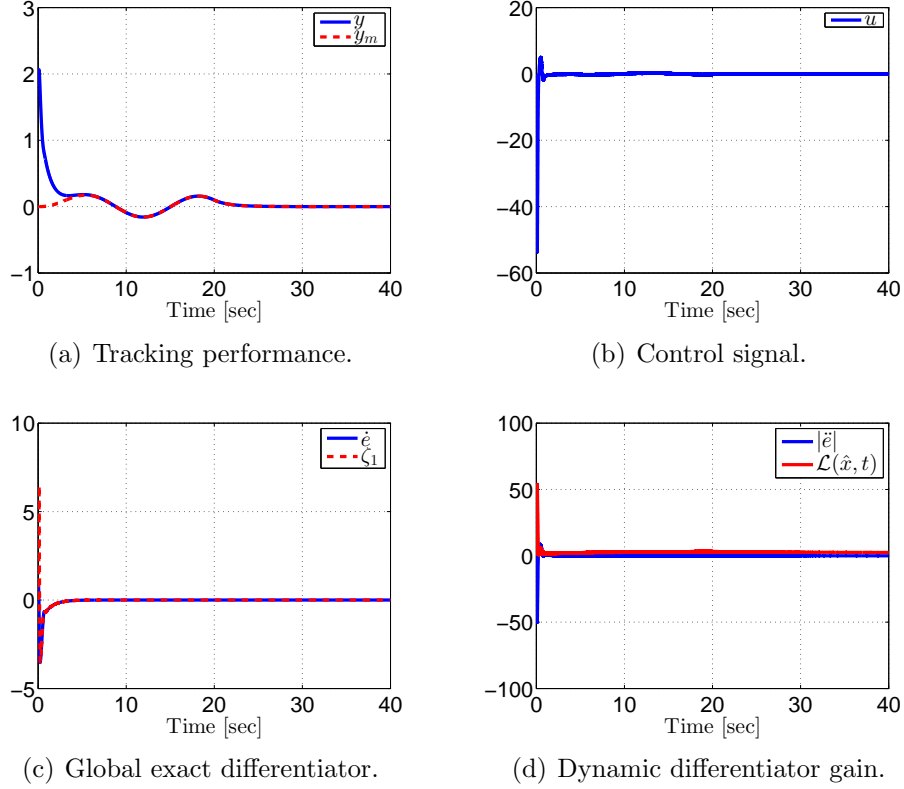
(d) Dynamic differentiator gain.

Figure 16 – Super-Twisting sliding mode - simulation results

$N_{i,\rho}$ and $\Psi_{i,\rho}$ are ρ-sliding homogeneous functions of the weights $\rho - i$ and 0 respectively, $N_{i,\rho}$ is also a positive-definite function of $\sigma, \dot{\sigma}, \ldots, \sigma^{(i-1)}$. Then the corresponding ρ-sliding homogeneous controller is defined as $u = -\alpha \Psi_{\rho-1,\rho} \left(\sigma, \dot{\sigma}, \ldots, \sigma^{(i-1)} \right)$.

For simulation, the parameter $\alpha = 1$, the sliding surface is chosen as $\hat{\sigma} = \zeta_0$, thus $\dot{\hat{\sigma}} = \zeta_1$ and therefore the controller is given by

$$u = -\varrho\left(t\right) \operatorname{sgn} \left(\zeta_1 - |\zeta_0|^{1/2} \operatorname{sgn}\left(\zeta_0\right) \right) \tag{235}$$

4.4.6 Quasi-Continuous Algorithm

If the relative degree $\rho > 1$, HOSM controllers can be constructed using a recursion. In [92], HOSM controllers were extended to include a variable gain and thus became non-homogeneous. In this case, the proposed output-feedback controller takes the form

$$u = -\alpha \Phi(t, \hat{x}) \Psi_{\rho-1,\rho} \left(\zeta_0, \zeta_1, \ldots, \zeta_{\rho-1} \right), \tag{236}$$

(a) Tracking performance.

(b) Control signal.

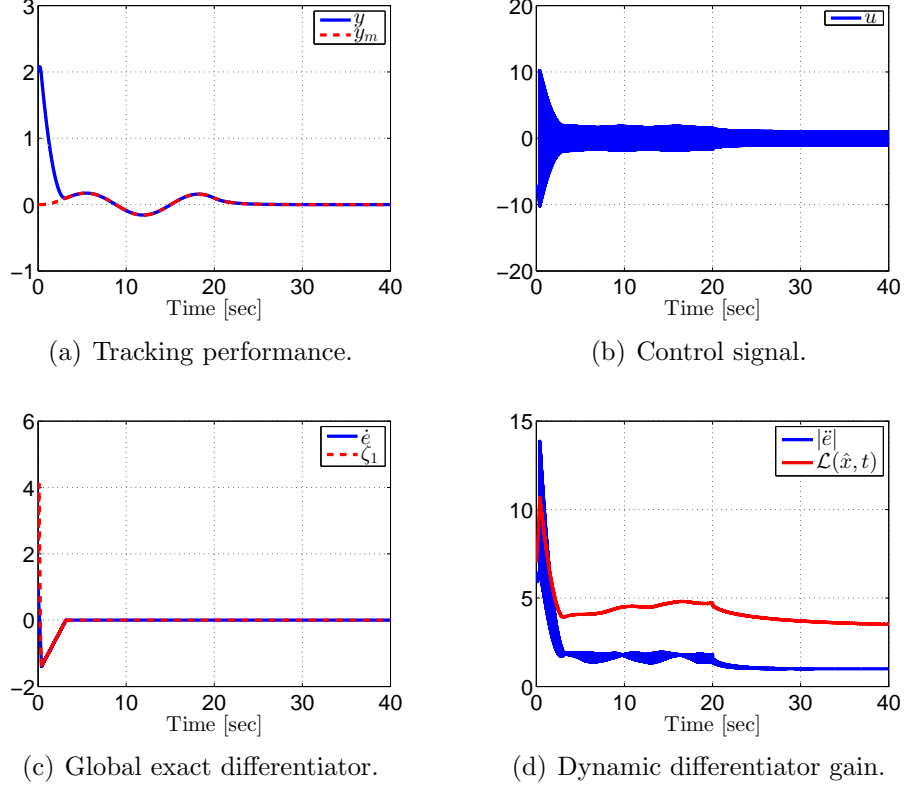(c) Global exact differentiator.

(d) Dynamic differentiator gain.

Figure 17 – Nested sliding mode - simulation results

where $\alpha > 0$ is an appropriate constant and the so-called "gain function" $\Phi(t, \hat{x}) > 0$ must satisfy (220), as was done before for $\varrho(t)$ in (221). The function $\Psi_{\rho-1,\rho}$ is a ρ-sliding homogeneous controller given by:

$$\varphi_{0,\rho} = \zeta_0 \,, \quad N_{0,\rho} = |\zeta_0| \,, \quad \Psi_{0,\rho} = \varphi_{0,\rho}/N_{0,\rho} \,, \tag{237}$$

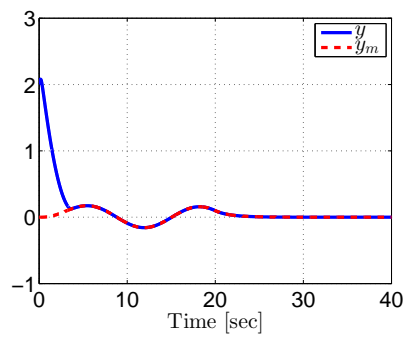$$\varphi_{i,\rho} = \zeta_i + \beta_i N_{i-1,\rho}^{(\rho-i)/(\rho-i+1)} \Psi_{i-1,\rho} \,, \tag{238}$$

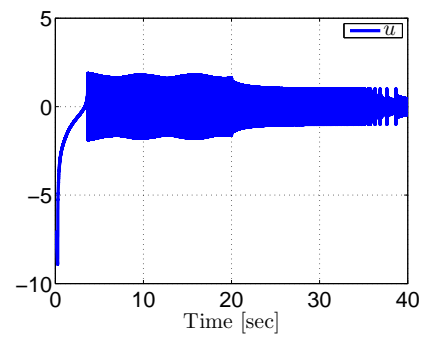$$N_{i,\rho} = |\zeta_i| + \beta_i N_{i-1,\rho}^{(\rho-i)/(\rho-i+1)} \,, \tag{239}$$

$$\Psi_{i,\rho}(\cdot) = \varphi_{i,\rho}/N_{i,\rho} \,, \quad i = 1, \ldots, \rho - 1 \,. \tag{240}$$

where $|\Psi_{\rho-1,\rho}| \leq 1$ and $\beta_1, \ldots, \beta_{\rho-1} > 0$ are constants. As usual, the idea is to replace the signals $e, \dot{e}, \ldots, e^{(\rho-1)}$ by their estimates $\zeta_0, \zeta_1, \ldots, \zeta_{\rho-1}$ and the state x by its norm bound $\hat{x}$, obtained with the global differentiator (218) and the norm observer (207), respectively.

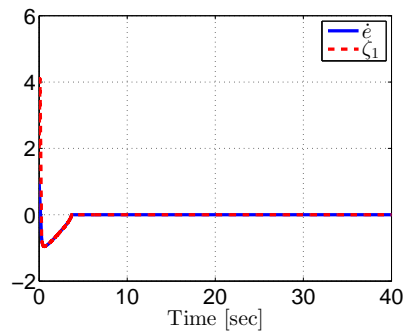For $\alpha > 0$ and $\beta_i > 0$, $i = 1, \ldots, \rho-1$, sufficiently large, the identity $\zeta_0 \equiv e \equiv 0$ is globally achieved in finite-time.
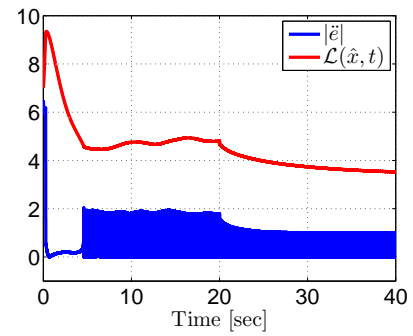
(a) Tracking performance.

(b) Control signal.

(c) Global exact differentiator.

(d) Dynamic differentiator gain.

Figure 18 – Quasi-continuous sliding mode - simulation results

5 GENERALIZED MODEL REFERENCE ADAPTIVE CONTROL

In this chapter, we combine a global differentiator based on higher-order sliding modes (HOSM) and dynamic gains with classical model reference adaptive control (MRAC) schemes to solve the problem of trajectory tracking via output feedback for uncertain linear plants of arbitrary relative degree. The gains of the differentiator are adapted through state-norm observers for the unmeasured state, whereas the control parametrization explores the input-output filters commonly used in MRAC design. Global asymptotic stability and robust exact tracking are rigorously demonstrated. The obtained results are easily extended to other adaptive laws using switching σ–modification or binary control concepts associated with parameter projection. Simulations highlight the claimed properties as well as the remarkable simplicity of the proposed adaptive control system using robust exact differentiators when compared to more involve alternatives found in standard approaches. The theoretical results are also illustrated with an application to bilateral teleoperation systems.

5.1 Problem Statement

Consider the following uncertain linear plant described by:

$$\dot{x} = A_p x + B_p u \,, \qquad y = H_p x \,, \tag{241}$$

where $x \in \mathbb{R}^n$ is the state, $u \in \mathbb{R}$ is the input and $y \in \mathbb{R}$ is the output. The uncertain matrices A_p, B_p and H_p belong to some compact set, such that the necessary uncertainty bounds to be defined later are available for design. The assumptions listed below are made in the chapter:

(A1) $G(s) = H_p(sI - A_p)^{-1}B_p$ is minimum phase.

(A2) The pairs (A_p, B_p) and (A_p, H_p) are controllable and observable, respectively.

(A3) The transfer function $G(s)$ has a known relative degree ρ and order n. The *high-frequency gain* (HFG) $K_p \in \mathbb{R}$ satisfies $K_p = \lim_{s \to \infty} s^\rho G(s) = H_p A_p^{\rho-1} B_p$. We just assume the sign of K_p is known.

Assumptions (A1)–(A3) are usual in model reference adaptive control (MRAC) [16].

Let the reference signal $y_m(t) \in \mathbb{R}$ be generated by the following reference model

$$y_m = W_m(s)\, r\,, \quad W_m(s) = (s + \gamma_m)^{-1} L_m^{-1}(s)\,, \quad \gamma_m > 0, \tag{242}$$

where $r(t) \in \mathbb{R}$ is an arbitrary uniformly bounded piecewise continuous reference signal and

$$L_m(s) = s^{(\rho-1)} + l_{\rho-2} s^{(\rho-2)} + \cdots + l_1 s + l_0\,, \tag{243}$$

with $L_m(s)$ being a Hurwitz polynomial. The transfer function matrix $W_m(s)$ has the same relative degree as $G(s)$ and its HFG is the unity.

The main objective is to find a control law u such that the output error

$$e(t) := y(t) - y_m(t) \tag{244}$$

is steered to zero, for arbitrary initial conditions.

The MRAC parametrization [16] using I/O filters is initially applied to obtain the *ideal matching control* [16] denoted by u^* and derive the dynamic error equations for the error system. In this sense, a control law which achieves the matching between the closed-loop transfer function matrix and $W_m(s)$ is given by

$$u^* = \theta^{*T} \omega\,, \quad \theta^* = \begin{bmatrix} \theta_1^{*T} & \theta_2^{*T} & \theta_3^* & \theta_4^* \end{bmatrix}^T, \tag{245}$$

where θ^* is the parameter vector with $\theta_1^*, \theta_2^* \in \mathbb{R}^{(n-1)}$ and $\theta_3^*, \theta_4^* \in \mathbb{R}$. The regressor vector $\omega = [\omega_u^T \ \omega_y^T \ y \ r]^T$, $w_u, w_y \in \mathbb{R}^{(n-1)}$ is obtained from I/O state variable filters given by:

$$\dot{\omega}_u = \Phi \omega_u + \Gamma u\,, \qquad \dot{\omega}_y = \Phi \omega_y + \Gamma y\,, \tag{246}$$

where $\Phi \in \mathbb{R}^{(n-1) \times (n-1)}$ is Hurwitz and $\Gamma \in \mathbb{R}^{(n-1)}$ is chosen such that the pair $(\Phi,\ \Gamma)$ is controllable. The matching conditions require that $\theta_4^* = K_p^{-1}$. Define the augmented state vector

$$X = [x^T, \omega_u^T, \omega_y^T]^T, \tag{247}$$

with dynamics described by $\dot{X} = A_0 X + B_0 u$, and output $y = H_0 X$, where

$$A_0 = \begin{bmatrix} A_p & 0 & 0 \\ 0 & \Phi & 0 \\ (\Gamma H_p) & 0 & \Phi \end{bmatrix}, \quad B_0 = \begin{bmatrix} B_p \\ \Gamma \\ 0 \end{bmatrix}, \tag{248}$$

$$H_0 = \begin{bmatrix} H_p & 0 & 0 \end{bmatrix}. \tag{249}$$

Then, adding and subtracting $B_0 \theta^{*T} \omega$ and noting that there exist matrices $\Omega_1 \in \mathbb{R}^{(2n-2) \times (3n-2)}$ and $\Omega_2 \in \mathbb{R}^{(2n-2)}$ such that [16]

$$\omega = \Omega_1 X + \Omega_2 r, \tag{250}$$

one has

$$\dot{X} = A_c X + B_c K_p [\theta_4^* r + u - u^*], \quad y = H_0 X, \tag{251}$$

where $A_c = A_0 + B_0 \theta^{*T} \Omega_1$ and $B_c = B_0 \theta_4^*$. Notice that (A_c, B_c, H_0) is a nonminimal realization of $W_m(s)$. For analysis purposes, the reference model can be described by

$$\dot{X}_m = A_c X_m + B_c K_p \theta_4^* r, \quad y_m = H_0 X_m. \tag{252}$$

Thus, the error dynamics with state

$$X_e := X - X_m \tag{253}$$

can be written in the the state-space representation by

$$\dot{X}_e = A_c X_e + B_c K_p [u - \theta^{*T} \omega], \tag{254}$$

$$e = H_0 X_e, \tag{255}$$

$$e = W_m(s) K_p \left[u - \theta^{*T} \omega \right], \tag{256}$$

where (256) is the I/O form of (254)–(255).

The importance of considering the augmented dynamics (251) with state X including the I/O filters (246) is not only to derive the full-error equation (254), but to create an output-feedback framework which allow us to derive norm bounds for the unmeasured state of a possible unstable plant (241), as discussed in the next section. As a

bonus, we use (254) in the proof of the main theorem to state global stability by means of input-to-state properties of the closed-loop system.

5.2   State-Norm Observer

Applying [8, Lemma 3] to (251), it is possible to find a norm bound for X and x that can be obtained through stable *first order approximation filters* (FOAFs) (see details in [8]). Thus, one has

$$|x(t)|, |X(t)| \leq |\hat{x}(t)| + \hat{\pi}(t),\tag{257}$$

$$\hat{x}(t) := \frac{c_x}{s + \lambda_x}|\omega(t)|,\tag{258}$$

with $c_x, \lambda_x > 0$ being appropriate constants that can be computed by the optimization methods mentioned in [8], such that, being $\{\lambda_i\}$ the eigenvalues of A_c, the stability margin of A_c is defined by $\lambda_x := \min_i[-\text{Re}(\lambda_i)]$.

In this sense, inequality (257)–(258) establishes that the norm observer estimate $\hat{x}(t)$ provides a valid norm bound for the unmeasured state x of the uncertain plant, *i.e.*, $|x| \leq |\hat{x}|$ except for exponentially decaying terms due to the system initial conditions, denoted here by $\hat{\pi}(t)$. From (257), we still can conclude the following norm bound

$$|x(t)|, |X(t)| \leq |\hat{x}(t)| + \delta_0, \quad \forall t \geq T_0,\tag{259}$$

valid after some finite time $T_0 > 0$, for any arbitrarily small positive constant δ_0 (independent of initial conditions) since $\hat{\pi}(t)$ is an exponentially decreasing term.

5.3   Global Differentiator with Dynamic Gains

In what follows, a HOSM differentiator with coefficients being adapted using the estimate for the norm of the state x provided in (257) is proposed to achieve global exact estimation, *i.e.*, exact differentiation of signals with any initial conditions and unbounded higher derivatives.

It is possible to show that the nonlinear system (241) can be transformed into the

normal form [80]:

$$\dot{\eta} \;=\; \mathcal{A}_0\eta + \mathcal{B}_0 y\,, \tag{260}$$

$$\dot{\xi} \;=\; \mathcal{A}_\rho\xi + \mathcal{B}_\rho K_p[u + d_e(x,t)]\,, \quad y = \mathcal{C}_\rho\xi\,, \tag{261}$$

where $z^T = [\eta^T\ \xi^T] \in \mathbb{R}^n$ with $\eta \in \mathbb{R}^{(n-\rho)}$ being referred to the state of the inverse or zero dynamics and $\xi = [y\ \dot{y}\ \dots\ y^{(\rho-1)}]^T$ the state of the external dynamics. The triple $(\mathcal{A}_\rho,\ \mathcal{B}_\rho,\ \mathcal{C}_\rho)$ is in the Brunovsky's controller form [80] and $\mathcal{A}_0$ is Hurwitz. The equivalent input disturbance $d_e(x,t) = K_p^{-1} H_p A_p^\rho x$ is affinely norm bounded by

$$|d_e(x,t)| \leq k_0|x|\,, \tag{262}$$

where $k_0 > |K_p^{-1}|\,|H_p A_p^\rho|$ is a known constant. We can conclude the following state-dependent upper bound for higher derivative (order ρ) of the output signal

$$|y^{(\rho)}| \leq |K_p|\,[k_0|x| + |u|]\,. \tag{263}$$

From (263) and (244), we can write

$$|e^{(\rho)}(t)| \leq L(x,t) = |K_p|\,[k_0|x| + |u|] + |y_m^{(\rho)}(t)|\,. \tag{264}$$

By applying (257) to (264), we can obtain the following upper bound with the norm observer variable $\hat{x}(t)$ in (257)–(259):

$$|e^{(\rho)}(t)| \leq |K_p|\,[k_0(|\hat{x}| + \delta_0) + |u|] + |y_m^{(\rho)}(t)|\,, \tag{265}$$

modulo exponential decaying terms due to initial conditions, which take into account the transient of the FOAF. By defining known positive constants k_1, k_2, k_3 and k_m satisfying $k_m \geq |y_m^{(\rho)}(t)|$, $k_1 \geq |K_p|k_0$ and $k_2 \geq |K_p|k_0\delta_0 + k_m$, we can define

$$\mathcal{L}(\hat{x},t) := k_1|\hat{x}| + k_2 + |u|\,, \tag{266}$$

and state the following upper bound constructed only with measurable signals

$$|e^{(\rho)}(t)| \leq \mathcal{L}(\hat{x}, t), \quad \forall t \geq T, \tag{267}$$

for some finite time $T > 0$.

In light of (266)–(267), we can introduce the following HOSM differentiator based on dynamic gains for the output error $e \in \mathbb{R}$, with state $\zeta = [\zeta_0 \ \ldots \ \zeta_{\rho-1}]^T$ and order $p = \rho - 1$:

$$\dot{\zeta}_0 = v_0 = -\lambda_0 \mathcal{L}(\hat{x}, t)^{\frac{1}{p+1}} |\zeta_0 - e(t)|^{\frac{p}{p+1}} \mathrm{sgn}(\zeta_0 - e(t)) + \zeta_1,$$

$$\vdots$$

$$\dot{\zeta}_i = v_i = -\lambda_i \mathcal{L}(\hat{x}, t)^{\frac{1}{p-i+1}} |\zeta_i - v_{i-1}|^{\frac{p-i}{p-i+1}} \mathrm{sgn}(\zeta_i - v_{i-1}) + \zeta_{i+1}, \tag{268}$$

$$\vdots$$

$$\dot{\zeta}_p = -\lambda_p \mathcal{L}(\hat{x}, t) \mathrm{sgn}(\zeta_p - v_{p-1}).$$

The dynamic gain of our differentiator must satisfy the same conditions for finite-convergence given in [11, 102]: the global upper bound $\mathcal{L}(\hat{x}, t)$ must be absolutely continuous with at least ultimate bounded logarithmic derivative ($|\dot{\mathcal{L}}/\mathcal{L}| \leq M$, for some constant $M > 0$). It implies that, after some finite time, $\mathcal{L}(\hat{x}, t)$ can grow at most exponentially as a result of $|\dot{\mathcal{L}}| \leq M|\mathcal{L}|$. Initially the variable gain may have an arbitrary growth so that $\dot{\mathcal{L}}(\hat{x}, t) \geq 0$ implies into faster convergence rates for the differentiator [102]. Our main contribution is to show how to construct the differentiator gain using only input-output information in order to satisfy the conditions raised in [11, 102].

Now, assume that the control input u in (266) satisfies

$$|u| \leq \bar{\theta}|\omega(t)| \leq k_3||X_t|| + k_4, \tag{269}$$

where $k_3, k_4 > 0$ are adequate constants, $\omega(t)$ is the regressor vector, and $\bar{\theta}$ is a constant norm bound for the estimate $\theta(t)$ of θ^* in (245) to be generated by an appropriate adaptive control law defined later on.

According to the *regularity condition* [57] assumed in (269) for the control signal, any finite-escape is precluded. Thus, if the parameters λ_i are properly recursively chosen [17], the following equalities

$$\zeta_0 = e(t), \quad \zeta_i = e^{(i)}(t), \quad i = 1, \ldots, p, \tag{270}$$

are established in finite time [17], but with the theoretical advantage of being globally valid (for any initial conditions) since it is not required *a priori* that the signal $e^{(\rho)}(t)$ be uniformly bounded, as assumed in the HOSM differentiator with fixed gains [17].

5.4   Adaptive Control for Global Exact Tracking via Output-feedback

The next step is to proposed output-feedback MRAC control laws which satisfy (269) such that the global differentiator above can be indeed constructed and applied.

5.4.1   Generalized MRAC for Arbitrary Relative Degrees

To overcome the challenge imposed by plants with higher relative degree, we could use the operator $L_m(s)$ defined in (243). The operator $L_m(s)$ is such that $L_m(s)G(s)$ and $L_m(s)W_m(s)$ have relative degree one. Thus, an auxiliary output error variable $S = L_m(s)e$ of relative degree one for the system (254) can be obtained, such that

$$S = e^{(\rho-1)} + \cdots + l_1\dot{e} + l_0 e \tag{271}$$
$$= \sum_{i=0}^{\rho-1} l_i H_0 A_c^i X_e = \bar{H}X_e \,,$$

where the second equality is derived from Assumption (A3) and (254). Notice that $\{A_c, B_c, \bar{H}\}$ is a nonminimal realization of $L_m(s)W_m(s)$. From (242)–(243), one has

$$S = L_m(s)W_m(s)K_p\left[u - \theta^{*^T}\omega\right]$$
$$= \frac{K_p}{s + \gamma_m}\left[u - \theta^{*^T}\omega\right] \,. \tag{272}$$

Now, if the MRAC law was chosen

$$u(t) = \theta^T(t)\omega(t) \,, \tag{273}$$
$$\dot{\theta}(t) = -\text{sgn}(K_p)\gamma S(t)\omega(t) \,, \tag{274}$$

where $\gamma > 0$ is the adaptation gain and $\theta(t)$ is the estimate of θ^*. Since $L_m(s)W_m(s)$ in (272) is SPR, it is easy to show that $S(t) \to 0$ as $t \to +\infty$, according to [16, Section 6.4.1]. Reminding that the error dynamics (254) is ISS with respect to $S(t)$, one can conclude

that $X_e(t)$ and $e(t)$ tend to zero at least asymptotically.

However, S is not directly available to implement the control law. Thus, using the proposed global HOSM differentiator, the following exact finite-time estimate for S can be obtained:

$$\hat{S} = \zeta_{\rho-1} + \cdots + l_1\zeta_1 + l_0\zeta_0 \,. \tag{275}$$

From (250) and (258), it is easy to show that the following adaptive control signal

$$u(t) = \theta^T(t)\omega(t) \,, \tag{276}$$

$$\dot{\theta}(t) = -\text{sgn}(K_p)\gamma\hat{S}(t)\omega(t) \,, \tag{277}$$

satisfies inequality (269) once $\theta(t)$ is uniformly bounded (as it will be shown in the proof of the main theorem). To show this property we just have to write $|\omega| \leq k_5|X| + k_6$ from (250), with $k_5 \geq |\Omega_1|$ and $k_6 \geq |\Omega_2|$, by considering that $r(t)$ is an uniformly bounded reference signal. Then, from (257) and the ISS relation of the filtered signal in (258) with respect to $|\omega|$, we conclude the norm bound (269). Thus, the global differentiator with dynamic gains given in (268) can indeed be constructed and its state exactly surrogates the time derivatives of the signal $e(t)$ in the variable $\hat{S}$ (275), after some finite time.

5.4.2 Stability Analysis

The next theorem states the global stability results with ultimate exact tracking for the output-feedback scheme.

Theorem 4. *Consider the plant (241) and the reference model (242)–(243). The output-feedback control law u is given by (276) with adaptive function θ defined in (277), the global exact estimate of S in (271) is $\hat{S}$ given by (275) and constructed with the state $\zeta = [\zeta_0 \ \ldots \ \zeta_{\rho-1}]^T$ of the proposed differentiator (268). Suppose that assumptions (A1) to (A3) hold. For λ_i, $i = 0,\ldots,\rho-1$, properly chosen and $\mathcal{L}(\hat{x},t)$ in (268) satisfying (266), the estimation of the variable S becomes exact after some finite time, i.e., $\hat{S} \equiv S$. Then, the closed-loop error system with dynamics (254) is uniformly globally asymptotically stable in the sense that X_e and, hence, the output tracking error e converge asymptotically to zero and all closed-loop signals remain uniformly bounded.*

Proof 4. *In what follows, $k_i > 0$ are new constants not depending on the initial conditi-*

ons. The demonstration is divided in three steps.

In the first one, it is necessary to show that the adaptation law (274) results in θ uniformly bounded. By contradiction, let us assume $\theta(t)$ grows unboundedly with the time variable, thus there exist finite-time instants $T_1 > 0$ and $T_2 > 0$ such that (259) and (267) are satisfied, $\forall t > \max\{T_1, T_2\}$. Then, the equations in (270) are verified and the variable S is exactly estimated, i.e., $\hat{S} \equiv S$ and the relative degree compensation is perfectly achieved. Thus, consider the following Lyapunov-like function

$$V(\tilde{\theta}, S) = \frac{|K_p|}{2\gamma}\tilde{\theta}^T\tilde{\theta} + \frac{1}{2}S^2, \quad \tilde{\theta}(t) := \theta(t) - \theta^*, \tag{278}$$

whose $\tilde{\theta}$ is the parameter error. By computing the time derivative of S, from (272), one can write:

$$\dot{S} = -\gamma_m S + K_p\tilde{\theta}^T\omega. \tag{279}$$

Thus, reminding that $\dot{\tilde{\theta}} = \dot{\theta}$, the time derivative of $V(\tilde{\theta}, S)$ in (278) is given by

$$\dot{V}(\tilde{\theta}, S) = \frac{|K_p|}{\gamma}\tilde{\theta}^T\dot{\tilde{\theta}} + S\dot{S},$$

and using (274), (279) and $K_p = |K_p|sgn(K_p)$, one gets

$$\dot{V}(\tilde{\theta}, S) = -\gamma_m S^2 \leq 0. \tag{280}$$

From (278) and (280), we can also conclude that the solutions $\tilde{\theta}(t), S(t)$ are uniformly bounded but nothing more. Consequently, θ in (277) tends to some constant value since θ^* is a constant parameter vector. Thus, we can prove that

$$|\theta(t)| \leq \bar{\theta}, \quad \forall t \geq 0, \tag{281}$$

where $\bar{\theta} > 0$ and u in (276) satisfies the first inequality in (269).

In addition, from (278) and (280), we conclude that $V(t) = V(\tilde{\theta}(t), S(t))$ is bounded from below and is nonincreasing with time, so it has a limit, i.e., $\lim_{t \to \infty} V(t) = V_\infty$. Therefore, from (280) one has

$$\lim_{t \to \infty} \int_0^t S^2 d\tau = \frac{V(0) - V_\infty}{\gamma_m} < \infty, \tag{282}$$

then, by invoking Barbalat's Lemma [16, 80], one can state $S(t) \to 0$ as $t \to +\infty$ since $S(t)$ is also a uniformly continuous function.

The second step of the proof shows that no finite time escape is possible signal in the closed-loop system. By using the relations (250) and (253), one has that $X = X_e + X_m$ and the regressor vector

$$\omega = \Omega_1 X_e + \Omega_1 X_m + \Omega_2 r \,. \tag{283}$$

Let $x_m := [y_m \;\; \dot{y}_m \;\; \ldots \;\; y_m^{(\rho-1)}]^T$ and $x_e := \xi - x_m$, with ξ in (261). From (254), it can be shown that $e^{(i)} = H_0 A^i X_e$, for $i = 0, \ldots, \rho-1$, hence $|x_e| \le k_0 |X_e|$. Therefore, since x_m is uniformly bounded, then $\xi = x_e + x_m$ can be affinely norm bounded in $|X_e|$. In addition, from (260), the η-dynamics is ISS with respect to $y = \mathcal{C}_\rho \xi$. Thus, one can conclude that $|x| \le k_1 \|\xi_t\| + k_2$, and consequently, $|x| \le k_3 \|(X_e)_t\| + k_4$ and, from (252), one has

$$|X_m| \le k_5 \|(X_e)_t\| + k_6 \,. \tag{284}$$

Finally, from (250), (283) and (284), we conclude which ω and consequently the control input u are all affinely norm bounded by X or X_e, i.e.,

$$|u|\,,|\omega| \;\; \le \;\; k_a \|X_t\| + k_b \,, \tag{285}$$

$$|u|\,,|\omega| \;\; \le \;\; k_c \|(X_e)_t\| + k_d \,, \tag{286}$$

which satisfy the second inequality in (269). Thus, the system signals will be regular and, therefore, can grow at most exponentially [57]. This fact lead us to the third step of the proof.

As mentioned earlier, it is possible to rewrite (254) into the normal form [80] such that the states of the error system are ISS with respect to S. It can be shown reminding that $L_m(s)W_m(s) = 1/(s + \gamma_m)$. From (254) and (272), one gets $\dot{X}_e = A_c X_e + B_c(\dot{S} + \gamma_m S)$. Further, using the transformation $X_e := \bar{X}_e + B_c S$, one has

$$\dot{\bar{X}}_e = A_c \bar{X}_e + (A_c B_c + \gamma_m B_c)S \,, \tag{287}$$

which clearly implies an ISS relationship from S to either X_e or $\bar{X}_e$ since A_c is Hurwitz. Thus, X_e and $e = H_0 X_e$ tends asymptotically to zero as well as the state ζ of the differentiator, which is also driven by e. From (286), we conclude all remaining signals are

uniformly bounded. □

5.5 MRAC Controllers with Parameter Projection

Although we have focused only on the generalization of classical MRAC, our results could be easily applied to other classes of adaptive controllers using some kind of *leakage* procedure [16] by means of switching σ–modification [16] or binary control concepts associated with parameter projection [66–68]. Such methodologies are well-known in the literature for allowing output tracking with better transient responses since the speed of adaptation (γ) can be increased while keeping the adjustable parameter vector θ inside some finite ball of appropriate radius.

The error system for such cases would be fundamentally the same as in (254)–(255). However, the control law (273) would be updated according to an adaptation law with a σ–modification given by:

$$\dot{\theta} = -\text{sgn}(K_p)[\sigma\theta + \gamma\hat{S}\omega]\,, \quad \sigma\text{sgn}(K_p) \geq 0\,, \tag{288}$$

where $\hat{S}$ is given in (275).

The σ–factor, also called projection factor, is defined by

$$\sigma = \begin{cases} 0\,, & \text{if } |\theta| < M_\theta \quad \text{or} \quad \sigma_{eq}\text{sgn}(K_p) < 0\,, \\ \sigma_{eq}\,, & \text{if } |\theta| \geq M_\theta \quad \text{and} \quad \sigma_{eq}\text{sgn}(K_p) \geq 0\,, \end{cases} \tag{289}$$

with

$$\sigma_{eq} = -\frac{\gamma\hat{S}\theta^T\omega}{|\theta|^2} \tag{290}$$

and $M_\theta(> |\theta^*|)$ is a constant. Notice that the stability analysis of the closed-loop system would follow the same steps that were given previously in the proof of Theorem 4. In particular, the regularity condition in (269) is directly satisfied with $\bar{\theta} = M_\theta$ since the boundedness of θ is guaranteed by the projection factor (289)–(290), as discussed in the following.

The control law $u = \theta^T\omega$ with adaptive law (288)–(290) is called B-MRAC in [67,68] due to its similarity to the *binary control* given in [66]. Indeed, in both cases, the

integral adaptation is applied inside some invariant compact set, for example, the finite ball M_θ for θ in B-MRAC. In latter case, considering that $|\theta(0)| \le M_\theta$, the projection of update vector can be understood geometrically as follows: if the term $-\gamma \hat{S} \omega$ points outwards the ball $|\theta| \le M_\theta$, the update vector is projected onto the tangent plane of the sphere; if it points inwards, the σ–factor is equal to zero and $\theta(t)$ moves to the interior of the ball, according to the standard MRAC gradient adaptation law. Then, it is straightforward to prove that the closed ball with radius M_θ is invariant, that is, $|\theta(t)| \le M_\theta, \forall t \ge 0$. A mathematical demonstration of that can be derived by considering the next Lyapunov function candidate

$$V_\theta = \frac{1}{2} \theta^T \theta . \tag{291}$$

Indeed, the time derivative of (291) along of (288) results in

$$\dot{V}_\theta = (\sigma_{eq} - \sigma)|\theta|^2 = 2(\sigma_{eq} - \sigma)V_\theta , \tag{292}$$

and $(\sigma_{eq} - \sigma) \le 0$ for $|\theta| \ge M_\theta$, by virtue of (289) and (290). Thus, the set $|\theta| \le M_\theta$ is positively invariant and therefore $\tilde{\theta}^T \tilde{\theta}$ is uniformly bounded by a constant (Q.E.D.).

5.6   Simulation Example

To show the efficacy of proposed adaptive control scheme, let us consider an example borrowed from [16, Example 6.4.3], where the objective is to ensure that a naturally unstable plant with relative degree three is stabilized and forced to track the output signal y_m of the reference model.

Consider the following linear unstable system (241) with relative degree $\rho = 3$:

$$\dot{x}(t) = \begin{bmatrix} 0 & 1 & 0 \\ 0 & 0 & 1 \\ 10 & -3 & -6 \end{bmatrix} x(t) + \begin{bmatrix} 0 \\ 0 \\ 1 \end{bmatrix} u(t) , \tag{293}$$

$$y(t) = \begin{bmatrix} 1 & 0 & 0 \end{bmatrix} x(t) . \tag{294}$$

The reference model is given by

$$y_m = \frac{1}{(s+2)^3} r = \frac{1}{(s+2)(s^2+4s+4)} r, \tag{295}$$

where r is

$$r(t) = \begin{cases} 20\sin(2t), & \text{for} \quad t < 25, \\ 0, & \text{for} \quad t \geq 25. \end{cases} \tag{296}$$

The regressor vector (246) is generated with I/O filters

$$\dot{\omega}_i = \begin{bmatrix} -10 & -25 \\ 1 & 0 \end{bmatrix} \omega_i + \begin{bmatrix} 1 \\ 0 \end{bmatrix} i, \quad i = u, y$$

and the norm observer (257) is obtained by $\hat{x} = \frac{0.1}{s+1}|\omega|$. The system (293) is already in the normal form (261), where $x = \xi \in \mathbb{R}^3$, and the η–dynamics in (260) is dropped out. The equivalent input disturbance is $d_e(x,t) = 10x_1 - 3x_2 - 6x_3$ so that $|d_e(x,t)| \leq 19|\hat{x}|$, according to (262). Since the global exact HOSM differentiator is employed, its dynamic gain must satisfy (266) with $\mathcal{L}(\hat{x},t) = 19|\hat{x}(t)| + |\dddot{y}_m(t)| + |u(t)|$ and $\dddot{y}_m(t) = -8y_m(t) - 12\dot{y}_m(t) - 6\ddot{y}_m(t) + r(t)$ being implemented from the state-space representation of the reference model. Finally, the differentiators can be written as

$$\dot{\zeta}_0 = v_0 = -5\mathcal{L}(\hat{x},t)^{1/3}|\zeta_0 - e|^{2/3}\text{sgn}(\zeta_0 - e) + \zeta_1,$$
$$\dot{\zeta}_1 = v_1 = -3\mathcal{L}(\hat{x},t)^{1/2}|\zeta_1 - v_0|^{1/2}\text{sgn}(\zeta_1 - v_0) + \zeta_2,$$
$$\dot{\zeta}_2 = v_2 = -1.5\mathcal{L}(\hat{x},t)\text{sgn}(\zeta_2 - v_1).$$

From (242)–(243) and (295), one can obtain $\gamma_m = 2$ and $L_m(s) = s^2 + 4s + 4$, which leads to $S = \ddot{e} + 4\dot{e} + 4e$ according to (271). Nevertheless, $\ddot{e}$ and $\dot{e}$ are not available, then HOSM differentiators are applied to construct $\hat{S} = \zeta_2 + 4\zeta_1 + 4\zeta_0$. Therefore, the control law $u(t) = \theta(t)^T\omega(t)$ with adaptive law $\dot{\theta}(t) = -8\hat{S}(t)\omega(t)$ can be implemented, according to (276)–(277), reminding that $K_p = 1$ in our example.

For comparison purposes, the classical MRAC for relative degree three presented

in [16] is also simulated. Its control law is given by

$$u = \theta^T \omega - \epsilon\mathrm{sgn}(K_p)(\phi^T\Gamma\phi_1) - \alpha_0(p_1 - p_0)(\phi^T\Gamma\phi)^2 r_0$$
$$- 4\alpha_0(\phi^T\Gamma\phi)(\phi^T\Gamma\dot\phi)r_0 + \alpha_0^2(\phi^T\Gamma\phi)^4 r_0$$
$$- \alpha_0(\phi^T\Gamma\phi)^3\epsilon\mathrm{sgn}(K_p) , \tag{297}$$

where the adaptation law is

$$\dot\theta = -\Gamma\epsilon\phi\mathrm{sgn}(K_p) , \quad \dot\rho_0 = \gamma\epsilon r_0 ,$$
$$\dot r_0 = -(p_0 + \alpha_0(\phi^T\Gamma\phi)^2)r_0 + (\phi^T\Gamma\phi)\epsilon\mathrm{sgn}(K_p) ,$$
$$\hat e = \frac{1}{s + q_0}\rho_0 r_0 , \quad \epsilon = e - \hat e ,$$
$$\phi_1 = \frac{1}{s + p_1}\omega , \quad \phi = \frac{1}{s + p_0}\phi_1 , \tag{298}$$

with the design parameters chosen as in [16, Example 6.4.3]: $\gamma = 8$, $\Gamma = 8I$, $p_0 = 2$, $p_1 = 2$, $q_0 = 2$ and $\alpha_0 = 0.01$. The plant initial conditions were $y(0) = x_1(0) = -1$ and $x_2(0) = x_3(0) = 0$, while the initial conditions for all remaining designed filters were set to zero.

The simulation results are presented in Figure 19 to Figure 21, where the Euler method with fixed step-size of 10^{-5} s was applied to numerical integration. In Figure 19, the generalized MRAC is compared to classical MRAC. As can be seen by Figure 19(a) and Figure 19(b), the tracking objective is reached with a better transient response when the generalized MRAC strategy is applied. Moreover, the latter has a less conservative control effort, see Figure 19(c) and Figure 19(d).

Figure 20 shows the responses of the estimated parameters $\theta_i(t)$, $i = 1, \ldots, 6$. Notice that the vector of ideal matching parameters is $\theta^* = [0, -9, 162, 810, -54, 1]^T$. In this case, $|\theta^*| = 827.8539$ and the constant upper bound M_θ for $|\theta|$ should be chosen at least equal to $|\theta^*|$. It suggests the use of projection factor described in Section 5.5 would not bring any advantage in our example since the updated parameters $\theta_i(t)$ do not reach values greater (lesser) than 20 (or -25), for all time. As usual in MRAC schemes, the convergence of the tracking error $e(t) \to 0$ can be achieved without the parameters convergence to θ^*.

In Figure 21(a), it can be seen how the norm observer state $\hat x$ overcomes after a finite time the actual value of the x-norm. Figure 21(b) shows the adaptive gain $\mathcal{L}(\hat x, t)$

(a) Generalized MRAC: output signals $y(t)$ and $y_m(t)$.

(b) MRAC: output signals $y(t)$ and $y_m(t)$.

(c) Generalized MRAC: control signal $u(t)$.

(d) MRAC: control signal $u(t)$.
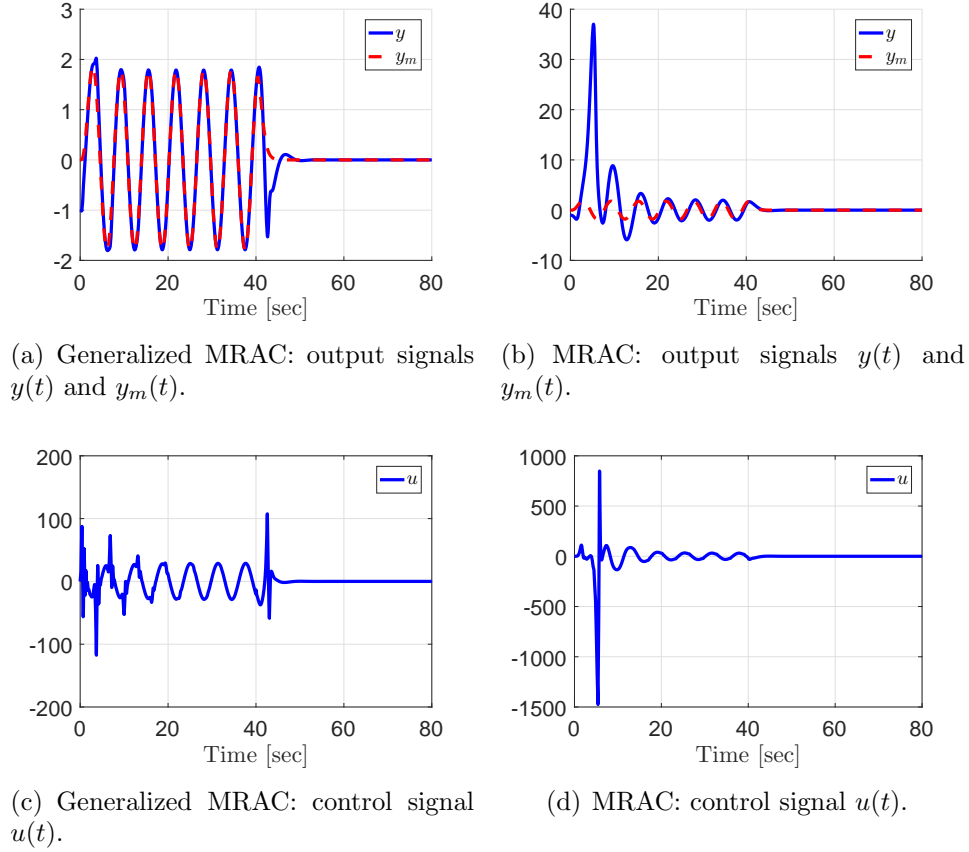
Figure 19 – Generalized MRAC $\times$ MRAC.
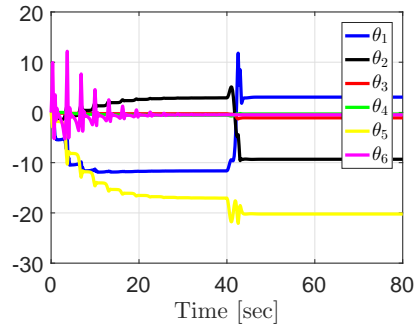
Figure 20 – Generalized MRAC: estimated parameter vector $\theta(t)$.

applied to upper bound the signal $|e^{(3)}(t)|$ used in the differentiator (268).

Remark 6. *The procedure for $\rho = 3$ given in (297)–(298) may be extended to the case of $\rho > 3$ by following similar steps [16]. However, the complexity of the control input signal u in (297) increases considerably with ρ to the point that it defeats any simplicity we may gain from analysis by using a single Lyapunov-like function to establish stability with an unnormalized adaptive law. In addition to complexity the highly nonlinear terms in the control law may lead to a "high bandwidth" control input that may have adverse effects on*

robustness with respect to modeling errors [16].

(a) Norm observer performance.

(b) Variable gain $\mathcal{L}(\hat{x}, t)$ (norm bound for $\dddot{e}(t)$) of the variable gain HOSM differentiator.

(c) Estimate of $\dot{e}(t)$ given by the proposed global hybrid adaptive HOSM differentiator.

(d) Estimate of $\ddot{e}(t)$ given by the proposed global hybrid adaptive HOSM differentiator.
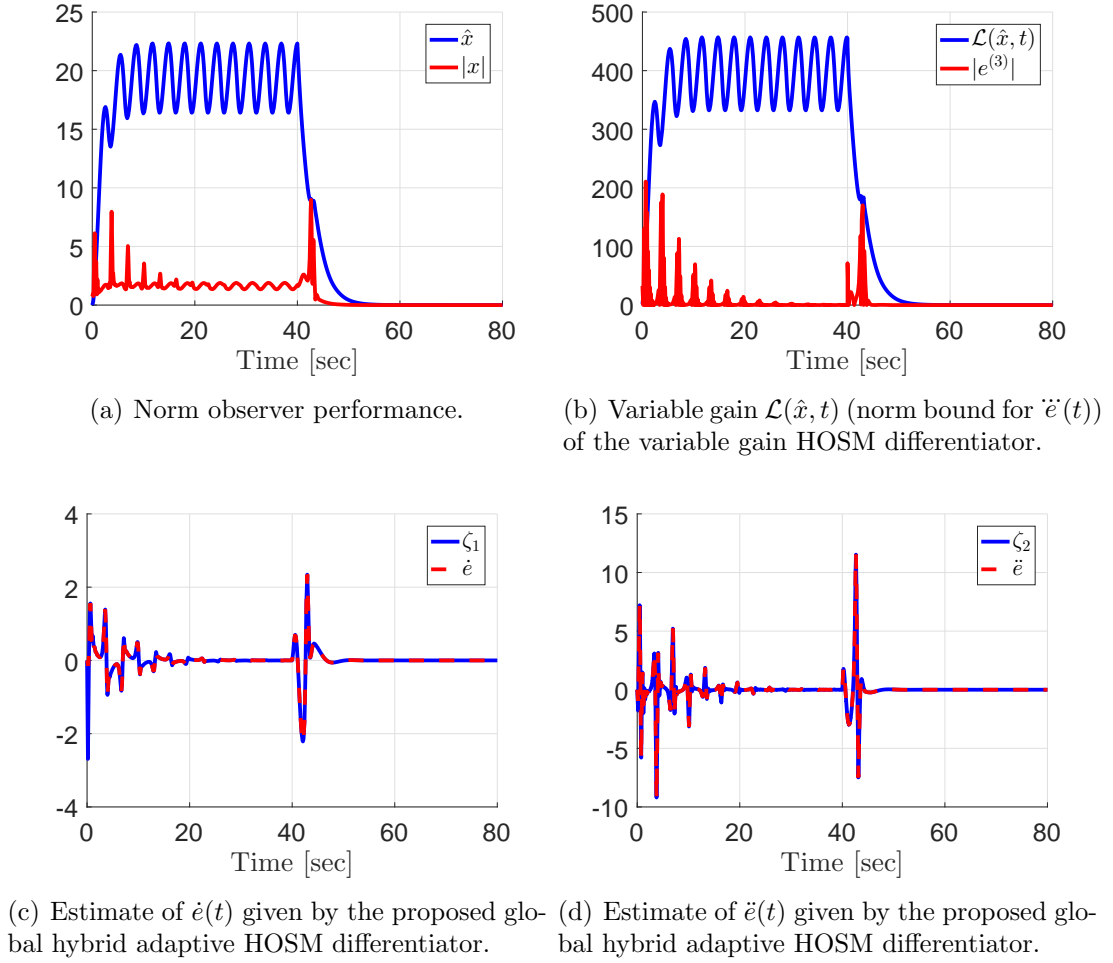
Figure 21 – Simulation Results.

5.7 Application to Bilateral Teleoperation

Teleoperation deals with a control system which the aim is to extend the human ability in manipulating devices remotely [70]. In bilateral teleoperation [71,72], the remote environment contains adverse conditions (reaction forces f_e), generated by the interaction between the slave and its environment. This force is reflected to the operator terminal acting into a joystick or manipulator (the master), which is similar to the plant (the slave). It gives to the operator a real feeling over the slave behavior. Thus, by controlling the master, it is expected that slave is being controlled too.

The master-slave manipulators with n degrees of freedom can be represented by

$$M_m \ddot{x}_m(t) + C_m \dot{x}_m(t) + K_m x_m(t) = u_m(t) + f_h(t) + f_e(t), \tag{299}$$

$$M_s \ddot{x}_s(t) + C_s \dot{x}_s(t) + K_s x_s(t) = u_s(t) + f_e(t), \tag{300}$$

where x_m, $x_s \in \mathbb{R}^n$ are the degrees of freedom of the manipulators; u_m, $u_s \in \mathbb{R}^n$ are force input signals; $f_h \in \mathbb{R}^n$ is the external force exerted on the master by the human operator; $f_e \in \mathbb{R}^n$ is the reaction force between the slave and its environment; M_m and M_s are symmetric positive definite inertia matrices; C_m and C_s are symmetric viscous matrices; K_m and K_s represent the compliance of the end-effector.

Transparency is the major goal in bilateral teleoperation architecture design [70]. A telerobotic system is transparent if the human operator feels as if directly interacting with the remote task. Formally, transparency is achieved if master and slave movements are equal $(x_s = x_m)$ and the force displayed to the human operator is exactly the reaction force from the environment.

For the sake of simplicity, in this chapter it is assumed robots of one degree of freedom without human operators in the loop $(f_h = 0)$, where the desired trajectories are generated automatically by a reference model. In what follows, the index $i = m, s$ is applied to indicate either master or slave manipulators, respectively. The parameters $M_i = 0.04 + \Delta_i$, $C_i = 3.424$ and $K_i = 0$ were chosen similarly to [71]. The uncertainty in the slave inertia matrix is chosen such that $\Delta_m = 0$ and $\Delta_s = 0.02$. The external force due to the environment can be simply modeled by $f_e = -k_e x_s$, where k_e is the stiffness coefficient [72]. The state-space description of (299)–(300) is

$$\dot{X}_i = \begin{bmatrix} 0 & 1 \\ 0 & -(M_i + \Delta_i)^{-1} C_i \end{bmatrix} X_i + \begin{bmatrix} 0 \\ (M_i + \Delta_i)^{-1} \end{bmatrix} (u_i + f_e),$$

$$y_i = \begin{bmatrix} 1 & 0 \end{bmatrix} X_i, \tag{301}$$

with $(M_m + \Delta_m)^{-1} C_m = 85.6$, $(M_s + \Delta_s)^{-1} C_s = 57.06$, $(M_m + \Delta_m)^{-1} = 25$ and $(M_s + \Delta_s)^{-1} = 16.66$. The state vectors are given by $X_i = [x_i, \dot{x}_i]^T$ and $f_e = -8.9 x_s$. The reference model selected by the designer is given by

$$M_d(\ddot{y}_r - \ddot{x}_d) + C_d(\dot{y}_r - \dot{x}_d) + K_d(y_r - x_d) = f_e, \tag{302}$$

where $M_d = 0.04$, $C_d = 0.4$, $K_d = 1$ and $x_d(t) = \sin(t)$ is a desired trajectory. Then, (302) can be represented in the following I/O form (242):

$$y_r = W_m(s)r = \frac{1}{s^2 + 10s + 25}r = \frac{1}{(s+5)^2}r\,, \tag{303}$$

$$r = 25f_e + \ddot{x}_d + 10\dot{x}_d + 25x_d \tag{304}$$

where y_m in (242) was replaced by y_r to avoid clutter with the master indexation, when $i = m$ in (301). Note that, we can obtain (256) directly from (301) and (303), which means the adaptive control methodology developed here is applicable to the teleoperation problem.

The regressor vector $\omega_i = [\omega_{u_i}, \omega_{y_i}, y_i, r]^T$ is generated by means of the I/O filters (246):

$$\dot{\omega}_{u_i} = -5\omega_{u_i} + u_i\,, \quad \dot{\omega}_{y_i} = -5\omega_{y_i} + y_i\,, \tag{305}$$

and the norm observer (257) is obtained by $\hat{x}_i = \frac{0.1}{s+1}|\omega_i|$, The systems represented by (301) are already in the normal form with $X_i = \xi_i \in \mathbb{R}^2$ and without η-dynamics. Hence, the equivalent input disturbance $d_{e_m}(x_m, t) = -85.6\dot{x}_m$ and $d_{e_s}(x_s, t) = -57.06\dot{x}_s$. From (259) and (262), we can write $|d_{e_i}(x, t)| \le 90|\hat{x}_i| + \delta_0^i$, where $\max\{|-85.6|, |-57.06|\} < 90$ and $\delta_0^s = \delta_0^m = 0.01$. The dynamic gains are chosen to satisfy (266) assuming the second derivatives $\ddot{e}_i$ of the error signals $e_m = x_m - x_r$ and $e_s = x_s - x_m$. We can obtain $\mathcal{L}_m(\hat{x}_m, t) = 90(|\hat{x}_m(t)| + \delta_0^m) + |\ddot{y}_r(t)| + 30(|u_m(t)| + |f_e(t)|)$, where $\ddot{y}_r(t) = -25y_r(t) - 10\dot{y}_r(t) + r(t)$ can be implemented from the state-space representation of (303), and $\mathcal{L}_s(\hat{x}_s, t) = 90(|\hat{x}_s(t)| + \delta_0^s) + k_s + 30(|u_s(t)| + |f_e(t)|)$, with constant $k_s > 0$ being a rough and known norm bound for $|\ddot{y}_r(t)| \le k_s$, since $\ddot{y}_m(t) \to \ddot{y}_r(t)$ as $t \to +\infty$. Hence, the HOSM differentiators (268) are implemented by

$$\dot{\zeta}_0^i = v_0^i = -5\mathcal{L}_i(\hat{x}_i, t)^{1/2}|\zeta_0^i - e_i|^{1/2}\operatorname{sgn}(\zeta_0^i - e_i) + \zeta_1^i\,,$$

$$\dot{\zeta}_1^i = v_1^i = -3\mathcal{L}_i(\hat{x}_i, t)\operatorname{sgn}(\zeta_1^i - v_0^i)\,.$$

By comparing (303) to (242)–(243), one can concluded that $\gamma_m = 5$ and $L_m(s) = s + 5$, which leads to $S_i = \dot{e}_i + 5e_i$ according to (271). Nevertheless, $\dot{e}_i$ is not available then HOSM differentiators are applied, such that $\hat{S}_i = \zeta_1^i + 5\zeta_0^i$.

In order to compare our adaptive controller with $\mathcal{L}_1$ adaptive control strategy introduced in [61] (see equations (3)–(8) therein), our control law $u_i = \theta_i^T \omega_i$ was implemented according to (276), adaptive law with parameter projection (288)–(290), adaptation gain $\gamma = 10^2$ and $M_\theta = 10$. In Figure 22(a), the *exact* tracking between the output signals of the master (y_m) and the slave (y_s) is reached by means of our B-MRAC generalization using HOSM differentiators given in Section 5.5. On the other hand, the slave control signal u_s provided by the projection based $\mathcal{L}_1$ adaptive controller cannot guarantee the synchronization of the slave and master $(y_s \neq y_m)$, even if the the adaptation gain Γ in [61] increases from 10^2 to 10^4, see Figure 22(b). The control signals u_s of each strategy are shown in Figure 22(c) and Figure 22(d).
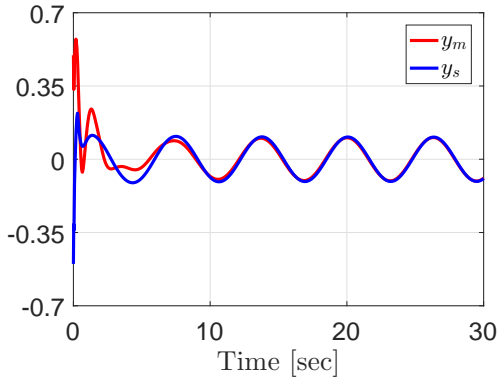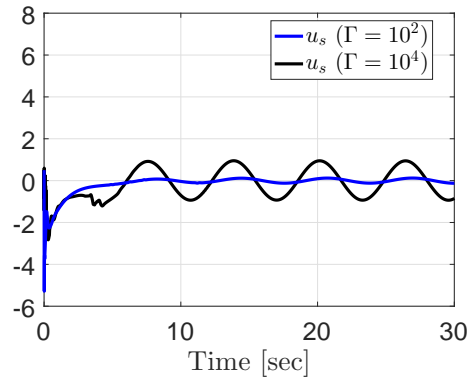

(a) **B-MRAC:** $y_m(t)$ and $y_s(t)$.
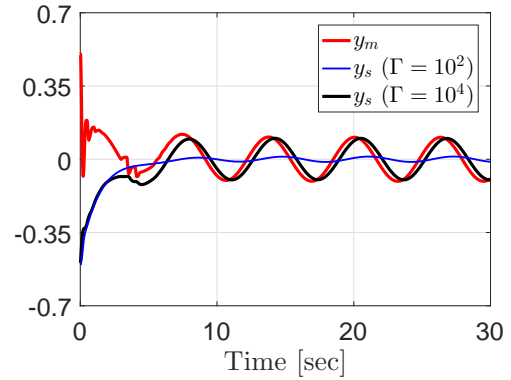
(b) $\mathcal{L}_1$: $y_s(t)$ and $y_m(t)$.
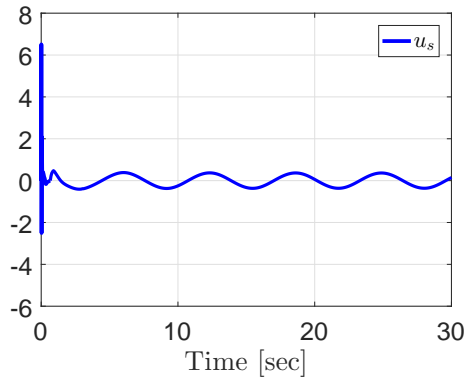
(c) **B-MRAC:** control signal $u_s(t)$.

(d) $\mathcal{L}_1$: control signal $u_s(t)$.

Figure 22 – Output-Feedback Adaptive Bilateral Teleoperation Scheme.

5.8 Conclusions

The global real-time differentiation issue and its application to obtain output-feedback model reference adaptive controllers for uncertain plants with arbitrary relative

degree have been explored in the present contribution. The proposed differentiator uses variable gains which are updated by a state-norm observer based on input-output filters. Global asymptotic stability of the overall closed-loop system was demonstrated and exact output tracking of a desired reference model is guaranteed. The generalization of the proposed methodology for other adaptation laws using parameter projection and leakage tools were also considered. Numerical results have shown the simplicity of the proposed approach when compared to classical adaptive controllers for higher relative degrees. An application to adaptive impedance force control for bilateral teleoperation was also addressed.

6 UNIT VECTOR SLIDING MODE CONTROL

In this chapter, we propose a unit vector control law by output feedback to solve the problem of global exact output tracking for a class of multivariable uncertain plants with nonlinear disturbances. In order to face the nonuniform arbitrary relative degree obstacle, we extend our ealier estimation scheme based on global finite-time differentiators using dynamic gains to a multivariable architecture.

A diagonally stable condition over the system high-frequency gain (HFG) matrix has to be assumed. Preserving the simplicity of its monovariable framework, variable gain super-twisting algorithm (STA) is employed to obtain the robust and exact multivariable differentiator. Moreover, state-norm observers for the unmeasured state variables are constructed to upper bound the disturbances as well as to update the differentiator gains, being both state dependent.

Uniform global exponential stability and ultimate exact tracking are proved. As an alternative to chattering alleviation, we appeal to the Emelyanov's concept of binary control in order to obtain a continuous control signal replacing the unit vector function in the controller by a high-gain gradient adaptive law with parameter projection. As shown in the existing literature for monovariable systems, the proposed multiparameter binary-adaptive formulation tends to the unit vector control as the adaptation gain increases to infinity, also smoothing the transition from adaptive to sliding mode control.

A numerical example is portrayed to illustrate the potentialities of the developed multivariable techniques.

6.1 Problem Formulation

Consider an uncertain MIMO system described by:

$$\dot{x} = A_p x + B_p [u + d(x,t)], \qquad y = H_p x, \tag{306}$$

where $x \in \mathbb{R}^n$ is the state, $u \in \mathbb{R}^m$ is the input, $y \in \mathbb{R}^m$ is the output and $d(x,t) \in \mathbb{R}^m$ is a state dependent uncertain nonlinear disturbance. The uncertain matrices A_p, B_p and H_p belong to some compact set, such that the necessary uncertainty bounds to be defined later are available for design. The following basic assumptions are usual in MIMO

adaptive control:

(A1) $G(s) = H_p(sI - A_p)^{-1}B_p$ is minimum phase and has full rank.

(A2) The linear subsystem is controllable and observable.

(A3) The observability index ν of $G(s)$ (see [103]), or an upper bound of ν, is known.

We also make the following assumptions that are discussed and motivated in [74].

(A4) The left interactor matrix $\Xi(s)$ (see [16]) is diagonal and $G(s)$ has a known global vector relative degree $\{\rho_1, \ldots, \rho_m\}$ (i.e., $\Xi(s) = \text{diag}\{s^{\rho_1}, \ldots, s^{\rho_m}\}$). The matrix $K_p \in \mathbb{R}^{m \times m}$, finite and nonsingular, is referred to as the *high-frequency gain* (HFG) matrix and satisfies $K_p = \lim_{s \to \infty} \Xi(s)G(s)$.

(A5) A nonsingular matrix S_p is known such that $-K_pS_p$ is diagonally stable, i.e. there exists a diagonal matrix $D > 0$ such that $DK + K^TD = -Q$, with $Q = Q^T > 0$ and $K = -K_pS_p$.

To achieve global exact tracking using only output feedback the following assumption is made.

(A6) The input disturbance $d(x,t)$ is assumed to be uncertain, locally integrable and norm bounded by $|d(x,t)| \leq k_x|x| + k_d$, $\forall x, t$, where $k_x, k_d \geq 0$ are *known* scalars.

Note that the relative degree of system (306) depends only on the linear part, being independent of the disturbance d. Although this assumption restricts the class of disturbances coped with, it represents a challenge in the context of output-feedback sliding mode control since global stability and exact tracking are still pursued. Despite the positive real diagonal Jordan form (PDJ) like conditions assumed for the HFG matrix in references [104], [105] are less conservative than that considered in (A5), no input disturbance ($d \equiv 0$) could be take into account in such previous designs.

Let the reference signal $y_m(t) \in \mathbb{R}^m$ be generated by the following reference model

$$y_m = W_m(s)\, r\,, \tag{307}$$

$$W_m(s) = \text{diag}\left\{(s+\gamma_1)^{-1}, \ldots, (s+\gamma_m)^{-1}\right\} L^{-1}(s)\,,$$

where $\gamma_i > 0$ $(i = 1, \cdots, m)$, $r(t) \in \mathbb{R}^m$ is an arbitrary uniformly bounded piecewise continuous reference signal and

$$L(s) = \text{diag}\{L_1(s), L_2(s), \ldots, L_m(s)\}\,, \tag{308}$$

with $L_i(s) = s^{(\rho_i-1)} + l^{[i]}_{\rho_i-2} s^{(\rho_i-2)} + \cdots + l^{[i]}_1 s + l^{[i]}_0$ $(i=1,\ldots,m)$ being Hurwitz polynomials and the superscript $^{[i]}$ indicating that a parameter belongs to $L_i(s)$. The transfer function matrix $W_m(s)$ has the same vector relative degree as $G(s)$ and its HFG is the identity matrix.

The main objective is to find a control law u such that the output error

$$e := y - y_m \tag{309}$$

tends asymptotically to zero, for arbitrary initial conditions. When the plant is known and $d(t) \equiv 0$, a control law which achieves the matching between the closed-loop transfer function matrix and $W_m(s)$ is given by $u^* = \theta^{*^T}\omega$, where the parameter matrix is written as $\theta^* = \begin{bmatrix} \theta_1^{*^T} & \theta_2^{*^T} & \theta_3^{*^T} & \theta_4^{*^T} \end{bmatrix}^T$, with $\theta_1^*, \theta_2^* \in \mathbb{R}^{m(\nu-1)\times m}$, $\theta_3^*, \theta_4^* \in \mathbb{R}^{m\times m}$ and the regressor vector $\omega = [\omega_u^T \ \omega_y^T \ y^T \ r^T]^T$ $(w_u, w_y \in \mathbb{R}^{m(\nu-1)})$ is obtained from I/O state variable filters given by:

$$\omega_u = A(s)\Lambda^{-1}(s)u\,, \quad \omega_y = A(s)\Lambda^{-1}(s)y\,, \tag{310}$$

where $A(s) = [Is^{\nu-2} \ Is^{\nu-3} \ \cdots \ Is \ I]^T$, $\Lambda(s) = \lambda(s)I$ with $\lambda(s)$ being a monic Hurwitz polynomial of degree $\nu - 1$. The matching conditions require that $\theta_4^{*^T} = K_p^{-1}$.

Consider the following realization of (310)

$$\dot{\omega}_u = \Phi\omega_u + \Gamma u\,, \quad \dot{\omega}_y = \Phi\omega_y + \Gamma y\,, \tag{311}$$

$$\Phi \in \mathbb{R}^{m(\nu-1)\times m(\nu-1)}\,, \quad \Gamma \in \mathbb{R}^{m(\nu-1)\times m} \tag{312}$$

where $\det(sI - \Phi) = \det(\Lambda(s)) = [\lambda(s)]^m$. Define the state vetor $X = [x^T, \omega_u^T, \omega_y^T]^T$ with dynamics described by $\dot{X} = A_0 X + B_0 u + B_0' d$, $y = H_o X$. Then, adding and subtracting $B_0\theta^{*^T}\omega$ and noting that there exist matrices Ω_1 and Ω_2 such that

$$\omega = \Omega_1 X + \Omega_2 r\,, \tag{313}$$

one has

$$\dot{X} = A_c X + B_c K_p[\theta_4^{*^T} r + u - u^*] + B_0' d\,, \quad y = H_o X\,, \tag{314}$$

where $A_c = A_0 + B_0\theta^{*^T}\Omega_1$ and $B_c = B_0\theta_4^{*^T}$. Notice that (A_c, B_c, H_o) is a nonminimal

realization of $W_m(s)$. For analysis purposes, the reference model can be described by

$$\dot{X}_m = A_c X_m + B_c K_p[\theta_4^{*T} r - d_f] + B_0' d, \quad y_m = H_o X_m, \tag{315}$$

the equivalent input disturbance

$$d_f = W_d(s)d, \tag{316}$$

where

$$W_d(s) = [W_m(s)K_p]^{-1} \bar{W}_d(s), \ \bar{W}_d(s) = H_o(sI - A_c)^{-1} B_0'. \tag{317}$$

Thus, $y_m = W_m(s)K_p\left[\theta_4^{*T} r - W_d(s)d\right] + \bar{W}_d(s)d$, it is straightforward to conclude that $y_m = W_m(s)r$. Thus, the error dynamics with state

$$X_e := X - X_m \tag{318}$$

is given by:

– State space –

$$\dot{X}_e = A_c X_e + B_c K_p[u - \theta^{*T}\omega + d_f], \ e = H_o X_e, \tag{319}$$

– Input-output form –

$$e = W_m(s)K_p\left[u - \theta^{*T}\omega + d_f\right]. \tag{320}$$

6.2   State-Norm Observer and Norm Bound for Equivalent Disturbance

In what follows we use state-norm observers to obtain a norm bound for x and $d_f(x, t)$.

Considering Assumption (A6) and applying [8, Lemma 3] to (314), it is possible to find $k_x^* > 0$ such that, for $k_x \in [0, k_x^*]$ a norm bound for X and x can be obtained through *first order approximation filters* (FOAFs) (see details in [8]). Thus, one has

$$|x(t)| \le |\hat{x}(t)| + \hat{\pi}(t), \tag{321}$$

where

$$\hat{x}(t) := \frac{1}{s + \lambda_x} \left[c_1 k_d + c_2 |\omega(t)| \right] , \qquad (322)$$

with $c_1, c_2, \lambda_x > 0$ being appropriate constants that can be computed by the optimization methods described in [56]. As in [8], the exponentially decaying term $\hat{\pi}$ accounts for the system initial conditions. Reminding that $d_f = W_d(s)d$ it is clear that $|d_f| \leq |W_d(s) * d|$, *modulo* an exponential decaying term depending on the initial conditions. Moreover, from (A6) and (322), one has $|d(x, t)| \leq k_x \hat{x}(t) + k_d$, *modulo* $\hat{\pi}$ term, and one can write $|d_f| \leq \hat{d}_f + \hat{\pi}_f$, where $\hat{\pi}_f$ is an exponentially decaying term,

$$\hat{d}_f(t) := \frac{c_f}{s + \lambda_f} \left[k_x \hat{x}(t) + k_d \right] , \qquad (323)$$

and $\frac{c_f}{s+\lambda_f}$ is a FOAF designed for $W_d(s)$, with adequate positive constants c_f and λ_f.

6.3 Unit Vector Control Design

For systems with uniform relative degree one, i.e. $\rho_1 = \rho_2 = \ldots \rho_m = 1$, the main idea is to close the control loop with a nominal control together with a unit vector control (UVC) term to cope with uncertainties and disturbances:

$$u = (\theta^{\text{nom}})^T \omega - \varrho(t) S_p \frac{e}{|e|} , \qquad (324)$$

where $e \in \mathbb{R}^m$, $S_p \in \mathbb{R}^{m \times m}$, $\varrho \in \mathbb{R}$, θ^{nom} is the nominal value for θ^*, S_p satisfies (A5) and the modulation function $\varrho(t) \geq 0$ is designed to induce a sliding mode on the manifold $e = 0$ and is such that:

$$\varrho(t) \geq (1 + c_d) |S_p^{-1} \left[(\theta^{\text{nom}} - \theta^*)^T \omega - d_f \right] | + \delta , \qquad (325)$$

where $c_d > 0$ is an appropriate constant and $\delta > 0$ can be arbitrarily small. Note that the nominal control signal allows the reduction of the modulation function amplitude if $|\theta^{\text{nom}} - \theta^*|$ is small. Since A_p, B_p and H_p belong to some known compact set, an upper bound $\bar{\theta} \geq |\theta^{\text{nom}} - \theta^*|$ can be obtained. Thus, a possible choice for the modulation function to satisfy (325) is given by

$$\varrho(t) = (1 + c_d) |S_p^{-1}| \left[\bar{\theta} |\omega| + |\hat{d}_f| \right] + \delta. \qquad (326)$$

For relative degree one plants, $W_m(s) = \text{diag}\left\{(s+\gamma_1)^{-1}, \ldots, (s+\gamma_m)^{-1}\right\}$ $(L(s) = I_m)$ and since $-K_p S_p$ is diagonally stable, by applying Lemma 1 in the appendix, one can conclude that the above scheme is uniformly globally exponentially stable and the output error e becomes identically zero after some finite time. For higher relative degree plants, one could use the operator $L(s)$ defined in (308), to overcome the relative degree obstacle. The operator $L(s)$ is such that $L(s)G(s)$ and $L(s)W_m(s)$ have uniform vector relative degree one. The ideal sliding variable $S = L(s)e \in \mathbb{R}^m$ is given by

$$
S = \begin{bmatrix} e_1^{(\rho_1-1)} + \cdots + l_1^{[1]}\dot{e}_1 + l_0^{[1]}\,e_1 \\ \vdots \\ e_m^{(\rho_m-1)} + \cdots + l_1^{[m]}\dot{e}_m + l_0^{[m]}e_m \end{bmatrix}
$$
$$
= \begin{bmatrix} \sum_{j=0}^{\rho_1-1} l_j^{[1]} h_1^T A_c^{(j)} X_e \\ \vdots \\ \sum_{j=0}^{\rho_m-1} l_j^{[m]} h_m^T A_c^{(j)} X_e \end{bmatrix} = \bar{H} X_e\,,
\tag{327}
$$

where $h_i \in \mathbb{R}^{n+2m(\nu-1)}$ is the i-th row of H_o matrix and the second equality is derived from Assumption (A4) and (319). From (307) and (308), one has

$$
\begin{aligned}
S &= L(s)W_m(s)Kp\left[u - \theta^{*T}\omega + d_f\right] \\
&= \text{diag}\left\{(s+\gamma_1)^{-1},\ \cdots,(s+\gamma_m)^{-1}\right\} K_p\left[u - \theta^{*T}\omega + d_f\right].
\end{aligned}
\tag{328}
$$

Notice that $\{A_c, B_c, \bar{H}\}$ is a nonminimal realization of $L(s)W_m(s)$. If the control signal is given by $u = (\theta^{nom})^T\omega - \varrho(t)S_p\frac{S}{|S|}$, with modulation function $\varrho(t)$ satisfying (325), then the closed-loop error system is uniformly globally exponentially stable and the ideal sliding variable S becomes identically zero after some finite time, according to Lemma 1 in the appendix. However, S is not directly available to implement the control law.

6.4 Global MIMO HOSM Differentiator with Dynamic Gains

In what follows, a MIMO HOSM differentiator with coefficients being adapted using the estimate for the norm of the state x provided in (321) is proposed to achieve global exact estimation, *i.e.*, exact differentiation of signals with any initial conditions and unbounded higher derivatives.

It is easy to show that the nonlinear system (306) can be transformed into the *normal form* [106, p. 224]:

$$\dot{\eta} = q(\xi, \eta), \tag{329}$$

$$\dot{\xi}_1^i = \xi_2^i,$$

$$\vdots \quad \vdots \tag{330}$$

$$\dot{\xi}_{\rho_i - 1}^i = \xi_{\rho_i}^i,$$

$$\dot{\xi}_{\rho_i}^i = b_i(\xi, \eta) + \sum_{j=1}^{m} a_{ij}(\xi, \eta),$$

$$y_i = \xi_1^i, \tag{331}$$

for all $1 \leq i \leq m$, where $z^T = [\eta^T \ \xi^T] \in \mathbb{R}^n$ with $\eta \in \mathbb{R}^{(n - \sum_{i=1}^m \rho_i)}$ being referred to the state of the inverse or zero dynamics and $\xi = [\xi_1^1, \ \ldots, \ \xi_{\rho_1 - 1}^1, \ \cdots, \ \xi_1^m, \ \ldots, \ \xi_{\rho_m - 1}^m]^T = [y_1, \ \ldots, \ y_1^{(\rho_1 - 1)}, \ \cdots, \ y_m, \ \ldots, \ y_m^{(\rho_m - 1)}]^T$ the external dynamics state. From Assumption (A1), we can concluded that η-dynamics is stable since the plant has minimum phase. Moreover, the terms $a_{ij}(\xi, \eta)$ and $b_i(\xi, \eta)$ are calculated by means of Lie Derivative such that $a_{ij}(\xi, \eta) = a_{ij}(x) = \sum_{j=1}^{m} H_p^{[i]} A_p^{\rho_i - 1} B_p^{[i,j]}(u_j + d_j(x, t))$ and $b_i(\xi, \eta) = b_i(x) = H_p^{[i]} A_p^{\rho_i} x$, where $H_p^{[i]}$ represents the i-th line matrix H_p and $B_p^{[i,j]}$ the element of line i-th line and j-th column of B_p. Therefore, for all $1 \leq i, j \leq m$, the ρ_i-derivative output y_i satisfy

$$y_i^{(\rho_i)} = H_p^{[i]} A_p^{\rho_i} x + \sum_{j=1}^{m} H_p^{[i]} A_p^{\rho_i - 1} B_p^{[i,j]}(u_j + d_j(x, t)). \tag{332}$$

The absolute value of $y_i^{(\rho_i)}$ satisfy

$$
\begin{aligned}
|y_i^{(\rho_i)}| &= \left| H_p^{[i]} A_p^{\rho_i} x + \sum_{j=1}^{m} H_p^{[i]} A_p^{\rho_i - 1} B_p^{[i,j]}(u_j + d_j(x, t)) \right| \\
&\leq \left| H_p^{[i]} A_p^{\rho_i} \right| |x| + \sum_{j=1}^{m} \left| H_p^{[i]} A_p^{\rho_i - 1} B_p^{[i,j]} \right| (|u_j| + |d_j(x, t)|) \\
&\leq \left| H_p^{[i]} A_p^{\rho_i} \right| |x| + \max_{k=1,\cdots,m} \left\{ \left| H_p^{[i]} A_p^{\rho_i - 1} B_p^{[i,j]} \right| \right\} \times \sum_{j=1}^{m} (|u_j| + |d_j(x, t)|) \\
&\leq \left| H_p^{[i]} A_p^{\rho_i} \right| |x| + \max_{k=1,\cdots,m} \left\{ \left| H_p^{[i]} A_p^{\rho_i - 1} B_p^{[i,j]} \right| \right\} \times m(|u| + |d|).
\end{aligned}
\tag{333}
$$

By using Assumption (A6) and (333), an upper for (332) is

$$|y_i^{(\rho_i)}| \leq \kappa_1^{[i]}|x| + \kappa_2^{[i]} + \kappa_3^{[i]}|u|\,, \tag{334}$$

where $\kappa_1^{[i]} > \left|H_p^{[i]}A_p^{\rho_i}\right| + m \max_{k=1,\cdots,m} \left\{\left|H_p^{[i]}A_p^{\rho_i-1}B_p^{[i,j]}\right|\right\}k_x$,

$\kappa_2^{[i]} > m \max_{k=1,\cdots,m} \left\{\left|H_p^{[i]}A_p^{\rho_i-1}B_p^{[i,j]}\right|\right\}k_d$ and

$\kappa_3^{[i]} > m \max_{k=1,\cdots,m} \left\{\left|H_p^{[i]}A_p^{\rho_i-1}B_p^{[i,j]}\right|\right\}$ are know constants.

From (334) and (309), we can write

$$|e_i^{(\rho_i)}(t)| \leq L_{\rho_i}^{[i]}(x,t) = \kappa_1^{[i]}|x| + \kappa_2^{[i]} + \kappa_3^{[i]}|u| + |y_{m_i}^{(\rho_i)}(t)|\,. \tag{335}$$

Now, assume that the control input satisfies the following *regularity condition* [57]:

$$|u| \leq k_\varrho \varrho(t) \leq \kappa_4\|X_t\| + \kappa_5\,, \tag{336}$$

for constants $\kappa_\varrho^{[i]}, \kappa_4^{[i]}, \kappa_5^{[i]} > 0$ and an appropriate continuous *modulation function* $\varrho(t) \geq 0$, to be defined later on. Then, applying (321), we can obtain the following upper bound with the norm observer variable $\hat{x}(t)$ in (321)–(322):

$$|e_i^{(\rho_i)}(t)| \leq \kappa_1^{[i]}(|\hat{x}| + \delta_0) + \kappa_2^{[i]} + \kappa_3^{[i]}\kappa_\varrho^{[i]}\varrho(t) + |y_{m_i}^{(\rho_i)}(t)|\,, \tag{337}$$

modulo exponential decaying terms due to initial conditions, which take into account the transient of the FOAF. By defining known positive constants $k_1^{[i]}$, $k_2^{[i]}$, $k_3^{[i]}$ and $\kappa_m^{[i]}$ satisfying $\kappa_m^{[i]} \geq |y_{m_i}^{(\rho_i)}(t)|$, $k_1^{[i]} \geq \kappa_1^{[i]}$, $k_2^{[i]} \geq \kappa_1^{[i]}\delta_0 + \kappa_2^{[i]} + \kappa_m^{[i]}$ and $k_3^{[i]} \geq \kappa_3^{[i]}\kappa_\varrho^{[i]}$, we can define

$$\mathcal{L}_{\rho_i}^{[i]}(\hat{x},t) := k_1^{[i]}|\hat{x}| + k_2^{[i]} + k_3^{[i]}\varrho(t)\,, \tag{338}$$

and state the following upper bound constructed only with measurable signals

$$|e_i^{(\rho_i)}(t)| \leq \mathcal{L}_{\rho_i}^{[i]}(\hat{x},t)\,, \quad \forall t \geq T\,, \tag{339}$$

for some finite time $T > 0$.

The sliding variable S can be estimated using a global MIMO extension of the

HOSM differentiator proposed in [17] such that exact tracking can be achieved. The idea here is to use a global HOSM differentiator with dynamic gains of order $p_i = \rho_i - 1$ for each output $e_i \in \mathbb{R}$, $i = 1, \ldots, m$ as follows:

$$
\begin{aligned}
\dot{\zeta}_0^{[i]} &= v_0^{[i]} = -\lambda_0^{[i]} \mathcal{L}_{\rho_i}^{[i]}(\hat{x}, t) |\zeta_0^{[i]} - e_i(t)|^{\frac{p_i}{p_i+1}} \mathrm{sgn}(\zeta_0^i - e_i(t)) + \zeta_1^{[i]} \\
&\vdots \\
\dot{\zeta}_j^{[i]} &= v_j^{[i]} = -\lambda_j^{[i]} \mathcal{L}_{\rho_i}^{[i]}(\hat{x}, t) |\zeta_j^{[i]} - v_{j-1}^{[i]}|^{\frac{p_i-j}{p_i-j+1}} \mathrm{sgn}(\zeta_j^{[i]} - v_{j-1}^{[i]}) + \zeta_{j+1}^{[i]}, \\
&\vdots \\
\dot{\zeta}_{p_i}^{[i]} &= -\lambda_{p_i}^{[i]} \mathcal{L}_{\rho_i}^{[i]}(\hat{x}, t) \mathrm{sgn}(\zeta_{p_i}^{[i]} - v_{p_i}^{[i]}),
\end{aligned}
\tag{340}
$$

where $\mathcal{L}_{\rho_i}^{[i]}(\hat{x}, t)$ is a variable gain designed such that $|e_i^{(\rho_i)}(t)| \leq \mathcal{L}_{\rho_i}^{[i]}(\hat{x}, t)$. A superscript $[i]$ is used to indicate that a particular parameter or variable belongs to a differentiator related with e_i.

If the parameters $\lambda_j^{[i]}$ are properly recursively chosen[4], then the equalities

$$
\zeta_0^{[i]} = e_i(t); \ \ \zeta_j^{[i]} = e_i^{(j)}(t), \quad i = 1, \ldots, m; \ j = 1, \ldots, p_i
$$

are established in finite time [11, 102]. Thus, using a global MIMO HOSM differentiator, composed by m differentiators of order $\rho_j - 1$ for each output e_j, the following estimate for S can be obtained:

$$
\hat{S} = \begin{bmatrix} \zeta_{\rho_1-1}^{[1]} + \cdots + l_1^{[1]} \zeta_1^{[1]} + l_0^{[1]} \zeta_0^{[1]} \\ \vdots \\ \zeta_{\rho_m-1}^{[m]} + \cdots + l_1^{[m]} \zeta_1^{[m]} + l_0^{[m]} \zeta_0^{[m]} \end{bmatrix}.
\tag{341}
$$

6.5 Global Output-feedback Unit Vector Control

Now, we propose a Global Output-feedback Unit Vector Sliding Mode Controller based on Multivariable HOSM differentiator. The Figure 23 shows a block diagram of our proposed control scheme.

The control law is given by:

$$
u = (\theta^{nom})^T \omega - \varrho(t) S_p \frac{\hat{S}}{|\hat{S}|},
\tag{342}
$$

---

[4]In particular, the following choice is valid for $p_i \leq 3$: $\lambda_0^{[i]} = 5, \lambda_1^{[i]} = 3, \lambda_2^{[i]} = 1.5, \lambda_3^{[i]} = 1.1$. For more details, see [17].
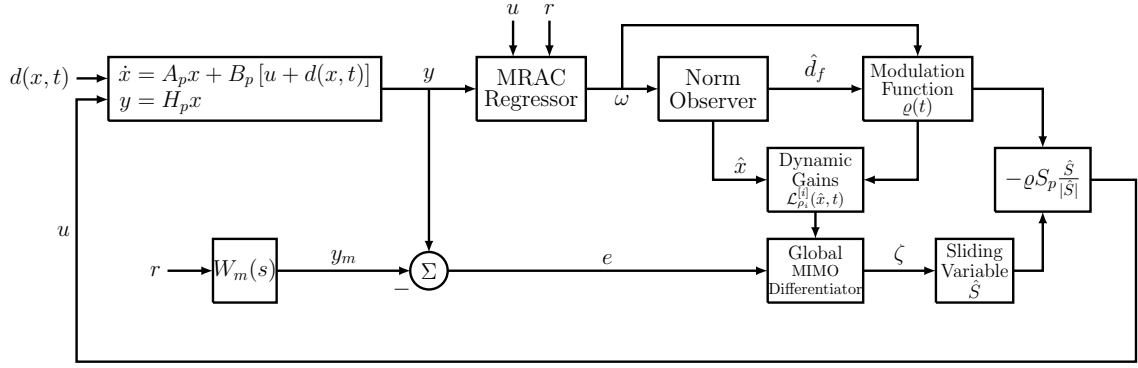
Figure 23 - Global Output-feedback Unit Vector Sliding Mode Controller based on Multivariable HOSM differentiator.

where the modulation function $\varrho(t)$ satisfies (325).

The following auxiliary lemma will be instrumental for the proof of Theorem 5.

Lemma 1. *Consider the MIMO system*

$$S(t) = M(s)K[u + d(t)], \tag{343}$$

where $M(s) = diag\{(s+\gamma_1)^{-1}, \ldots, (s+\gamma_m)^{-1}\}$, $\gamma_j > 0$, $K \in \mathbb{R}^{m \times m}$ is the high-frequency gain matrix and is such that $-K$ is diagonally stable, and $d(t)$ is locally integrable (LI). If $u = -\varrho(t)\frac{S}{|S|}$, $\quad \varrho \geq (1+c_d)|d(t)| + \delta$, where $\varrho(t)$ is LI, $c_d > 0$ is an appropriate constant, $\delta \geq 0$ is an arbitrary constant, then, the inequality

$$|S(t)| \text{ and } |x_e(t)| \leq c|x_e(0)|e^{-\lambda t} \tag{344}$$

holds $\forall t \geq 0$ for some positive constants c, λ, where x_e is the state of any stabilizable and detectable realization of (343) (possibly nonminimal). Moreover, if $\delta > 0$, then $S(t)$ becomes identically zero after some finite time $t_s \geq 0$.

Proof 1. *Consider a stabilizable and detectable realization of (343) described by $\dot{x} = Ax + B(u+d)$, $S = Hx$. From (343), one can obtain the normal form $\dot{\eta} = A_{11}\eta + A_{22}S$, $\quad \dot{S} = A_m S + K(u + d + \pi_\eta)$, where $A_m = diag\{-\gamma_1, \ldots, -\gamma_m\}$, $|\pi_\eta| \leq c_\eta|\eta(0)|e^{-\lambda_\eta t}$ and the zero dynamics given by $\dot{\eta} = A_{11}\eta$ is stable, since $M(s)$ is minimum phase. The state vector of this realization is $x_e^T = [\eta^T \ S^T]$. Consider the function $V(S) = S^T D S$, where $K^T D + DK = Q$, $Q = Q^T > 0$ for some diagonal matrix $D > 0$. The time derivative of $V(S)$ can be upper bounded by $\dot{V} \leq 2S^T DA_m S - \varrho\frac{S^T Q S}{|S|} + 2|DK||S|(|d| + |\pi_\eta|)$, Choosing $c_d \geq 2|DK|/\lambda_{min}(Q) - 1$, it can be verified that $\dot{V} \leq -\kappa_1|S|^2 - \delta|S| + |\bar{\pi}_\eta||S|$. Now, following the*

proof of Lemma 1 given in [8], one can conclude that $S(t) \leq \left(\kappa_2 |S(0)| + \kappa_3 |\eta(0)| \right) e^{-\bar{\lambda} t}$.
Moreover, if $\delta > 0$, it can be shown that S becomes identically zero in some finite time t_s.
Since A_{11} is Hurwitz, one can further conclude that (344) holds. □

The proposed control scheme guarantees global stability properties with ultimate exact tracking, as stated in the following theorem.

Theorem 5. *Consider the plant (306), the reference model (307)–(308) and the control law given by (342) with modulation function ϱ defined in (326) satisfying (325). The estimate $\hat{S}$ in (341) is given by the global MIMO Differentiator (340). Suppose that assumptions (A1) to (A6) hold. For $\lambda_j^{[i]}$, $i = 1, \ldots, m$, $j = 0, \ldots, \rho_i - 1$, properly chosen and $\mathcal{L}_{\rho_i}^{[i]}(\hat{x}, t)$ in (340) satisfying (338), the estimation of the ideal sliding variable S^T becomes exact after some finite time, i.e., $\hat{S}^T \equiv S^T$. Then, the closed-loop error system with dynamics (319) is uniformly globally exponentially stable in the sense that $X_e(t)$ and, hence, the output tracking error $e(t)$ converge exponentially to zero and all closed-loop signals remain uniformly bounded.*

Proof 5. *In what follows, $k_i > 0$ are constants not depending on the initial conditions. The demonstration is divided in two steps. In the first one, it is necessary to show that no finite time escape in the closed-loop system signals is possible. By using the relations (313) and (318), one has that $X = X_e + X_m$ and the regressor vector*

$$\omega = \Omega_1 X_e + \Omega_1 X_m + \Omega_2 r \,. \tag{345}$$

Let $x_m := [y_{m_1}, \ldots, y_{m_1}^{(\rho_1 - 1)}, \cdots, y_{m_m}, \ldots, y_{m_m}^{(\rho_m - 1)}]^T$ and $x_e := \xi - x_m$, with ξ in (330). From (319), it can be shown that $e_i^{(j)} = H_0^{[i]} A^j X_e$, for $j = 0, \ldots, \rho_i - 1$, hence $|x_e| \leq k_0 |X_e|$. Therefore, since x_m is uniformly bounded, then $\xi = x_e + x_m$ can be affinely norm bounded in $|X_e|$. In addition, from the minimum-phase assumption in (A1), we conclude the η-dynamics in (329) is input-to-state stable (ISS) – see [80] – with respect to ξ. Thus, one can conclude that $|x| \leq k_1 \|\xi_t\| + k_2$, and consequently, $|x| \leq k_3 \|(X_e)_t\| + k_4$. Due to assumption (A4) concerning the linear growth condition of the nonlinear disturbances with respect to the unmeasured state x, from (315) and (316), one has

$$|X_m| \leq k_5 \|(X_e)_t\| + k_6 \,. \tag{346}$$

Finally, from (313), (345) and (346), we conclude ω, the term d_f in (319), and consequently the control input u with modulation function ϱ in (326) are all affinely norm bounded by X or X_e, i.e.,

$$|u|, |d_f|, |\omega| \leq k_a \|X_t\| + k_b, \qquad (347)$$

$$|u|, |d_f|, |\omega| \leq k_c \|(X_e)_t\| + k_d. \qquad (348)$$

Thus, the system signals will be regular and, therefore, can grow at most exponentially [57]. Then, each dynamic gain $\mathcal{L}_{\rho_i}^{[i]}(\hat{x}, t)$ of our MIMO differentiator satisfy the following conditions introduced in [11] and [102] for fast and finite-convergence:

- *The global upper bound $\mathcal{L}_{\rho_i}^{[i]}$ is absolutely continuous with at least ultimate bounded logarithmic derivative ($|\dot{\mathcal{L}}_{\rho_i}^{[i]}/\mathcal{L}_{\rho_i}^{[i]}| \leq M_i$, for some constants $M_i > 0$) [11].*

- *Initially, the variable gain may have an arbitrary growth so that $\dot{\mathcal{L}}_{\rho_i}^{[i]}(\hat{x}, t) \geq 0$ implies into faster convergence rates for the differentiator [102].*

This fact lead us to the second step of the proof. There exist two finite-time instants $T_1 > 0$ and $T_2 > 0$ such that (339) and (325) are satisfied, $\forall t > \max\{T_1, T_2\}$. Then, the ideal sliding variable is exactly estimated, i.e., $\hat{S} \equiv S$ and the relative degree compensation is perfectly achieved. Moreover, from Lemma 1 (see Appendix) the ideal sliding mode $\hat{S}(t) \equiv S(t) \equiv 0$ is achieved in finite time. Since S in (327) is the relative degree one output for (319), it is possible to rewrite it into the normal form [106] such that the states of the error system are ISS with respect to S, for a particular exponential class-$\mathcal{KL}$ function. It can be shown reminding that $L(s)W_m(s) = diag\{(s + \gamma_1)^{-1}, \cdots, (s + \gamma_m)^{-1}\}$. From (319) and (328), one gets $\dot{X}_e = A_c X_e + B_c(\dot{S} + A_m S)$, where $A_m = diag\{-\gamma_1, \ldots, -\gamma_m\}$. Further, using the transformation $X_e := \bar{X}_e + B_c S$, one has

$$\dot{\bar{X}}_e = A_c \bar{X}_e + (A_c B_c + A_m B_c)S, \qquad (349)$$

which clearly implies an ISS relationship from S to either X_e or $\bar{X}_e$ since A_c is Hurwitz. Thus, X_e and $e = H_0 X_e$ tends exponentially to zero as well as the state ζ of the differentiator, which is also driven by e. From (348), we conclude that all remaining signals are uniformly bounded. □

6.6   Chattering Alleviation

Although the sliding mode controllers are known for its robustness with respect to parametric uncertainties and disturbances, the presence of chattering in the control signal is frequently an issue. An alternative to alleviate chattering employing continuous control signals is given by the B-MRAC. The B-MRAC is able to combine the good transient and robustness of sliding mode controllers while maintaining the typical smoothness of adaptive control.

6.6.1   Multivariable B-MRAC

The B-MRAC was originally proposed to deal with SISO plants [67] and only recently its MIMO version was presented [105] for plants with relative degree one. In this section, we consider the MIMO B-MRAC as in [104], which is deals with a further extension to plants of arbitrary relative degree. The control law is given by

$$u(t) = \theta^T(t)\omega(t) \tag{350}$$

where θ is an estimate of θ^* provided by an adaptive law. Moreover, a modified regressor matrix and vector parameter, respectively Ω and ϑ, are employed as

$$\Omega(t) = \begin{bmatrix} \omega(t) & & \\ & \ddots & \\ & & \omega(t) \end{bmatrix} , \ \vartheta(t) = \text{vec}(\theta) = \begin{bmatrix} \theta_1(t) \\ \vdots \\ \theta_m(t) \end{bmatrix} , \tag{351}$$

with dimensions $\Omega \in \mathbb{R}^{Nm \times n}$, $\vartheta \in \mathbb{R}^{Nm}$, being N the dimension of ω and θ_i is the i-th column of parameter θ. Finally, the adaptation law is

$$\dot{\vartheta}(t) = -\vartheta(t)\sigma - \gamma\Omega(t)\hat{S}(t) , \tag{352}$$

where $\hat{S}$ in (341) is the exact estimate of S given in (327) and σ generated by projection

$$\sigma = \begin{cases} 0 , & \text{if } |\vartheta| < M_\vartheta \quad \text{or} \quad \sigma_{eq} < 0 , \\ \sigma_{eq} , & \text{if } |\vartheta| \geq M_\vartheta \quad \text{and} \quad \sigma_{eq} \geq 0 , \end{cases} \tag{353}$$

with

$$\sigma_{eq} = -\frac{\gamma \vartheta^T \Omega \hat{S}}{|\vartheta|^2}, \tag{354}$$

and $M_\vartheta > |\vartheta^*|$ is a constant. Thus, the adaptive control law can be rewritten as

$$u(t) = \theta^T(t)\omega(t) = \Omega^T(t)\vartheta(t). \tag{355}$$

The control law (355) with adaptive law (352)–(354) is called B-MRAC in [67,68] due to its similarity to the *binary control* given in [66] – in [107], such liaison between adaptive and variable structure systems was named *dual-mode*. Indeed, in both cases, the integral adaptation is applied in some invariant compact set, such as the finite ball M_ϑ for ϑ. In B-MRAC, by considering that $|\vartheta(0)| \le M_\vartheta$, the projection of update vector can be understood geometrically as follows: if the term $-\gamma \vartheta^T \Omega \hat{S}$ points outwards the ball $|\vartheta| \le M_\vartheta$, the update vector is projected onto the tangent plane of the sphere; if it points inwards, the σ–factor is equal to zero and $\vartheta(t)$ moves to the interior of the ball, according to the standard MRAC gradient adaptation law [16]. Then, it is straightforward to prove that the closed ball with radius M_ϑ is invariant, that is, $|\vartheta(t)| \le M_\vartheta$, $\forall t \ge 0$. A mathematical demonstration of that can be derived considering the following Lyapunov function candidate

$$V_\vartheta = \frac{1}{2}\vartheta^T\vartheta. \tag{356}$$

Indeed, the time derivative of (356) along (352) results in

$$\dot{V}_\vartheta = (\sigma_{eq} - \sigma)|\vartheta|^2 = 2(\sigma_{eq} - \sigma)V_\vartheta, \tag{357}$$

and $(\sigma_{eq} - \sigma) \le 0$ for $|\vartheta| \ge M_\vartheta$, by virtue of (353) and (354). Thus, the set $|\vartheta| \le M_\vartheta$ is positively invariant and therefore $\tilde{\vartheta}^T\tilde{\vartheta}$ is uniformly bounded by a constant.

A similar regularity condition to (336) is directly satisfied as follows since the boundedness of ϑ is guaranteed by the parameter projection (353)–(354). Recalling that $\vartheta = \text{vec}(\theta)$ is uniformly bounded by a constant, one can conclude that θ is also uniformly bounded by a constant, such that, $|\theta| < \bar{\theta}$. Then, the control law (355) satisfies inequality

$$|u| \le \bar{\theta}|\omega(t)| \le k_7||X_t|| + k_8. \tag{358}$$

This property is established writing $|\omega| \leq k_9|X| + k_{10}$ from (313), with $k_9 \geq |\Omega_1|$ and $k_{10} \geq |\Omega_2 r|$, and reminding that $r(t)$ is a uniformly bounded reference signal. Then, we obtain the norm bound (358) from the norm bound for $|\omega|$. Thus, the global differentiator with dynamic gains given in (340) can indeed be constructed and its state exactly surrogates the time derivatives of the signal $e(t)$ in the variable $\hat{S} \equiv S$ (341), after some finite time. From (328), it is easy to show that $S(t) \to 0$ as $t \to +\infty$ since $L(s)W_m(s)$ is SPR, according to [16, Section 6.4.1]. Reminding that the error dynamics (319) is ISS with respect to $S(t)$, so one can conclude that $X_e(t)$ and $e(t)$ tend to zero at least asymptotically.

6.6.2   A Bridge Between B-MRAC and UVC

A relationship between the UVC and B-MRAC can be established considering increasing adaptation gains in B-MRAC. Following the steps given in [105], we consider the simplified unit vector control law (342) with $\theta^{nom} = 0$:

$$u = -\varrho S_p \frac{\hat{S}}{|\hat{S}|} \, , \tag{359}$$

with $\hat{S}$ in (341) and $\varrho(t)$ being its modulation function.

From adaptation law (352), one can write

$$\gamma^{-1}\dot{\vartheta} = -\vartheta\tilde{\sigma} - \Omega\hat{S} \, , \quad \tilde{\sigma} = \gamma^{-1}\sigma_{eq} \, , \tag{360}$$

where $\tilde{\sigma}$ is a scalar and σ_{eq} is defined in (354). As the adaptation gain increases such that $\gamma \to \infty$ ($\gamma^{-1} \to 0$), ϑ is given as the solution of $\vartheta\tilde{\sigma} + \Omega\hat{S} = 0$. From (354), we verify that for $\Omega\hat{S} \neq 0$ the equation $\vartheta\left(\frac{\vartheta^T \Omega\hat{S}}{M_\vartheta^2}\right) = \Omega\hat{S}$ must be satisfied. Thus, ϑ is collinear with the vector $\Omega\hat{S}$, and therefore ϑ can be expressed as $\vartheta = -M_\vartheta\frac{\Omega\hat{S}}{|\Omega\hat{S}|}$. Noting that $|\Omega\hat{S}| = |\omega||\hat{S}|$, it follows that

$$\vartheta = -M_\vartheta \frac{\Omega}{|\omega|} \frac{\hat{S}}{|\hat{S}|} \, , \tag{361}$$

where the negative sign is due to the fact that $\sigma \neq 0$, only if $\sigma_{eq} > 0$. Substituting (361)

into (355) and since $\Omega^T \Omega = |\omega|^2$, one has that

$$u = -M_\vartheta |\omega| \frac{\hat{S}}{|\hat{S}|}, \tag{362}$$

which is a UVC law with modulation function $\varrho = S_p^{-1} M_\vartheta |\omega|$.

6.7 Simulation Example

6.7.1 Results with UVC

In order to illustrate the proposed control strategy, we consider a nonlinear plant with nonuniform relative degree ($\rho_1 = 2$, $\rho_2 = 3$) described by (306), with

$$A_p = \begin{bmatrix} -2 & 3 & 0 & 0 & 0 \\ 1 & 0 & 0 & 0 & 0 \\ 1 & 2 & -6 & -11 & -6 \\ 0 & 0 & 1 & 0 & 0 \\ 0 & 0 & 0 & 1 & 0 \end{bmatrix}, \quad B_p^T = \begin{bmatrix} 1 & 0 & 0 & 0 & 0 \\ 0 & 0 & 1 & 0 & 0 \end{bmatrix},$$

$$H_p = \begin{bmatrix} 0 & \kappa & 0 & \kappa & 3\kappa \\ 0 & 0 & 0 & 0 & 1 \end{bmatrix},$$

$$G(s) = \begin{bmatrix} \frac{\kappa(s+2)}{(s-1)(s+1)(s+3)} & \frac{\kappa}{(s+1)(s+2)} \\ \frac{1}{(s-1)(s+1)(s+3)^2} & \frac{1}{(s+1)(s+2)(s+3)} \end{bmatrix},$$

where the constant $\kappa \in [4, 10]$ is uncertain and $K_p = \begin{bmatrix} \kappa & \kappa \\ 0 & 1 \end{bmatrix}$ is the linear subsystem HFG matrix. The input disturbance is considered uncertain for control design and is given by $d(x) = \begin{bmatrix} 0.2 \cos(t) \sin(x_2 \, x_3)|x_4| & \frac{1}{2\pi} \left(e^{-|x_5|}|x_1| + |x_2| \right) \end{bmatrix}^T$. This particular choice is motivated by the example considered in [108]. The reference signal and model are chosen as $r = [\sin(t) \; \sin(0.5t)] \, [\mathbb{1}(t) - \mathbb{1}(t - 20)]$ and $W_m(s) = \text{diag} \left\{ \frac{1}{(s+1)^2}, \frac{1}{(s+1)^2(s+2)} \right\}$.

To perform the simulations, the actual parameter κ is set to 10, while $\kappa^{nom} = 7$ is chosen for control purposes. For $\kappa^{nom} = 7$ and $\kappa \in [4, 10]$, it follows that $|(\theta^{\text{nom}} - \theta^*)^T| \leq 2$ and Assumption (A5) is satisfied with $S_p = I$. Then, in (342) the modulation function $\varrho(t)$ is given by (326), with $c_d = 2.25$, $|d_f| \leq \hat{d}_f$ and $\delta = 1$. The signal $\hat{d}_f$ is obtained by the FOAF described in (323), with $k_x = 0.2$, $k_d = 1$, $c_f = 5$, $\lambda_f = 0.5$ and $\hat{x}$ is a state-norm observer given by (322), with $c_1 = 1.2$, $c_2 = 2$ and $\lambda_x = 0.1$.

Other design parameters are listed as follows: I/O filters (310): $\lambda(s) = (s+2)^2$ and
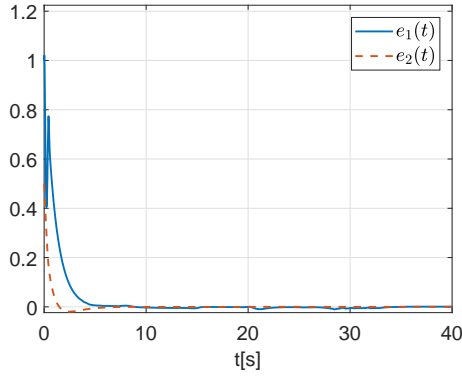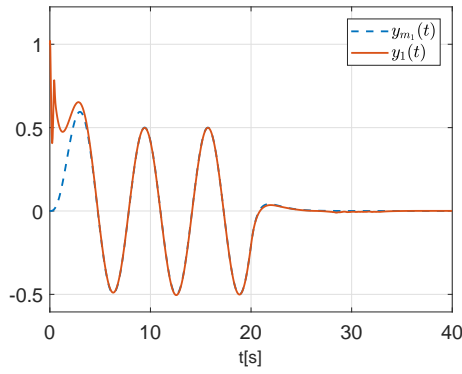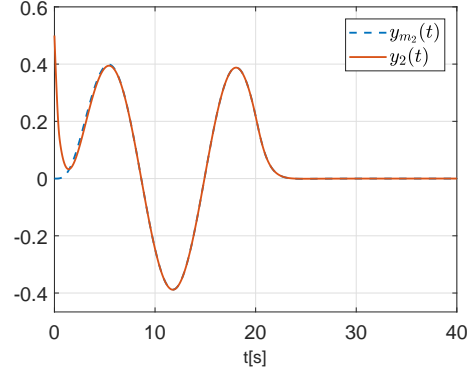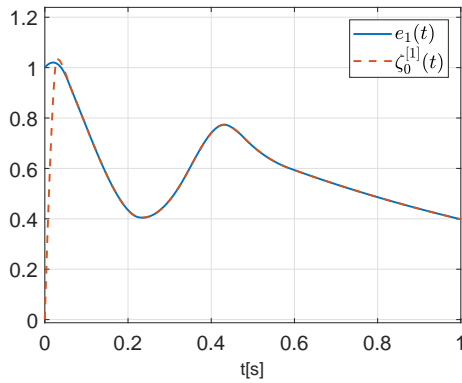
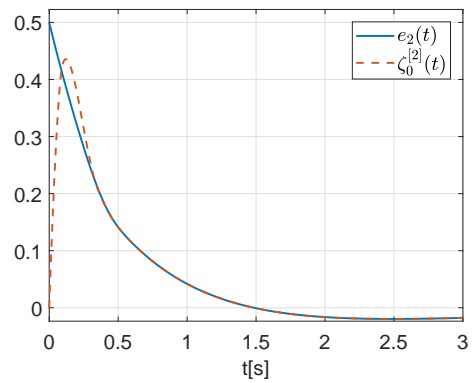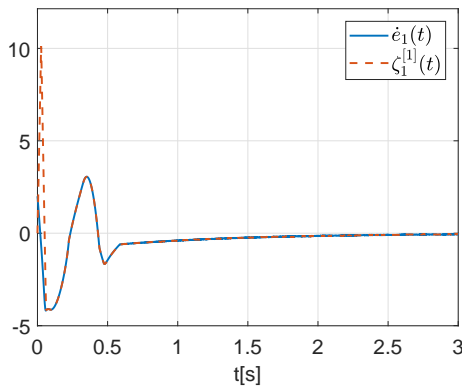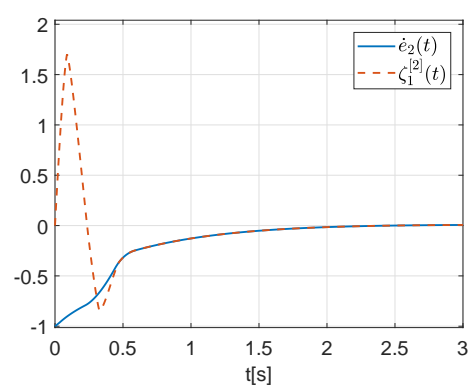(a) tracking errors.
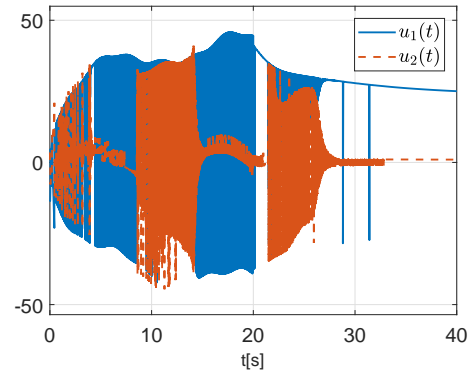
(b) control inputs.

(c) tracking performance for $y_1(t)$.

(d) tracking performance for $y_2(t)$.

(e) signal $e_1(t)$ and its estimate $\zeta_0^{[1]}(t)$.

(f) signal $e_2(t)$ and its estimate $\zeta_0^{[2]}(t)$.

(g) signal $\dot{e}_1(t)$ and its estimate $\zeta_1^{[1]}(t)$.

(h) signal $\dot{e}_1(t)$ and its estimate $\zeta_1^{[1]}(t)$.

Figure 24 - Numerical simulations of UVC – to be continued...

(a) signal $\ddot{e}_2(t)$ and its estimate $\zeta_2^{[2]}(t)$.

(b) dynamic gain and error bound.

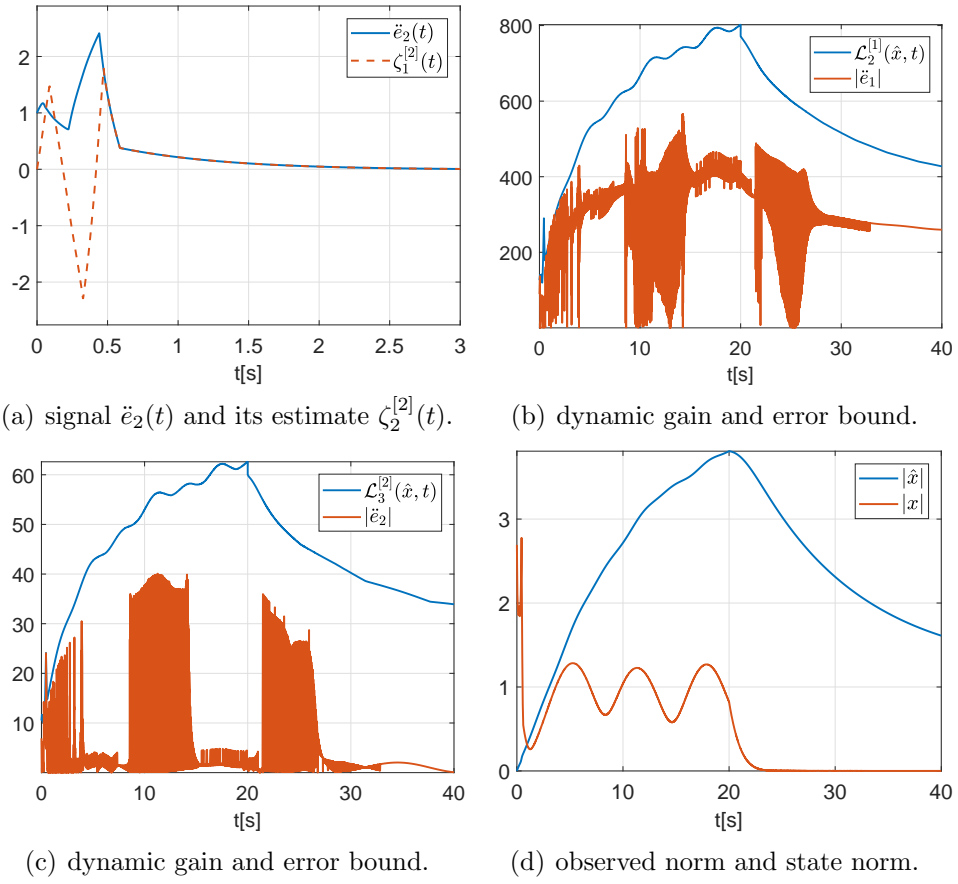(c) dynamic gain and error bound.

(d) observed norm and state norm.

Figure 25 - Numerical simulations of UVC.

$\nu = 3$; $L(s) = \text{diag}\{(s+1), (s+1)^2\}$; $K_p^{nom} = K_p$ with $\kappa = 7$; $N_a^{[1]} = s^2 + 2s + 1$, $N_a^{[2]} = s^3 + 3s^2 + 3s + 1$, $H_a^{[1]} = [2\ 1]^T$, $H_a^{[2]} = [4\ 5\ 2]^T$, $\bar{H}_M^{[1]} = [-1\ 1]^T$, $\bar{H}_M^{[2]} = [4\ -2\ 1]^T$; HOSM differentiator (340): $\lambda_0^{[1]} = 1.5$, $\lambda_1^{[1]} = 1.1$ and $\mathcal{L}_{\rho_1}^{[1]}(\hat{x}, t) = 130|\hat{x}| + 10\varrho + |y_{m_1}| + 2|\dot{y}_{m_1}| + |r_1|$; $\lambda_0^{[2]} = 3$, $\lambda_1^{[2]} = 1.5$, $\lambda_2^{[2]} = 1.1$ and $\mathcal{L}_{\rho_2}^{[2]}(\hat{x}, t) = 26|\hat{x}| + \varrho + 2|y_{m_2}| + 5|\dot{y}_{m_2}| + 4|\ddot{y}_{m_2}| + |r_2|$; note that y_{m_1}, y_{m_2} and their respective derivatives can be found by employing a state space implementation of the reference model. We consider the following plant initial conditions: $y_1(0) = 1$, $\dot{y}_1(0) = 2$, $y_2(0) = 0.5$, $\dot{y}_2(0) = -1$, $\ddot{y}_2(0) = 1$. The remaining system initial conditions are set to zero.

The Euler Method with step-size $h = 10^{-5}$ is used for numerical integration. Figure 24(a)-Figure 24(d) show good tracking performance with the control signals seen in Figure 24(b). The estimates given by the HOSM differentiatores are compared to estimated variables $e_j(t)$ and $\dot{e}_j(t)$ in Figure 24(e)–Figure 24(h), while the estimate for $\ddot{e}_2(t)$ is seen in Figure 25(a). In Figure 25(b) to Figure 25(d), we also show the time-history of the differentiator gains as well as the state-norm observer. Unlike other publications in the literature which applies strictly increasing gains [13, 49], our variable gains are decreasing with the state variables.

6.7.2 Results with Multivariable B-MRAC

To illustrate the performance of the B-MRAC strategy, we revisit the previous example. The parameter upper bound is $M_\vartheta = 12$ and the adaptation gain is initially set to $\gamma = 40$. The error signals and tracking performance are seen in Figure 26(a), Figure 26(c) and Figure 26(d), respectively, whereas the continuous control signals of B-MRAC are given in Figure 26(b). It is possible to note the fast convergence and good transient behavior achieved with the proposed smooth binary approach employing a projection-based adaptation law, as illustrated in Figure 27.

To illustrate the transition to UVC, the previous simulation is repeated with $\gamma = 100$ and $\gamma = 2000$. In Figs. Figure 28 and Figure 29 is possible to note that the control signals resemble the ones obtained in discontinuous UVC, as the adaptation gain γ increases.
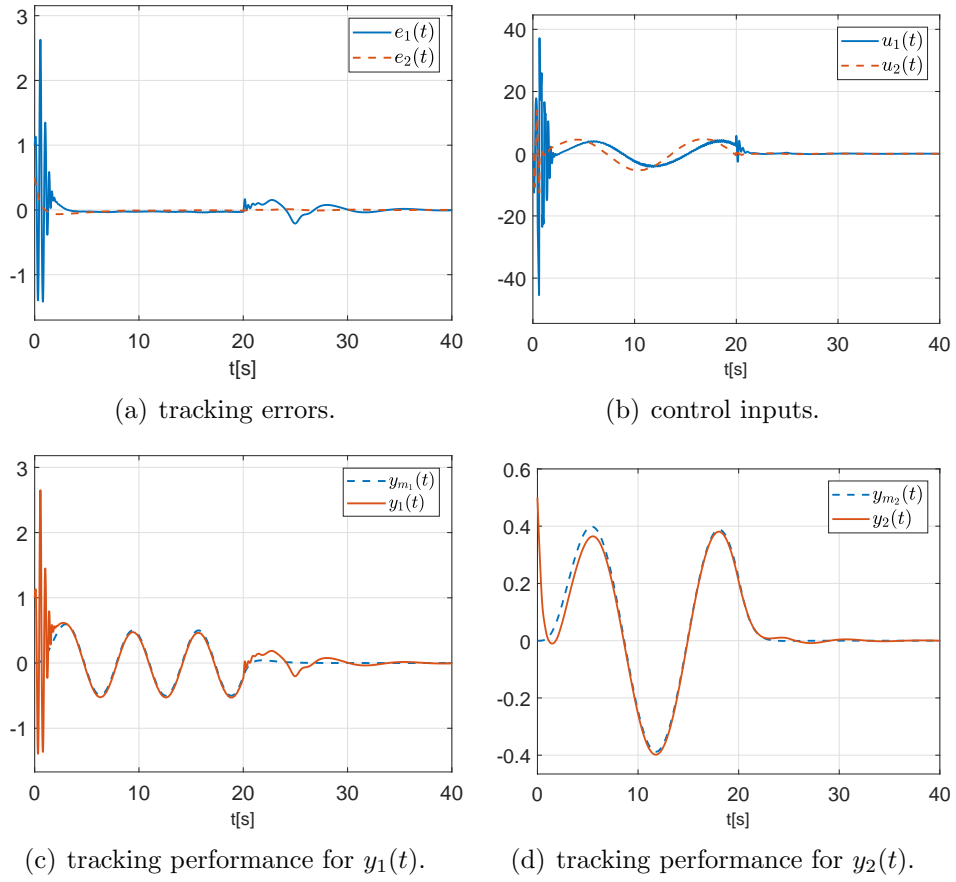
(a) tracking errors.

(b) control inputs.

(c) tracking performance for $y_1(t)$.

(d) tracking performance for $y_2(t)$.

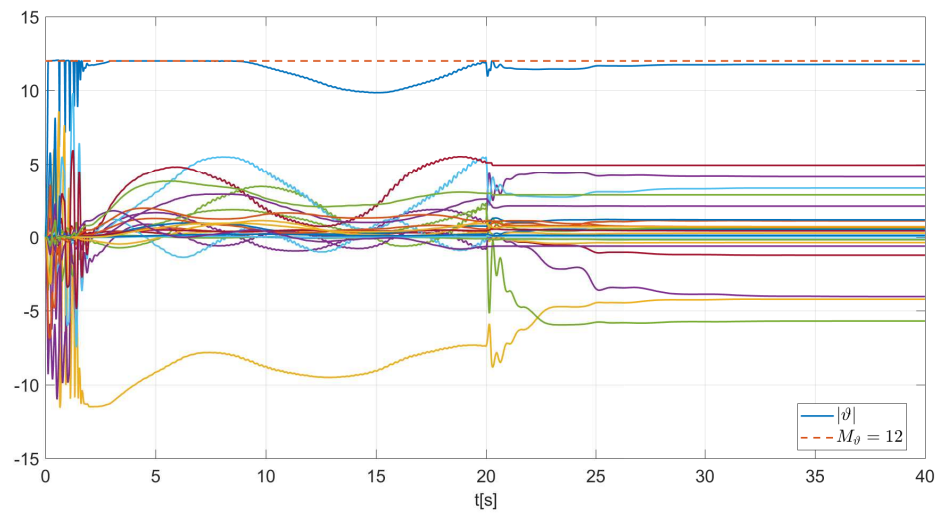Figure 26 - Numerical simulations of B-MRAC with $\gamma = 40$.

Figure 27 - Projection-based adaptive law in B-MRAC: adapted parameters (ϑ), parameters norm ($|\vartheta|$), and its upper bound (M_ϑ).
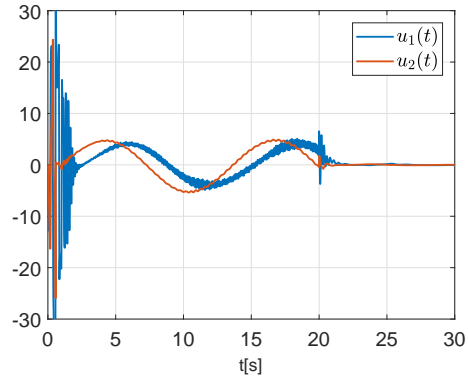
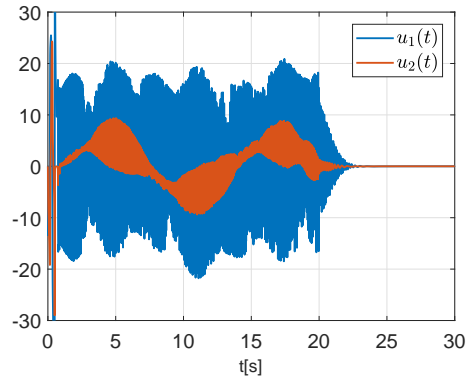Figure 28 - Control signals for B-MRAC with $\gamma = 100$.

Figure 29 - Control signals for B-MRAC with $\gamma = 2000$.

CONCLUSION

In Chapter 1, the problem of global differentiation and its application to output-feedback has been addressed. Instead of using a sufficiently large constant bound or strictly increasing time-varying gains, our differentiator applies for dynamic gains updated by a state-norm observer using only input-output information. In particular, such gains become necessarily large in order to guarantee the globality and then become smaller as possible under the control action, decreasing with the system states and improving the precision performance of the differentiator. Output-feedback sliding mode controllers based on the global differentiator are proposed for arbitrary relative degree plants with nonlinear disturbances and uncertainties. Both matched and unmatched disturbances were allowed. The former can grow inclusive with the unmeasured state. Uniform global stability and robust exact output tracking of a desirable reference model is guaranteed.

In Chapter 2, the problem of global adaptive and exact differentiation for output feedback has been solved. The gains of the proposed HOSM differentiator are dynamically updated according to the norm bound for the unmeasured state provided by a hybrid state-norm observer driven by a switching monitoring function. First order output-feedback sliding mode controller employing the adaptive differentiator is proposed for arbitrary relative degree plants with nonlinear matched disturbances/uncertainties with unknown and state-dependent bounds. The developed strategy assures ideal sliding modes in theory (and chattering alleviation in practice) as well as global stability results. Robust exact trajectory tracking is illustrated by simulations. An engineering application on the wing rock control problem for aircraft with high angles of attack was solved by means of the proposed control algorithm.

In Chapter 3, we have generalized Variable Gain Super-Twisting algorithm (VGSTA) using output feedback. The inclusion of the (non) homogeneous HOSM differentiator with dynamic gains in the control loop was the key element to achieve this extension. The limitation on conventional super twisting algorithm (STA) application restricted to relative degree one systems is eliminated. The gains of the differentiator and the controller were adapted according to the norm bound estimate for the unmeasured state provided by a norm observer to tackle the gain overestimation problem using only input-output information. The proposed gains are decreasing together with the system states and, consequently,

the precision of the tracking is growing. In practice, if the gains decrease, the sensitivity of the overall closed-loop system is reduced with respect to noise and signal sampling. The proposed output-feedback VGSTA can substitute the discontinuous first-order sliding mode control by an absolutely continuous controller ensuring chattering reduction, while guaranteeing global/semi-global stability properties and the exact compensation of uncertainties/disturbances for a class of systems with arbitrary relative degree. The main advantages of the proposed design were verified by numerical simulations concerning the trajectory tracking problem in an academic example and with stabilization experiments on a seesaw real-world control system as well.

In Chapter 4, the problem of adaptive differentiation for output-feedback has been solved for distinct families sliding mode controllers. The differentiator gains are dynamically updated according to the norm bound for the unmeassured state provided by a state-norm observer. The adaptive differentiator are proposed for arbitrary relative degree plants with nonlinear matched and unmacthed disturbances/uncertainties. The developed strategies assure ideal sliding modes in theory (and chattering alleviation in practice) as well as global or semi-global stability results. Robust exact trajectory tracking is illustrated by means of simulations.

In Chapter 5, the global real-time differentiation issue and its application to obtain output-feedback model reference adaptive controllers for uncertain plants with arbitrary relative degree have been explored in the present contribution. The proposed differentiator uses variable gains which are updated by a state-norm observer based on input-output filters. Global asymptotic stability of the overall closed-loop system was demonstrated and exact output tracking of a desired reference model is guaranteed. The generalization of the proposed methodology for other adaptation laws using parameter projection and leakage tools were also considered. Numerical results have shown the simplicity of the proposed approach when compared to classical adaptive controllers for higher relative degrees. An application to adaptive impedance force control for bilateral teleoperation was also addressed.

In Chapter 6, a new output feedback sliding mode tracking controller has been proposed for uncertain MIMO plants with nonuniform arbitrary relative degree in the presence of nonlinear state-dependent growing disturbances. The unit vector controller is based on a global multivariable HOSM differentiation scheme, which employs state-norm

observers to adapt the differentiator gains. Global exponential stability is guaranteed as well as ultimate exact output tracking of a reference model. The scheme allows ideal sliding modes in theory such that chattering is precluded in the ideal case. Indeed, the estimated sliding variable provided by the global MIMO HOSM differentiator, which drives the unit vector function, becomes identically zero after some finite time. As an alternative for chattering alleviation in practical scenarios under real-life imperfections such as measurement noise, unmodeled dynamics and switching delays, we employ binary control concepts to replace the unit vector function in the control law, thus obtaining a continuous control signal. Consistent simulation results are provided to support the theoretical developments.

FUTURE WORKS

Regarding the future directions, one can point out the extension of our results to more general classes of multivariable systems and the obtainment of new and general nonlinear sliding surfaces which allow us to conclude finite-time convergence for the tracking error signal rather than exponential one. The latter topic is really hardy since only the existence of such general nonlinear sliding surfaces were proved in the current literature, but the design of them were not presented yet. Some advances were restricted to finite-time stabilization of linear plants represented by a chain of integrators, as discussed in [95].

SCIENTIFIC PRODUCTION

I started my academic life at State University of Rio de Janeiro (UERJ) in 2009, as an undergraduate student in the bachelor course of Electrical Engineering. Since 2011, I have been advised by Professor Tiago Roux Oliveira in his research line, working on the fields of: control and synchronization of complex systems, estimation of nonlinear systems, adaptive control, extremum seeking and sliding mode control. I had the opportunity of participating in several international and national scientific events and I have published over fifteen archived journal and conference papers.

Bibliographical Production

Articles in Scientific Journals

1. OLIVEIRA, T. R. ; **RODRIGUES, V. H. P.** ; FRIDMAN, L. M. . *Generalized Model Reference Adaptive Control by means of Global HOSM Differentiators.* IEEE Transactions on Automatic Control.

2. OLIVEIRA, T. R. ; **RODRIGUES, V. H. P.** ; ESTRADA, A. ; FRIDMAN, L. M. . *Output-Feedback Variable Gain Super-Twisting Algorithm for Arbitrary Relative Degree Systems.* International Journal of Control.

3. **RODRIGUES, V. H. P.** ; OLIVEIRA, T. R. . *Global Adaptive HOSM Differentiators via Monitoring Functions and Hybrid Norm-State Observers for Output Feedback.* International Journal of Control.

4. **RODRIGUES, V. H. P.** ; OLIVEIRA, T. R. ; CUNHA, J. P. V. S. . *Globally Stable Synchronization of Chaotic Systems Based on Norm Observers Connected in Cascade.* IEEE Transactions on Circuits and Systems. II, Express Briefs, v. 63, p. 883-887, 2016.

Complete works published in proceedings of conferences

1. OLIVEIRA, T. R. ; **RODRIGUES, V. H. P.** ; ESTRADA, A. ; FRIDMAN, L. M. . *Adaptive HOSM Differentiator for Global/Semi-Global Output Feedback.* In: 20th World Congress of the International Federation of Automatic Control (IFAC'2017), 2017, Toulouse.

2. **RODRIGUES, V. H. P.**; OLIVEIRA, T. R. . *Monitoring Function for Switching Adaptation in Control and Estimation Schemes with Sliding Modes.* In: 2017 IEEE Conference on Control Technology and Applications, 2017, Kohala Coast.

3. OLIVEIRA, T. R.; **RODRIGUES, V. H. P.** . *Generalização do Controle Adaptativo por Modelo de Referência Através de Diferenciadores Globais.* In: XIII Simpósio Brasileiro de Automação Inteligente (SBAI'2017), 2017, Porto Alegre.

4. OLIVEIRA, T. R. ; KRSTIC, M. ; **RODRIGUES, V. H. P.**. *Busca Extremal Baseada no Método de Newton na Presença de Atrasos.* In: XXI Congresso Brasileiro de Automática (CBA'2016), 2016, Vitória.

5. **RODRIGUES, V. H. P.**; DANSA, M. M. ; OLIVEIRA, T. R. . *Estabilização Global para uma Classe de Sistemas Hipercaóticos através de Observadores da Norma em Cascata.* In: XII Simpósio Brasileiro de Automação Inteligente (SBAI'2015), 2015, Natal.

6. OLIVEIRA, T. R. ; KRSTIC, M. ; **RODRIGUES, V. H. P.**. *Realimentação por Preditor para Busca Extremal com Atrasos.* In: XII Simpósio Brasileiro de Automação Inteligente, 2015, Natal.

7. **RODRIGUES, VICTOR HUGO PEREIRA**; OLIVEIRA, TIAGO ROUX . *Chaos synchronization applied to secure communication via sliding mode control and norm state observers.* In: 2014 13th International Workshop on Variable Structure Systems (VSS), 2014, Nantes.

8. **RODRIGUES, V. H. P.**; OLIVEIRA, T. R. . *Sincronização Caótica Aplicada à Comunicação Segura Via Controle Por Modos Deslizantes.* In: XX Congresso Brasileiro de Automática (CBA'2014), 2014, Belo Horizonte.

9. OLIVEIRA, T. R. ; HSU, L. ; CUNHA, J. P. V. S. ; **RODRIGUES, V. H. P.** . *Controle Extremal via Função de Monitoração e Escalonamento Temporal para Grau Relativo Arbitrário.* In: XX Congresso Brasileiro de Automática (CBA'2014), 2014, Belo Horizonte.

10. **RODRIGUES, V. H. P.**; OLIVEIRA, T. R. . *Estabilização Global do Sistema Caótico de Lorenz através do Controle por Modos Deslizantes via Observadores da*

Norma. In: XII Conferência Brasileira de Dinâmica, Controle e Aplicações (DIN-CON'2013), 2013, Fortaleza.

Summary published in proceedings of conferences

1. **RODRIGUES, V. H. P.**; OLIVEIRA, T. R. . *Comunicação Caótica através do Controle Equivalente e Realimentação de Saída.* In: XXVI UERJ Sem Muros, 2015, Rio de Janeiro.

2. **RODRIGUES, V. H. P.**; OLIVEIRA, T. R. . *Controle por modos deslizantes via realimentação de saída para sistemas hiper-caóticos de classe ISS.* In: XXIII Semana de Iniciação Científica da UERJ, 2014, Rio de Janeiro. p. 796-796.

3. **RODRIGUES, V. H. P.**; OLIVEIRA, T. R. . *Sincronização do Caos aplicada à Comunicação Segura.* In: XXII Semana de Iniciação Científica da UERJ, 2013, Rio de Janeiro.

4. **RODRIGUES, V. H. P.** ; OLIVEIRA, T. R. . *Trazendo Ordem ao Caos: uma abordagem utilizando a teoria de controle por modos deslizantes.* In: XXI Semana de Iniciação Científica da UERJ, 2012, Rio de Janeiro.

Interview

1. **RODRIGUES, V. H. P.**. Student of State University of Rio de Janeiro receives Honorable Mention at the 20th Brazilian Congress of Automatica. 2014.

2. **RODRIGUES, V. H. P.**. Student of State University of Rio de Janeiro presents work at international congress held in France and receives Honorable Mention from Brazilian Society of Automatica. 2014.

Awards

Some of our contributions were recognized by important scientific and technological Brazilian Institutes. For instance, the project "Sincronização Global de Sistemas Caóticos via Realimentação de Saída com Observadores da Norma" received in 2017 the *V CREA-RJ Award for Scientific and Technological Projects* from Regional Council of Engineering and Architecture of Rio de Janeiro (CREA-RJ). The extended abstract published in

XXV Scientific Initiation Program of UERJ, "Comunicação Caótica através do Controle Equivalente e Realimentação de Saída", was awarded with Honorable Mention title from the Magnificent Dean of UERJ. The article presented in XX Brazilian Conference of Automatica (2014), entitled "Sincronização Caótica Aplicada à Comunicação Segura Via Controle Por Modos Deslizantes", received the Student Best Paper Awards of the Brazilian Society of Automatica. In 2012, for the participation and organization of scientific and technological activities, the Faculty of Engineering of UERJ, during the commemoration of its fifty years, granted me the Certificate of Merit.

1. V CREA-RJ Award for Scientific and Technological Works, CREA/RJ - Regional Council of Engineering and Architecture of Rio de Janeiro, 2017

2. Honorable Mention, UERJ - State University of Rio de Janeiro, 2015.

3. Honorable Mention, SBA - Brazilian Society of Automatica, 2014.

4. Honor to Merit, FEN/UERJ - Faculty of Engineering of the State University of Rio de Janeiro, 2012.

REFERENCES

[1] UTKIN, V. I.; GULDNER, J.; SHI, J. *Sliding Mode Control in Electro-Mechanical Systems*. CRC Press, 2009.

[2] ANGULO, M. T.; FRIDMAN, L.; MORENO, J. A. Output-feedback finite-time stabilization of disturbed feedback linearizable nonlinear systems. *Automatica*, v. 49, n. 9, p. 2767–2773, 2013.

[3] ANGULO, M. T.; FRIDMAN, L.; LEVANT, A. Output-feedback finite-time stabilization of disturbed LTI systems. *Automatica*, v. 48, n. 4, p. 606–611, 2012.

[4] PLESTAN, F.; SHTESSEL, Y.; BRéGEAULT, V.; POZNYAK, A. New methodologies for adaptive sliding mode control. *International Journal of Control*, v. 83, n. 9, p. 1907–1919, 2010.

[5] SHTESSEL, Y.; TALEB, M.; PLESTAN, F. A novel adaptive-gain supertwisting sliding mode controller: methodology and application. *Automatica*, v. 48, n. 5, p. 759–769, 2012.

[6] EDWARDS, C.; FLOQUET, T.; SPURGEON, S. Springer-Verlag, 2008. Cap. Circumventing the relative degree condition in sliding mode design, p. 137–158.

[7] POLYAKOV, A.; EFIMOV, D.; PERRUQUETTI, W. Finite-time and fixed-time stabilization: Implicit Lyapunov function approach. *Automatica*, v. 51, n. 1, p. 332–340, 2015.

[8] HSU, L.; COSTA, R. R.; CUNHA, J. P. V. S. Model-reference output-feedback sliding mode controller for a class of multivariable nonlinear systems. *Asian Journal of Control*, v. 5, n. 4, p. 543–556, 2003.

[9] CUNHA, J. P. V. S.; COSTA, R. R.; LIZARRALDE, F.; HSU, L. Peaking free variable structure control of uncertain linear systems based on a high-gain observer. *Automatica*, v. 45, p. 1156–1164, 2009.

[10] ESFANDIARI, F.; KHALIL, H. K. Output feedback stabilization of fully linearizable systems. *International Journal of Control*, v. 56, n. 10, p. 1007–1037, 1992.

[11] LEVANT, A.; LIVNE, M. Adjustment of higher-order sliding-mode controllers. *International Journal of Robust and Nonlinear Control*, v. 19, n. 15, p. 1657–1672, 2012.

[12] VAZQUEZ, C.; ARANOVSKIY, S.; FREIDOVICH, L. B.; FRIDMAN, L. M. Time-varying gain differentiator: A mobile hydraulic system case study. *IEEE Transactions on Control Systems Technology*, v. 24, n. 5, p. 1740–1750, 2016.

[13] EFIMOV, D.; FRIDMAN, L. A hybrid robust non-homogeneous finite-time differentiator. *IEEE Transactions on Automatic Control*, v. 56, n. 5, p. 1213–1219, 2011.

[14] NUNES, E. V. L.; HSU, L.; LIZARRALDE, F. Global tracking for uncertain systems using output-feedback sliding mode control. *IEEE Trans. Aut. Contr.*, v. 54, n. 5, p. 1141–1147, 2009.

[15] KRICHMAN, M.; SONTAG, E. D.; WANG, Y. Input-output-to-state stability. *SIAM J. Control Optim.*, v. 39, n. 6, p. 1874–1928, 2001.

[16] IOANNOU, P.; SUN, J. *Robust Adaptive Control.* Prentice Hall, 1996.

[17] LEVANT, A. Higher-order sliding modes, differentiation and output-feedback control. *International Journal of Control*, v. 76, n. 9, p. 924–941, 2003.

[18] CAPISANI, L. M.; FERRARA, A.; DE LOZA, A. F.; FRIDMAN, L. M. Manipulator fault diagnosis via higher order sliding-mode observers. *IEEE Transactions on Industrial Electronics*, v. 59, n. 10, p. 3979–3986, 2012.

[19] CHALANGA, A.; KAMAL, S.; FRIDMAN, L. M.; BANDYOPADHYAY, B.; MORENO, J. A. Implementation of super-twisting control: super-twisting and higher order sliding-mode observer-based approaches. *IEEE Transactions on Industrial Electronics*, v. 63, n. 6, p. 3677–3685, 2016.

[20] PILLONI, A.; PISANO, A.; USAI, E. Observer-based air excess ratio control of a PEM fuel cell system via high-order sliding Mode. *IEEE Transactions on Industrial Electronics*, v. 62, n. 8, p. 5236–5246, 2015.

[21] PLESTAN, F.; MOULAY, E.; GLUMINEAU, A.; CHEVIRON, T. Robust output feedback sampling control based on second-order sliding mode. *Automatica*, v. 46, n. 6, p. 1096–1100, 2010.

[22] REICHHARTINGER, M.; HORN, M. Application of higher order sliding-mode concepts to a throttle actuator for gasoline engines. *IEEE Transactions on Industrial Electronics*, v. 56, n. 9, p. 3322–3329, 2009.

[23] LEVANT, A. Sliding order and sliding accuracy in sliding mode control. *International Journal of Control*, v. 58, n. 6, p. 1247–1263, 1993.

[24] SHTESSEL, Y.; FRIDMAN, L.; PLESTAN, F. Adaptive sliding mode control and observation. *International Journal of Control*, v. 89, n. 9, p. 1743–1746, 2016.

[25] OLIVEIRA, T. R.; FRIDMAN, L. M.; ORTEGA, R. From adaptive control to variable structure systems – seeking harmony. *International Journal of Adaptive Control and Signal Processing*, v. 30, n. 8–10, p. 1074–1079, 2016.

[26] ESTRADA, A.; FRIDMAN, L. Integral HOSM semiglobal controller for finite-time exact compensation of unmatched perturbations. *IEEE Transactions on Automatic Control*, v. 55, n. 11, p. 2645–2649, 2010.

[27] VAZQUEZ, C.; ARANOVSKIY, S.; FREIDOVICH, L. B.; FRIDMAN, L. M. Time-varying gain differentiator: A mobile hydraulic system case study. *IEEE Transactions on Control Systems Technology*, v. 24, n. 5, p. 1740–1750, 2016.

[28] LEVANT, A. Globally convergent fast exact differentiator with variable gains. *European Control Conference*, p. 2925–2930, 2014.

[29] OLIVEIRA, T. R.; PEIXOTO, A. J.; NUNES, E. V. L.; HSU, L. Control of uncertain nonlinear systems with arbitrary relative degree and unknown control direction using sliding modes. *International Journal of Adaptive Control and Signal Processing*, v. 21, n. 8–9, p. 692–707, 2007.

[30] GOEBEL, R.; SANFELICE, R. G.; TEEL, A. R. *Hybrid Dynamical Systems - Modeling, Stability, and Robustness*. Princeton University Press, 2012.

[31] HUNG, J. Y.; GAO, W.; HUNG, J. C. Variable structure control: a survey. *IEEE Transactions on Industrial Electronics*, v. 40, n. 1, p. 2–22, 1993.

[32] UTKIN, V. I. Sliding mode control design principles and applications to electric drives. *IEEE Transactions on Industrial Electronics*, v. 40, n. 1, p. 23–36, 1993.

[33] YU, X.; KAYNAK, O. Sliding mode control with soft computing: A survey. *IEEE Transactions on Industrial Electronics*, v. 56, n. 9, p. 3275–3285, 2009.

[34] BARTOLINI, G.; FERRARA, A.; USAI, E. Chattering avoidance by second order sliding mode control. *IEEE Transactions on Automatic Control*, v. 43, n. 2, p. 241–246, 1998.

[35] LEVANT, A. Construction Principles of 2-sliding mode design. *Automatica*, v. 43, n. 5, p. 576–586, 2007.

[36] ORLOV, Y. *Discontinuous Control*. Springer-Verlag, 2009.

[37] PISANO, A.; USAI, E. Contact force regulation in wire-actuated pantographs via variable structure control and frequency-domain techniques. *International Journal of Control*, v. 81, n. 11, p. 1747–1762, 2008.

[38] SHTESSEL, Y.; BAEV, S.; SHKOLNIKOV, I. Nonminimum-phase output tracking in causal systems using higher order sliding modes. *International Journal of Robust and Nonlinear Control*, v. 18, n. 4-5, p. 454–467, 2008.

[39] BUTT, Q. R.; BHATTI, A. I. Estimation of gasoline–engine parameters using higher order sliding mode. *IEEE Transactions on Industrial Electronics*, v. 55, n. 11, p. 3891–3898, 2008.

[40] AHMED, Q.; BHATTI, A. I. Estimating SI engine efficiencies and parameters in second-order sliding modes. *IEEE Transactions on Industrial Electronics*, v. 58, n. 10, p. 4837–4846, 2011.

[41] EVANGELISTA, C.; PULESTON, P.; VALENCIAGA, F.; FRIDMAN, L. M. Lyapunov-designed super-twisting sliding mode control for wind energy conversion optimization. *IEEE Transactions on Industrial Electronics*, v. 60, n. 2, p. 538–545, 2013.

[42] CASTAÑEDA, H.; PLESTAN, F.; CHRIETTE, A.; LEÓN-MORALES, J. D. Continuous differentiator based on adaptive second-order sliding-mode control for a 3-DOF helicopter. *IEEE Transactions on Industrial Electronics*, v. 63, n. 9, p. 5786–5793, 2016.

[43] GENNARO, S. D.; DOMÍNGUEZ, J. R.; MEZA, M. A. Sensorless high order sliding mode control of induction motors with core loss. *IEEE Transactions on Industrial Electronics*, v. 61, n. 26, p. 2678–2689, 2014.

[44] ALWI, H.; EDWARDS, C.; STROOSMA, O.; MULDER, J. A.; HAMAYUN, M. T. Real-time implementation of an ISM fault tolerant control scheme for LPV plants. *IEEE Transactions on Industrial Electronics*, v. 62, n. 6, p. 3896–3905, 2014.

[45] NAGESH, I.; EDWARDS, C. A multivariable super-twisting sliding mode approach. *Automatica*, v. 50, n. 3, p. 984–988, 2014.

[46] EDWARDS, C.; SHTESSEL, Y. Adaptive dual-layer super-twisting control and observation. *International Journal of Control*, v. 89, n. 9, p. 1759–1766, 2016.

[47] BARTH, A.; REICHHARTINGER, M.; WULFF, K.; HORN, M.; REGER, J. Certainty equivalence adaptation combined with super-twisting sliding-mode control. *International Journal of Control*, v. 89, n. 9, p. 1767–1776, 2016.

[48] BARTOLINI, G.; LEVANT, A.; PISANO, A.; USAI, E. Adaptive second-order sliding mode control with uncertainty compensation. *International Journal of Control*, v. 89, n. 9, p. 1747–1758, 2016.

[49] NEGRETE-CHÁVEZ, D. Y.; MORENO, J. Second-order sliding mode output feedback controller with adaptation. *International Journal of Adaptive Control and Signal Processing*, v. 30, n. 8–10, p. 1523–1543, 2016.

[50] MORENO, J. A. Levant's Arbitrary Order Differentiator with Varying Gain. *Proceedings of the 20th World Congress of the International Federation of Automatic Control*, p. 1741–1746, 2017.

[51] GONZALEZ, T.; MORENO, J. A.; FRIDMAN, L. Variable gain super-twisting sliding mode control. *IEEE Transactions on Automatic Control*, v. 57, n. 8, p. 2100–2105, 2012.

[52] MORENO, J. A. A linear framework for the robust stability analysis of a Generalized Super-Twisting Algorithm. *6th International Conference on Electrical Engineering, Computing Science and Automatic Control*, p. 1–6, 2009.

[53] LI, Y.; TONG, S.; LIU, L.; FENG, G. Adaptive output-feedback control design with prescribed performance for switched nonlinear systems. *Automatica*, v. 80, n. 6, p. 225–231, 2017.

[54] OLIVEIRA, T. R.; ESTRADA, A.; FRIDMAN, L. M. Global exact differentiator based on higher-order sliding modes and dynamic gains for globally stable output-feedback control. *54th IEEE Conference on Decision and Control*, p. 4109–4114, 2015.

[55] OLIVEIRA, T. R.; ESTRADA, A.; FRIDMAN, L. M. Output-Feedback Generalization of Variable Gain Super-Twisting Sliding Mode Control via Global HOSM Differentiators. *14th International Workshop on Variable Structure Systems*, p. 257–262, 2016.

[56] CUNHA, J. P. V. S.; COSTA, R. R.; HSU, L. Design of first-order approximation filters for sliding-mode control of uncertain systems. *IEEE Transactions on Industrial Electronics*, v. 55, n. 11, p. 4037–4046, 2008.

[57] SASTRY, S. S.; BODSON, M. *Adaptive Control: Stability, Convergence and Robustness.* Prentice Hall, 1989.

[58] MONOPOLI, R. V. Model reference adaptive control with an augmented error signal. *IEEE Transactions on Automatic Control*, v. 19, p. 474–484, 1974.

[59] FEUER, A.; MORSE, A. S. Adaptive control of single-input, single-output linear systems. *IEEE Transactions on Automatic Control*, v. 23, p. 557–569, 1978.

[60] KRSTIC, M.; KANELLAKOPOULOS, I.; KOKOTOVIC, P. V. *Nonlinear and adaptive control design.* Wiley, 1995.

[61] CAO, C.; HOVAKIMYAN, N. Design and analysis of a novel $\mathcal{L}_1$ adaptive control architecture with guaranteed transient performance. *IEEE Transactions on Automatic Control*, v. 53, n. 2, p. 586–591, 2008.

[62] ORTEGA, R.; PANTELEY, E. Comments on $\mathcal{L}_1$–adaptive control: Stabilization mechanism, existing conditions for stability and performance limitations. *International Journal of Control*, v. 87, n. 3, p. 581–588, 2014.

[63] IOANNOU, P. A.; ANNASWAMY, A. M.; NARENDRA, K. S.; JAFARI, S.; RUDD, L.; ORTEGA, R.; BOSKOVIC, J. $\mathcal{L}_1$–adaptive control: Stability, robustness and interpretations. *IEEE Transactions on Automatic Control*, v. 59, n. 11, p. 3075–3080, 2014.

[64] ORTEGA, R.; PANTELEY, E. Adaptation is unnecessary in $\mathcal{L}_1$–adaptive control: what makes an adaptive controller adaptive? *IEEE Control Systems Magazine*, v. 36, n. 1, p. 47–52, 2016.

[65] HOVAKIMYAN, N.; CAO, C. $\mathcal{L}_1$ *adaptive control theory: Guaranteed robustness with fast adaptation*. SIAM, 2010.

[66] EMELYANOV, S. V. *Binary automatic control systems*. MIR Publishers, 1987.

[67] HSU, L.; COSTA, R. R. B-MRAC: Global exponential stability with a new model reference adaptive controller based on binary control theory. *Control-Theory and Advance Technology*, v. 10, n. 4, p. 649–668, 1994.

[68] OLIVEIRA, T. R.; PEIXOTO, A. J.; NUNES, E. V. L. Binary robust adaptive control with monitoring functions for systems under unknown high-frequency-gain sign, parametric uncertainties and unmodeled dynamics. *International Journal of Adaptive Control and Signal Processing*, v. 30, n. 8-10, p. 1184–1202, 2016.

[69] HSU, L.; COSTA, R. R. Bursting phenomena in continuous-time adaptive systems with a σ–modification. *IEEE Transactions on Automatic Control*, v. 32, p. 84–86, 1987.

[70] FERRE, M.; BUSS, M.; ARACIL, R.; MELCHIORRI, C.; BALAGUER, C. *Advances in telerobotics*. Springer, 2007.

[71] LOVE, L. J.; BOOK, W. J. Force reflecting teleoperation with adaptive impedance control. *IEEE Transactions on Systems, Man, and Cybernetics, Part B: Cybernetics*, v. 34, n. 1, p. 159–165, 2004.

[72] HOKAYEM, P. F.; SPONG, M. W. Bilateral teleoperation: an historical survey. *Automatica*, v. 42, n. 12, p. 2035–2057, 2006.

[73] BARTOLINI, G.; FERRARA, A.; USAI, E.; UTKIN, V. I. On multi-input chattering-free second-order sliding mode control. *IEEE Transactions on Automatic Control*, v. 45, n. 9, p. 1711–1717, 2000.

[74] NUNES, E. V. L.; PEIXOTO, A. J.; OLIVEIRA, T. R.; HSU, L. Global exact tracking for uncertain MIMO linear systems by output feedback sliding mode control. *Journal of the Franklin Institute*, v. 351, n. 4, p. 2015–2032, 2014.

[75] OLIVEIRA, T. R.; ESTRADA, A.; FRIDMAN, L. M. Global and exact HOSM differentiator with dynamic gains for output-feedback sliding mode control. *Automatica*, v. 81, n. 7, p. 156–163, 2015.

[76] OLIVEIRA, T. R.; RODRIGUES, V. H. P.; ESTRADA, A.; FRIDMAN, L. M. HOSM Differentiator with Varying Gains for Global/Semi-Global Output Feedback. In: . c2017. p. 1728–1735.

[77] OLIVEIRA, T. R.; RODRIGUES, V. H. P.; ESTRADA, A.; FRIDMAN, L. M. Output-Feedback Variable Gain Super-Twisting Algorithm for Arbitrary Relative Degree Systems. *International Journal of Control*, 2017.

[78] RODRIGUES, V. H. P.; OLIVEIRA, T. R. Global Adaptive HOSM Differentiators via Monitoring Functions and Hybrid State-Norm Observers for Output Feedback. *International Journal of Control*, 2017.

[79] NAGESH, I.; EDWARDS, C. A multivariable super-twisting sliding mode approach. *Automatica*, v. 50, n. 3, p. 984–988, 2014.

[80] KHALIL, H. K. *Nonlinear Systems*. Prentice Hall, 2002.

[81] FILIPPOV, A. F. *Differential equations with discontinuous right-hand side*. American Mathematical Society Translations, 1964. v. 42.

[82] HSU, L.; PEIXOTO, A. J.; CUNHA, J. P. V.; COSTA, R. R.; LIZARRALDE, F. Springer, Berlin, Heidelberg, 2006. Cap. Output-feedback sliding mode control for a class of uncertain multivariable systems with unmatched nonlinear disturbances.

[83] LEVANT, A. Globally convergent fast exact differentiator with variable gains. In: . Strasbourg, France: , c2014. p. 2925–2930.

[84] HSU, L.; LIZARRALDE, F.; ARAUJO, A. D. New results on output-feedback variable structure model-reference adaptive control: design and stability analysis. *IEEE Transactions on Automatic Control*, v. 42, n. 3, p. 386–393, 1997.

[85] YANQUE, I.; NUNES, E. V. L.; COSTA, R. R.; HSU, L. Binary MIMO MRAC using a Passifying Multiplier - A smooth transition to Sliding Mode Control. In: . c2012. p. 1925–1930.

[86] NAYFEH, A. H.; ELZEBDA, J. M.; MOOK, D. T. Analytical Study of the Subsonic Wing-Rock Phenomenon for Slender Delta Wings. *Journal of Aircraft*, v. 26, n. 9, p. 805–809, 1989.

[87] JOSHI, S. V.; SREENTHA, A. G.; CHANDRASEKHAR, J. Suppression of wing rock of slender delta wings using a single neuron controller. *IEEE Transactions on Control Systems Technology*, v. 6, n. 5, p. 671–677, 1998.

[88] VIDAL, P. V. N. M.; NUNES, E. V. L.; HSU, L. Output-Feedback Multivariable Global Variable Gain Super-Twisting Algorithm. *IEEE Transactions on Automatic Control*, v. 62, n. 6, p. 2999–3005, 2017.

[89] CASTILLO, I.; FRIDMAN, L.; MORENO, J. A. Super-Twisting Algorithm in presence of time and state dependent perturbations. *International Journal of Control*, p. 1–14, 2017.

[90] BASIN, M. V.; RAMIREZ, P. C. R. A Supertwisting Algorithm for Systems of Dimension More Than One. *IEEE Transactions on Industrial Electronics*, v. 61, n. 11, p. 6472–6480, 2014.

[91] BASIN, M. V.; PANATHULA, C. B.; SHTESSEL, Y. B.; RAMIREZ, P. C. R. Continuous Finite-Time Higher Order Output Regulators for Systems with Unmatched Unbounded Disturbances. *IEEE Transactions on Industrial Electronics*, v. 63, n. 8, p. 5036–5043, 2014.

[92] LEVANT, A.; MICHAEL, A. Adjustment of higher-order sliding-mode controllers. *International Journal of Robust and Nonlinear Control*, v. 19, n. 15, p. 1657–1672, 2009.

[93] LEVANT, A. Non-homogeneous finite-time-convergent differentiator. *Joint 48th IEEE Conference on Decision and Control and 28th Chinese Control Conference*, p. 8399–8404, 2009.

[94] UTKIN, V. I. Discussion aspects of high-order sliding mode control. *IEEE Transactions on Automatic Control*, v. 61, n. 3, p. 829–833, 2016.

[95] BHAT, S. P.; BERNSTEIN, D. S. Geometric homogeneity with applications to finite-time stability. *Mathematics of Control, Signals and Systems*, v. 17, p. 101–127, 2005.

[96] DEIMLING, D. *Multivalued Differential Equations*. De Gruyter, 1992.

[97] ACKERMANN, J.; UTKIN, V. Sliding mode control design based on Ackermann's formula. *IEEE Transactions on Automatic Control*, v. 43, n. 2, p. 234–237, 1998.

[98] APKARIAN, J. A comprehensive and modular laboratory for control systems design and implementation. *Markham, ON, Canada: Quanser Consulting*, 1995.

[99] VENTURA, U. P.; FRIDMAN, L. Is It Reasonable to Substitute Discontinuous SMC by Continuous HOSMC? *https://www.researchgate.net/publication/317229996*, 2017.

[100] OLIVEIRA, T. R.; RODRIGUES, V. H. P.; ESTRADA, A.; FRIDMAN, L. M. HOSM Differentiator with Varying Gains for Global/Semi-Global Output Feedback. *Proceedings of the 20th World Congress of the International Federation of Automatic Control*, p. 1764–1771, 2017.

[101] FENG, Y.; YU, X.; MAN, Z. Non-singular terminal sliding mode control of rigid manipulators. *Automatica*, v. 38, n. 12, p. 2159–2167, 2002.

[102] MORENO, J. A. Exact differentiator with varying gains. *International Journal of Control*, , n. DOI: 10.1080/00207179.2017.1390262, p. online version: pp. 1–23, 2017.

[103] KAILATH, T. *Linear Systems.* Prentice Hall, 1980.

[104] BATTISTEL, A.; NUNES, E. V. L.; HSU, L. Multivariable B-MRAC extension to arbitrary relative degree using global robust exact differentiators. *Proc. of the 13th IEEE Workshop on Variable Structure Systems*, p. 1–6, 2014.

[105] YANQUE, I.; NUNES, E. V. L.; COSTA, R. R.; HSU, L. Binary MIMO MRAC using a Passifying Multiplier - A smooth transition to Sliding Mode Control. *Proc. of the 2012 American Control Conference*, p. 1925–1930, 2012.

[106] ISIDORI, A. *Nonlinear Control Systems.* Springer, 1995.

[107] CUNHA, C. D.; ARAUJO, A. D.; BARBALHO, D. S.; MOTA, F. C. A dual-mode adaptive robust controller applied to the speed control of a three-phase induction motor. *Asian Journal of Control*, v. 7, n. 2, p. 197–201, 2005.

[108] EMELYANOV, S. V.; KOROVINJ, S. K.; NERSISIAN, A. L.; NISENZON, Y. Y. Discontinuous output feedback stabilizing an uncertain MIMO plant. *International Journal of Control*, v. 55, n. 1, p. 83–109, 1992.